UNIVERSITY OF BIRMINGHAM

ELUCIDATING THE BIOCHEMICAL PROPERTY OF MURF1 E3 LIGASE FUNCTION

By

Peter William James Dawson BSc (Hons), MSc

A thesis submitted to

The School of Sport, Exercise and Rehabilitation Sciences

The University of Birmingham

for the degree of

DOCTOR OF PHILOSOPHY

The School of Sports, Exercise and Rehabilitation Sciences

University of Birmingham

March 2024

Abstract

The preservation of skeletal muscle mass is crucial for maintaining metabolic function, depending on the intricate balance between muscle protein synthesis (MPS) and muscle protein breakdown (MPB). Skeletal muscle atrophy occurs when MPB surpasses MPS. Although MuRF1 (Muscle-specific ubiquitin ring finger 1), an E3 ligase, is recognized as a marker for skeletal muscle atrophy, its precise molecular function in controlling muscle mass remains unclear. While MuRF1 is known for its role in degrading muscle proteins, little knowledge exists about its discreet mechanisms as a ubiquitin E3 ligase. This thesis aims to fill existing knowledge gaps, advancing our understanding of skeletal muscle mass regulation at the molecular level using *in-vitro* biochemical assays.

The present thesis elucidates, *in-vitro*, the auto-ubiquitylation of MuRF1, generating various ubiquitin chain types in a UBE2-dependent manner. Furthermore, MuRF1 exhibits the ability to produce K48 and K63 polyubiquitin chains on substrates when interacting with UBE2D and UBE2E enzymes. Remarkably, it can generate unanchored K63 chains in association with UBE2N/V and mono-ubiquitylation with UBE2W. Notably, the mono-ubiquitin serves as an anchor for these unanchored K63 chains. This thesis demonstrates the direct ubiquitylation of previously suspected MuRF1 substrates and that MuRF1 ubiquitylates via the same mechanisms, whether with a substrate or through auto-ubiquitylation.

These novel findings establish a ubiquitylation mechanism, cooperating UBE2s, and potential substrates of MuRF1. This knowledge can be used to further explore the role of MuRF1 in skeletal muscle atrophy and present targets for future therapies.

Acknowledgements

I greatly appreciate CMAR and Arthritis UK for the opportunity to train as a scientist and learn the skills that got me here.

Thank you to all the mentors who have supported my academic career and help provide opportunities, advice, and model a scientific philosophy – Yu-Chiang Lai, Jonny Barlow, Thomas Solomon, Leigh Breen, Martin Whitham, and Michael Parkes.

A special thank you to all the lab mates who I've had the privilege of working with, you really made the experience fun, and I have learned lots from all of you. Thanks to Sam, Ibrahim, Jitpisute, and Alex for your input, assistance, and superb comradery. In addition to these qualities, Yusuke you were a fun housemate and a great friend to have close by.

I am very grateful to my collaborators that offered the chance to elevate my early career – Kishan Adoni, Sue Bodine, David Hughes, Leslie Baehr, Daniela Nasteska, and David Hodson. I am also grateful to the other labs and support staff at Sportex for keeping the school as a reputable research institution.

A huge thank you to my friends and family that provided the scaffolding that allowed my academic career to grow, even when things were tough - Mom and Dad, Ida, Anthony, Lauren, Tom, Laura, and all the wonderful crew at Aldi Studley. You helped

me weather a pandemic, break-up, moving house, a job change, and all the mental health struggles while training as a scientist. I dedicate this thesis to you all.

Declarations

I affirm that the thesis presented herein is a product of my own research endeavours and composition. This work has not been submitted, either in full or in part, for any other advanced degree. Any contributions from sources other than my own have been properly acknowledged within the text, with clear citations to the respective researchers and their publications.

I declare that all the work presented in this thesis is mine, with exception of the proteomic investigation and analysis which was performed by Kishan Adoni.

Peter Dawson

List of Publications

Nasteska, D., Fine, N., Ashford, F., Cuozzo, F., Viloria, K., Smith, G., Dahir, A., **Dawson, P.**, Lai, Y.-C., Bastidas-Ponce, A., Bakhti, M., Rutter, G., Fiancette, R., Nano, R., Piemonti, L., Lickert, H., Zhou, Q., & Akerman, I., Hodson, D (2021). PDX1LOW MAFALOW β-cells contribute to islet function and insulin release. Nature Communications, 12, 674. DOI: 10.1038/s41467-020-20632-z

Nasteska, D., Fine, N., Ashford, F., Cuozzo, F., Viloria, K., Smith, G., Dahir, A., **Dawson, P.**, Lai, Y.-C., Bastidas-Ponce, A., Bakhti, M., Rutter, G., Fiancette, R., Nano, R., Piemonti, L., Lickert, H., Zhou, Q., & Akerman, I., Hodson, D. (2020). Mature and immature β-cells both contribute to islet function and insulin release. Research Square. DOI: OI: 10.21203/rs.3.rs-40718/v1

Dawson, P. W. J., Ng, J., & Lai, Y.-C. (2023). The Mechanisms of MuRF1 Ubiquitylation. Physical Activity, 1(1), 18-27. DOI: 10.1016/j.bbrep.2023.101636

Dawson, P. W. J., Baehr, L. M., Hughes, D. C., Knowles, T. J., Sridhar, P., Bodine, S. C., & Lai, Y.-C. (2022). The Role of UBE2-Conjugating Enzymes in the Mechanism of MuRF1 Ubiquitylation. bioRxiv, 2022.06.13.495268. DOI: 10.1101/2022.06.13.495268

Net-anong, S., Prommee, N., Dechayont, B., Prajuabjinda, O., Yangthaworn, K., Chunthorng-Orn, J., Phuaklee, P., **Dawson, P. W. J.**, & Juckmeta, T. (2023, August 1). Calamus caesius (Rattan) wood: Chemical constituents, biological activities' relative medicinal properties from Thai medicinal scriptures, and in silico antioxidant activity. Arabian Journal of Chemistry, 16(8), 104990. DOI: 10.1016/j.arabjc.2023.104990

Lord, S. O., **Dawson, P. W. J.**, Chunthorng-Orn, J., Ng, J., Baehr, L. M., Hughes, D. C., Sridhar, P., Knowles, T., Bodine, S. C., & Lai, Y.-C. (2024, March 1). Uncovering the mechanisms of MuRF1-induced ubiquitylation and revealing similarities with MuRF2 and MuRF3. Biochemistry and Biophysics Reports, 37, 101636. DOI: 10.1016/j.bbrep.2023.101636

Nishimura, Y., Chunthorng-Orn, J., Lord, S., Musa, I., **Dawson, P.**, Holm, L., & Lai, Y.-C. (2022, July 1). Ubiquitin E3 ligase Atrogin-1 protein is regulated via the rapamycin-sensitive mTOR-S6K1 signaling pathway in C2C12 muscle cells. American Journal of Physiology-Cell Physiology, 323(1), C215-C225.

List of Abbreviations

AR	Acidic Region
ATG7	Autophagy Related 7
CHIP	Carboxy-terminus of Hsc70 interacting protein
COS	C-terminal Subgroup One Signature
CSA	Cross-Sectional Area
DCAF8	DDB1 And CUL4 Associated Factor 8
DUB	Deubiquitylase
ELISA	Enzyme-linked immunosorbent assay
FBS	Fetal Bovine Serum
FBxl	F-Histidine
HIS	Box And Leucine Rich Repeat Protein
IGF1	Insulin-like growth factor 1
IL-6	Interleukin 6
IPTG	Isopropyl β- d-1-thiogalactopyranoside
IRS-1	Insulin receptor substrate 1
LB	Lysogeny Broth
LDS	Lithium dodecyl sulfate
MAFbx	Muscle Atrophy F-box
MBP	Muscle Protein Breakdown
MFC	MuRF Family Conserved
MPS	Muscle Protein Synthesis

MuRF	Muscle-specific RING finger protein
MUSA1	Muscle ubiquitin ligase of SCF complex in atrophy-1
MYLPF	Myosin light chain, phosphorylatable, fast skeletal muscle
NBR1	Neighbour of BRCA1 gene 1
PDK-1	Phosphoinositide-dependent kinase-1
PI3K	Phosphoinositide 3-kinase
PKB	Protein kinase B
PTM	Post-translational Modification
RBCC	RING–B-box–coiled-coil; RING
RF	Restriction-Free
RING	Really Interesting New Gene
SPR	Surface Plasmon Resonance
SUMO	Small Ubiquitin-like Modifier
TBST	Tris-Buffered saline with Tween-20
T63	TRIM63/MuRF1
TNF	Tumour Necrosis Factor
TTN	Titin
TRIM	Tripartite motif
UBE1	Ubiquitin Activating Enzyme
UBE2	Ubiquitin Conjugating Enzyme
UBE3	Ubiquitin Ligase Enzyme
UPS	Ubiquitin-Proteasome System
VCP	Valosin-containing protein

ZNF	Zinc Ring Finger

Table of Contents

List of Figures

List of Tables

Chapter 1 Introduction

1.1 Skeletal Muscle

Skeletal muscle plays a vital role in both structure and metabolism, making up around half of the total body mass (1,2). Beyond providing support and allowing for movement, muscle is deeply involved in processes like metabolic regulation and insulin-dependent glucose absorption. However, health conditions such as cancer, diabetes, sepsis and heart failure can significantly impact muscle quantity and quality through pathologies like myopathies (3).

An equilibrium between muscle protein synthesis and breakdown maintains these important functions, and while muscle mass is robust in resisting changes to short-term stimulus, such as acute dietary or activity changes, these can be detrimental when they become chronic. Furthermore, the more clinically urgent population are those with rapid and severe muscle wasting from infection, sepsis, or cancer. (4–8). Any disruptions to the balance regulated by the ubiquitin-proteasome system (UPS) can induce loss of muscle mass (9). Scientists are studying the complex molecular underpinnings of how the UPS impacts protein dynamics within muscles. The goal is to elucidate this mechanism in hopes of discovering targeted therapies that could exploit it for medical benefit. Further unveiling these intricacies may provide opportunities to prevent or treat muscle-wasting diseases. Continuous research aims to enhance our understanding of skeletal muscle at the cellular level and identify potential mechanisms for therapeutic intervention.

1.2 Skeletal Muscle Loss and Disease

1.2.1 Sarcopenia

Sarcopenia refers to the age-related loss of skeletal muscle mass and function experienced by older adults (10). It represents a major health issue due to its propensity to exacerbate physical frailty and dependency. As muscle tissues naturally weaken with aging, sarcopenia impairs mobility and increases susceptibility to falls (11). This contributes to heightened fracture risk as muscle is closely tied to bone health (12,13).

Quantitatively measuring sarcopenia is challenging due to variations in body composition with age (14). Defining thresholds for low muscle mass or weakness can be arbitrary. Nonetheless, research increasingly demonstrates that even modest sarcopenia independently predicts negative health outcomes (15). Longitudinal studies show associations between declining muscle mass and strength and elevated risks of mortality, disability, institutionalization and healthcare expenses over time (16).

The molecular mechanisms governing age-related muscle loss are multi-factorial. Accumulating knowledge points to roles for inflammation, oxidative stress, anabolic resistance and mitochondrial dysfunction (17,18). Unfortunately, available interventions remain relatively untargeted. Resistance exercise shows benefits but adherence often declines with age (19). Further elucidating the pathophysiology of

sarcopenia could help optimize prevention and treatment strategies to support healthy aging (20).

Anabolic resistance, a diminished ability of muscle tissue to synthesise new proteins in response to anabolic stimuli such as dietary protein intake and resistance exercise, plays a pivotal role in the pathogenesis of sarcopenia ((21,22), (22). This condition, characterized by the progressive loss of muscle mass and strength in aging individuals, is primarily driven by the impaired anabolic signalling pathways rather than excessive protein breakdown. The inefficiency in muscle protein synthesis means that even with adequate protein consumption, the elderly cannot effectively utilize the amino acids for muscle maintenance and growth. Consequently, therapeutic strategies should prioritize enhancing protein anabolism—improving the muscle's responsiveness to anabolic stimuli—over merely inhibiting protein catabolism. This focus is critical because targeting protein breakdown alone does not address the fundamental issue of impaired muscle protein synthesis (23,24), which is central to the development and progression of sarcopenia(See also – (25)). Hence, interventions aimed at overcoming anabolic resistance, such as optimizing protein intake timing and incorporating resistance training, are more likely to be effective in mitigating sarcopenia than those solely aimed at reducing protein degradation.

Continued research aims to address functionality decline and dependence accompanying this progressive condition.

1.2.2 Cancer Cachexia

Cancer cachexia is a wasting condition characterized by concurrent loss of both adipose and skeletal muscle mass (26). Patients experience a reduction in food intake, general weakness, weight loss and low blood cell counts (27). Unlike common malnutrition, cachexia uniquely targets both fat and muscle tissues (28). This makes it a serious concern for cancer prognosis and survival (29).

The skeletal muscle depletion caused by cachexia has been directly associated with reduced survival time in cancer patients, as those with more advanced muscle wasting tend to have poorer outcomes and shorter lifespans (30). Even early muscle loss during tumour progression can influence a patient's survival chances (31). As skeletal muscle is vital for mobility, functioning, and general health, its cachexia-related atrophy seriously threatens quality of life during cancer treatment (32).

Despite its impacts, there remain many unknowns regarding the molecular mechanisms that drive cancer cachexia. While pro-inflammatory cytokines like TNF-α and IL-6 produced by the tumour may instigate muscle wasting (33), the precise signalling pathways and factors involved are still being uncovered (34). More research is needed to comprehend how and why cachexia differentially targets muscle and fat depletion at the genetic and protein level (35). A better molecular understanding of variations between cancer types and patients could help tailor new targeted treatments (36). However, the complex interactions between the systemic

effects of cancer and localized tissue changes continue to challenge researchers seeking to explain cachexia progression (37).

1.3 Molecular Mechanisms of Muscle Protein Breakdown

Skeletal muscle mass is regulated through a dynamic balance between the rates of protein synthesis and breakdown (38). Increased protein degradation contributes to muscle atrophy in various conditions including aging, disuse, and chronic diseases (39,40). The ubiquitin proteasome system (UPS) and lysosomal/autophagy pathways are the primary intracellular mechanisms for regulated muscle protein breakdown (41).

Net muscle protein turnover can be measured using techniques such as deuterium oxide labelling or stable isotope tracer infusion – This can be used to approximately infer MPS. Deuterium oxide labelling allows for muscle biopsies to determine the incorporation of deuterium into amino acids. Stable isotope tracers enable the inference of synthesis by calculating the balance of a tracer between arterial and venous blood in the muscle. However, measuring muscle protein breakdown (MPB) presents challenges. Current tracer methods cannot distinguish whether amino acids are being recycled within the muscle, leading to potential underestimation of MPB. Additionally, it is currently not possible to quantify the accumulation of tracers within muscle protein, and it is therefore not possible to accurately measure the breakdown and release of these tracers (42).

Research is ongoing to explore the measurement of 3- methylhistidine (3-MH) as a byproduct of MPB (43). It is hypothesised that as 3-MH is in high concentrations in muscle, as actin and myosin contain high amounts of histidine subject to methylation (44). During MPB this will be broken down and released into the bloodstream and is

measured via mass spectrometry. This method is subject to having it's data obscured as 3-MH is not exclusive to muscle protein, just more abundant in muscle. Additionally, the consumption of meat also increases circulating 3-MH, further confounding the detection of muscle-specific 3-MH (45)(46).
This lack of ability to reliably measure MPB means that it is important to identify other quantitative measures of MBP signalling. This can be done by measuring the biochemical pathways that regulate protein breakdown in muscle.

The UPS involves substrate protein marking via ubiquitin conjugation, recognition by the 26S proteasome, and degradation into oligopeptides (47). E3 ubiquitin ligases facilitate substrate specificity through catalysing ubiquitin transfer (48). Their expression is regulated by the transcription factor FoxO, which is activated under catabolic conditions by upstream kinase pathways, such as disinhibition of the Pi3K-AKT pathway, or inflammatory-stimulated activation of the JNK→p38 and IKK→NF- κB pathways- (49,50).

Autophagy similarly degrades proteins and organelles through the lysosomal machinery (51). During macroautophagy, cytoplasmic contents are sequestered within double-membrane autophagosomes and delivered to lysosomes for breakdown. Autophagy-related gene 7 (Atg7) is required for autophagosome biogenesis, while microtubule-associated protein 1 light chain 3 (LC3) associates with autophagosomal membranes and serves as a marker of autophagic flux (52). While

baseline autophagy maintains protein quality control, elevated autophagy also contributes to net muscle protein loss during atrophy (41,53).

Crosstalk exists between the UPS and autophagy pathways, as autophagy can degrade ubiquitylated protein aggregates unable to enter the proteasome (54). Dysregulation of specific E3 ligases, autophagy-related genes, and upstream signalling kinase cascades like PI3K-Akt-FoxO are all implicated in pathological muscle wasting disorders (55). Elucidating the nuanced molecular choreography governing muscle protein breakdown could reveal novel treatment targets.

In summary, tightly regulating protein synthesis and several degradation mechanisms, especially the UPS and autophagy, is pivotal for maintaining skeletal muscle mass. Imbalances contribute to muscle loss in various conditions. Further elucidating these pathways may help optimize anti-atrophy therapies.

1.4 The Ubiquitin Proteasome System

1.4.1 Ubiquitylation: An Overview

The ubiquitin proteasome system (UPS) is a highly organized pathway that mediates the regulated degradation of intracellular proteins in eukaryotic cells (56). Precise control over protein turnover via the UPS is essential for many basic cellular processes such as cell cycle progression (57), transcriptional regulation (Davie and Murphy, 1990), signal transduction (58), and responses to stress (59). Dysregulation of the UPS is associated with various disease states including cancer (60), neurological disorders (61), and muscle wasting conditions (62).

The first step in the UPS involves tagging target proteins with ubiquitin, a small regulatory protein of 76 amino acids (63). Ubiquitin is attached through an enzymatic cascade involving E1 ubiquitin-activating enzyme, E2 ubiquitin-conjugating enzyme, and E3 ubiquitin ligase (64). The E3 ligase confers substrate specificity by facilitating the transfer of ubiquitin from the E2 enzyme to lysine residues on the target protein (65). Ubiquitylation involves the formation of an isopeptide bond between the C-terminal glycine of ubiquitin and the epsilon-amino group of a lysine residue on the target substrate (66). While lysine 48-linked polyubiquitylation signals proteasomal degradation, other ubiquitin chain linkages mediate non-proteolytic functions.

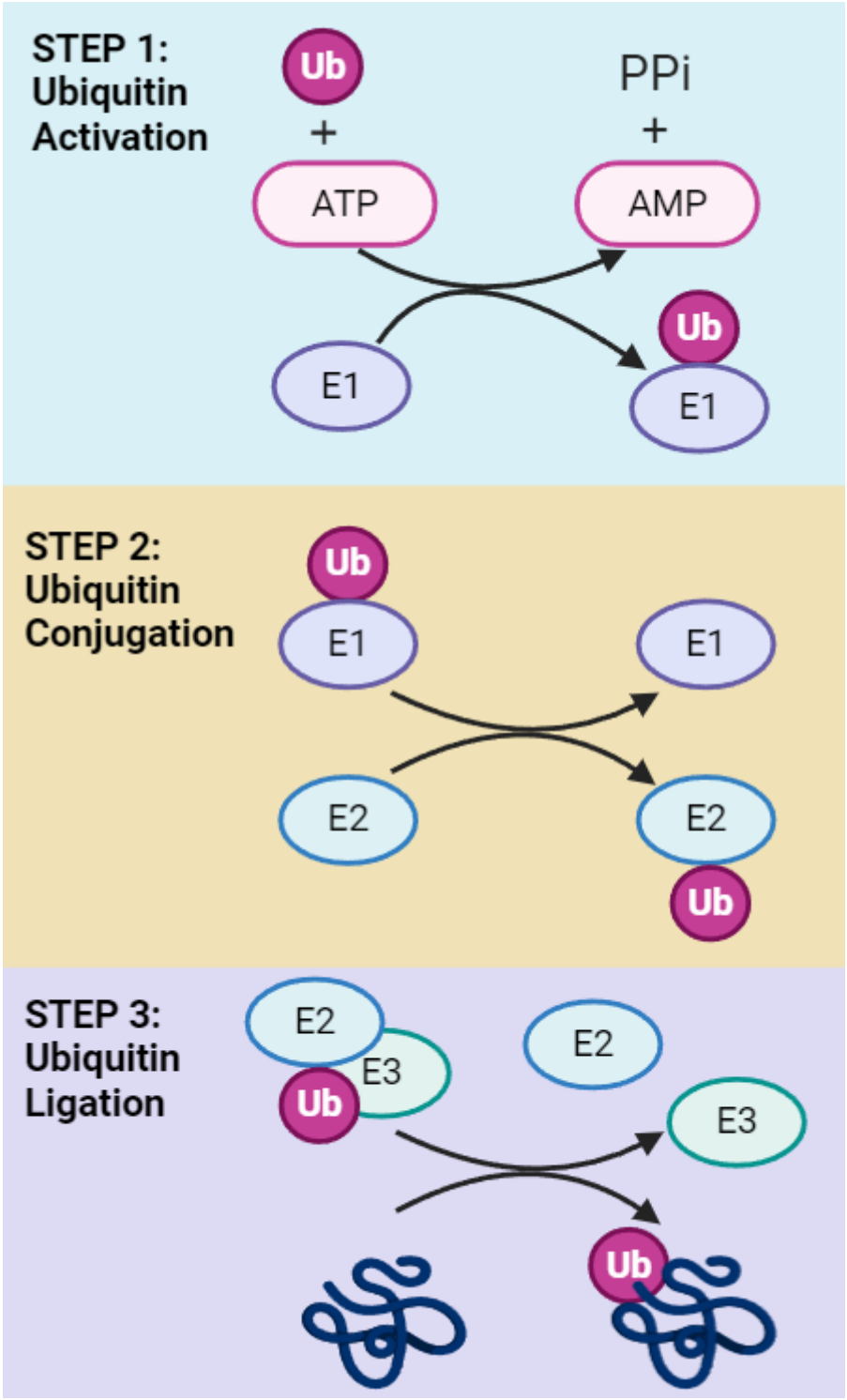

Figure 1.1 – The three-step process of ubiquitylation.

Lysine 63-linked chains participate in DNA repair, cell signalling, and endosomal sorting (67). Monoubiquitylation and lysine 11-, 29- or 63-linked chains help regulate processes like DNA damage response, kinase activation, and membrane protein trafficking (68). Lysine 27- and lysine 33-linked chains are also involved in regulating gene expression and DNA replication (69).

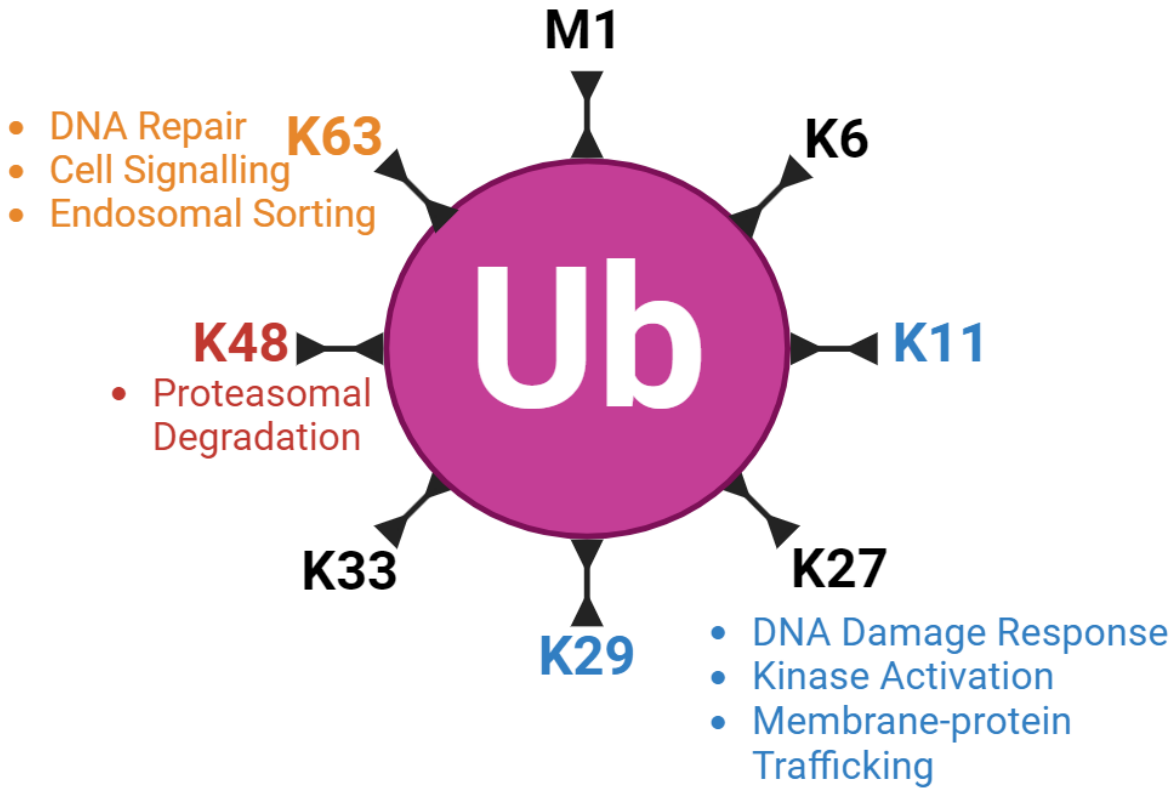

Figure 1.2 – Diagram of the ubiquitin protein and the amino acids that allow ubiquitin-ubiquitin linkages. Coloured amino acids highlight known functions of these linkages.

Non-canonical ubiquitylation can occur through attachment to alternate residues besides lysine. For example, ubiquitin conjugation to the alpha-amino group of protein N-termini or internal cysteine, serine, or threonine residues mediates specific outcomes (70). N-terminal ubiquitylation regulates mitochondrial import and proteasomal delivery, while cysteine ubiquitylation controls zinc finger transcription factor activity (71,72).

The linkages, chains lengths and internal positions of ubiquitin attachments all contribute to determining substrate fate. Interpreting these diverse "ubiquitin codes" requires deciphering context-dependent interactions between ubiquitylated proteins and effector domains on ubiquitin-binding partners (73). Elucidating non-proteolytic and non-canonical ubiquitylation mechanisms remains an ongoing area of research.

The 26S proteasome is a 2.5 MDa ATP-dependent complex that recognizes, unfolds and degrades polyubiquitylated proteins (74). It is composed of a 20S core particle which contains the proteolytic active sites, and one or two 19S regulatory particles at either end (75). The 19S caps recognize ubiquitylated proteins and open the core for protein translocation (76). Once unfolded proteins enter the 20S chamber, ubiquitin is cleaved off and recycled, and proteolytic subunits use ATP hydrolysis to degrade substrate proteins into small peptide fragments (77).

1.4.2 Mechanisms of Ubiquitylation

The three main classes of enzymes that cooperate to carry out ubiquitylation are E1, E2, and E3 enzymes. E1 enzymes, also called ubiquitin-activating enzymes, catalyse the first step by activating ubiquitin in an ATP-dependent manner. This leads to the formation of a high-energy thioester bond between the active-site cysteine on the E1 and the Gly76 carboxyl group of ubiquitin (78).

There are only 2 E1 enzymes in humans that activate ubiquitin (79). The E1 then works with various E2 enzymes, also known as ubiquitin-conjugating enzymes, which receive the ubiquitin cargo from the E1 via transesterification (80). E2s are responsible for shuttling and presenting ubiquitin for attachment to target proteins. There are approximately 40 different E2 enzymes that determine ubiquitin chain topology (81,82).

E3 ubiquitin ligases are the largest family of ubiquitylation enzymes, with over 600 different E3s identified in humans (83). They confer substrate specificity by directly interacting with target proteins and facilitating the transfer of ubiquitin from the E2 to a lysine residue on the substrate (65).

Together, the sequential cooperation between E1, E2, and E3 enzymes tightly regulates substrate selection and polyubiquitin chain assembly, determining eventual protein fate in the cell.

1.4.3 E3 Ubiquitin Ligases

E3 ubiquitin ligases are the largest family of enzymes involved in ubiquitylation, conferring substrate specificity through direct physical interaction. They are categorized into three main classes based on their mechanism of catalysis (83).

HECT (Homologous to E6AP Carboxyl Terminus) domain E3s contain a conserved HECT domain of around 350 amino acids. This domain forms a thioester intermediate with ubiquitin from the E2 before transferring it to substrate lysines. Examples include E6AP, Nedd4 and Herc2 which regulate processes like receptor endocytosis and cell signalling cascades (84).

RING (Really Interesting New Gene) finger E3s represent the largest E3 class, utilizing a RING domain structural motif to bind E2~ubiquitin conjugates (85). Rather than forming intermediates, RING E3s juxtapose E2 and substrate for direct transfer (86). Vast RING E3 subclasses include SCF complexes important for cell cycle regulation, and MDM2 inhibiting p53 tumour suppressor activity (65).

U-box E3s are structurally similar to RING fingers but use a U-box domain and lack zinc-binding ability (87). They work with E2s in a RING-like manner without thioester formation. Examples are CHIP and UBR proteins involved in endoplasmic reticulum-associated degradation (ERAD) and N-end rule pathways (87,88).

RING-between-RING (RBR) E3s combine RING1 and RING2 domains with an additional in-between region. This region adopts a HECT-like fold assisting transfer from an intermediate cysteine, displaying characteristics of both RING and HECT E3 classes (89). RBR E3s such as HOIL-1 and PARKIN are implicated in mitochondrial quality control and neurodegeneration (90).

Through distinct mechanisms, diverse E3 ligases impart exquisite control over ubiquitylation and protein fate. Elucidating their tissue-specific roles and regulation promises mechanistic insights relevant to disease pathology and therapy (84).

1.5 MuRF1 as a Ubiquitin E3 Ligase Regulating Muscle Mass

1.5.1 Discovery of MuRF1 Association with Muscle

The muscle-specific E3 ubiquitin ligase MuRF1 was initially discovered through its interaction with the titin kinase domain (91). Centner and colleagues (92) sought to characterize binding partners of the A167 and M2 regions of titin utilizing a yeast two-hybrid system. Through screening of cDNA libraries derived from human heart and skeletal muscle, they identified 22 potential interactors via β-galactosidase activity. Subsequent sequencing revealed that two of the four confirmed positives corresponded to MuRF1. Deletion mapping demonstrated the necessity of the A168/A169 domains for this interaction.

To elucidate the MuRF1 cDNA sequence, the authors conducted further screening of human muscle cDNA libraries (91). Systematic deletion analysis of both titin and cloned MuRF1 constructs coupled with two-hybrid assays revealed a central 144-residue region facilitated the interaction between MuRF1 and the titin A168-A169 segment. Additionally, a GST pull-down assay using purified recombinant titin A168/A169 and total muscle lysates confirmed the binding via western blot detection of MuRF1 (91).

While this study represented a seminal finding as the first to implicate MuRF1 as a titin binding partner, its functional role remained unknown at the time of publication

(91). Subsequent investigations would be crucial to elucidate MuRF1's importance in regulating muscle mass through orchestrating ubiquitin-mediated protein degradation (93–95).

1.5.2 Identification of MuRF1 as an E3 Ligase

Bodine et al, 2001 (96), sought to elucidate the molecular underpinnings of skeletal muscle atrophy by investigating differential gene expression patterns. They employed a rat immobilization model involving fixation of one gastrocnemius via casting for three days, with the contralateral limb serving as an ambulatory control. Gene-tag differential display compared mRNA from immobilized and control muscles, focusing on genes upregulated over three-fold (93).

Comparative analysis across immobilization, denervation, and unweighting paradigms spanning one to fourteen days found that denervation and immobilization induced similar transcriptional perturbations, while unweighting had a more limited impact (93). Two E3 ubiquitin ligases, muscle RING-finger protein-1 (MuRF1) and Muscle Atrophy F-Box (MAFBx), were identified as consistently induced across all models.

To gauge the ubiquitylation of MuRF1 and MAFBx as atrophy markers, the authors assessed expression following interleukin-1 (IL-1) and dexamethasone treatments, inducing cachexia and wasting via distinct mechanisms (93). Both upregulated MuRF1 and MAFBx over ten-fold, implicating their central role in mediating muscle loss.

Next, Bodine et al aimed to characterize MuRF1's function. *In-vitro* ubiquitylation assays incubated E1, E2, glutathione S-transferase-fused MuRF1, ubiquitin, and ATP, revealing polyubiquitin chain formation only in MuRF1-containing reactions via immunoblot, confirming MuRF1 acts as an E3 ligase.

To interrogate MuRF1's *in-vivo* significance, genetically engineered mice with the MuRF1 locus replaced by β-galactosidase/neomycin were generated (93). Sciatic nerve ablation in these mice induced expression at the MuRF1 locus, demonstrating direct transcriptional induction by denervation. Additionally, MuRF1 knockout mice were protected from denervation-induced atrophy, retaining 36% greater muscle mass versus controls at fourteen days (93).

Collectively, this seminal study established a definitive causal linkage between elevated MuRF1 and MAFBx expression and muscle wasting. Robust upregulation across multiple atrophy models highlighted their potential as universal catabolic markers. Characterization of MuRF1's E3 ligase activity *in-vitro* and indispensable catabolic role *in-vivo* mechanistically implicated MuRF1 as a central mediator of muscle proteolysis.

1.5.3 The Impacts of MuRF1 Knockout in-vivo

Since the initial characterization of MuRF1 by Bodine et al. (96), knockout mouse models have provided valuable insight into MuRF1's critical role as a driver of muscle loss. Unlike denervation, hindlimb suspension induces atrophy while maintaining neurologic integrity, avoiding stress-induced pathways (97). This study subjected MuRF1-knockout mice to 10 days of suspension. The soleus displayed near-complete resistance to wasting compared to wildtype littermates.

Baehr and colleagues (98) treated MuRF1-knockout mice with the glucocorticoid dexamethasone, another robust atrophy agent, for 14 days. Various parameters including muscle cross-sectional area, tibialis anterior mass, and triceps surae mass indicated attenuated atrophy compared to wildtype mice. Dexamethasone induced over 2-fold MuRF1 upregulation in wildtype mice by RT-PCR. ELISA assays found knockout mice exhibited lower total and polyubiquitin levels versus wildtype following dexamethasone, implicating MuRF1's role in ubiquitin-mediated proteolysis (98).

Hwee and coworkers (99) aged MuRF1 knockout and wildtype mice to 24 months to assess age-related wasting. Knockouts alone displayed muscle mass and cross-sectional area preservation without loss reported in aged wildtypes. Moreover, functional overload-induced hypertrophy was maintained in aged knockouts versus impaired growth in old wildtypes.

The mice were genetically modified to generate MuRF1 knockout (MuRF1-KO), MuRF1 ring-domain deleted, and wild type control mice (100). They underwent sciatic nerve ablation to induce muscle atrophy. Wildtype mice lost 36% of gastrocnemius muscle mass, whereas ring-domain mutant mice only lost 22% of muscle mass. This level of muscle mass loss in ring-domain mutant mice was similar to what was seen in full MuRF1 knockout mice, which lost 20% of muscle mass. These findings suggest that MuRF1's ubiquitylation activity, not just its presence, mediates muscle atrophy. By deleting the ring domain required for ubiquitylation, muscle mass loss during atrophy was attenuated, demonstrating the importance of MuRF1's E3 ligase function in driving protein breakdown and muscle wasting (100).

Collectively, knockout models demonstrate MuRF1 depletion robustly rescues multiple acute and chronic catabolic paradigms from denervation to aging (97–99). The RING mutant further implicates MuRF1's E3 activity rather than absence as critical for driving muscle loss (100). These studies establish MuRF1's central pathogenic role in skeletal muscle wasting.

1.5.4 The Impacts of MuRF1 Overexpression in-vivo

While MuRF1 knockout models demonstrate its necessity for muscle wasting, MuRF1 overexpression has comparatively little effect in skeletal muscle (101). Mice constitutively overexpressing MuRF1 in skeletal muscle displayed normal viability, muscle mass, myofibrillar structure, and ubiquitylated protein levels versus wildtypes under standard housing conditions.

Willis et al. (2009) investigated cardiac-specific MuRF1 overexpression utilizing transgenic mice (102). At baseline, prior to surgical induction of heart failure via transaortic constriction (TAC), MuRF1 overexpression impaired cardiac function. Transgenic mice exhibited enlarged left ventricular dimensions and significantly thinner anterior and posterior ventricular walls (27.6% and 32.5% reductions during diastole, respectively) compared to wildtypes. Following TAC, MuRF1 transgenic mice experienced progressive declines in fractional shortening over 70% lower than controls. In contrast, wildtype mice underwent compensatory hypertrophy of the left ventricular walls in response to the pressure overload. These findings implicated MuRF1 in deterioration of cardiac muscle tissue, as its elevated expression correlated with thinner myocardium unable to hypertrophy in response to stress (102).

The discrepancy between MuRF1 knockout and overexpression models requires consideration of potential mechanistic differences between cardiac and skeletal muscle. While MuRF1 ablation robustly rescues muscle from various atrophy stimuli,

overexpression alone does not induce skeletal muscle loss (101). However, in the heart, MuRF1 overexpression appears detrimental, hindering adaptive hypertrophic responses and exacerbating dysfunction (102).

Future work should aim to elucidate distinct MuRF1 functions and regulated pathways in these tissues. For example, cardiac myocytes experience continual remodelling demands not required of post-mitotic myofibers. Differential MuRF1 phosphorylation, localization, or substrate targeting based on tissue-specific signalling could functionally diverge its role in maintaining myocardium versus skeletal muscle mass homeostasis.

1.5.5 MuRF1 and Hypertrophic Cardiomyopathy

Investigations have explored associations between MuRF1 and human heart disease through sequencing studies (103). A cohort of 594 hypertrophic cardiomyopathy (HCM) patients underwent TRIM63 (encoding MuRF1) sequencing, compared to 307 non-HCM controls. Heterozygous TRIM63 mutations were enriched in HCM cases relative to controls. Two missense variants (p.Ala48Val and p.Ile130Met) and a deletion (p.Gln247Ter) identified in HCM patients were expressed in mouse hearts. Each variant induced cardiac hypertrophy, implicating dysfunctional MuRF1 in HCM pathogenesis (103).

Jokela and colleagues, 2019 (27), presented a case study of an HCM patient also harbouring the p.Gln247Ter deletion. Interestingly, this individual displayed mild skeletal myopathy with upper limb fatigability. Muscle biopsy from the vastus lateralis identified myopathic changes, suggesting MuRF1 mutations may confer pleiotropic effects on both cardiac and skeletal muscle (104).

This human epidemiological and functional data correspondingly supported prior mouse experimentation, further linking MuRF1 dysfunction to hypertrophic cardiomyopathy (103). The case report also highlighted MuRF1's potential importance in skeletal muscle, given extra-cardiac myopathic involvement (104).

Together, these cohort, mechanistic, and case studies substantiate observations from animal models and hypothesize roles for MuRF1 beyond the heart (103–105). They warrant future investigation to elucidate pleiotropic MuRF1 mechanisms, as its precise functions in both cardiac and skeletal muscle remain to be fully characterized. Elucidating MuRF1's diverse tissue-specific functions may yield novel therapeutic strategies for myopathies.

1.5.6 Limitations of Current MuRF1 Research

A major limitation in furthering the understanding of MuRF1 function has been over-reliance on mRNA expression analyses to infer protein activity and importance. While a necessary initial step, transcript levels alone provide an incomplete picture, as post-transcriptional and post-translational modifications profoundly influence MuRF1 regulation and substrate targeting (106). Many studies conclude MuRF1 drives atrophy primarily based on its elevated mRNA in catabolic conditions without direct assessment of protein levels, localization, phosphorylation state, interaction partners, or E3 ligase enzymatic activity (3,100). This leaves key aspects of MuRF1 physiology uncertain. More robust validation at the protein level through techniques like immunoblotting, immunohistochemistry, and interactomics is still lacking but would confirm functional implications of transcriptional changes.

Another limitation arises from the lack of in-depth mechanistic studies exploring MuRF1's interactions with specific E2 conjugating enzymes. MuRF1 participates in dynamic associations with UBE2s that likely confer substrate selectivity, yet the biophysical properties, enzymology, and regulation of discrete MuRF1-UBE2 pairs remain poorly defined (107). While sensitive methods identified preferred E2 partners like E2E1, E2G1, E2J1, E2J2, and E2L3 (108), little is known about binding affinities, catalytic efficiencies, or allosteric effects of substrates on these. More rigorous characterization of MuRF1-E2 pairs through co-precipitation experiments and biochemical ubiquitylation assays.

A further limitation arises from the general lack of demonstrable ubiquitylation of specific MuRF1 substrates. Application of protocols like immunoprecipitation followed by ubiquitin remnant profiling or mutational disruption of predicted lysine acceptor sites has been limited. Without unequivocally visualizing MuRF1-mediated ubiquitylation of candidates in relevant cellular or animal models, the field retains considerable uncertainty surrounding MuRF1's true *in-vivo* substrates. Additional investigation employing proteomics, ubiquitin linkage-specific antibodies, and competitive substrate mutants could validate MuRF1’s precisely regulated ubiquitylation activities and help reconcile discrepancies between putative and bona fide targets reported to date. ***A***ddressing these gaps through application of more rigorous mechanistic, protein-level, and substrate- focused methodologies would substantially advance understanding of MuRF1 physiology. Only with deeper insights into its regulation and substrate targeting precision will researchers realize MuRF1's full potential as a therapeutic target (106,109).

1.6 Significance of Thesis

Skeletal muscle atrophy is a serious medical condition affecting millions, compromising mobility and quality of life. Unfortunately, there are currently no effective pharmaceutical therapies due in large part to incomplete mechanistic understanding of its pathogenesis. While MuRF1 is robustly linked to muscle wasting through transcriptional profiling, precisely how this E3 ligase orchestrates loss of mass remains unclear when considering post-transcriptional regulation.

This thesis aims to address this knowledge gap and propel development of targeted treatments. A comprehensive investigation of MuRF1's regulation and activity at the protein level will provide novel insights into its role coordinating ubiquitin-mediated proteolysis. Directly visualizing the ubiquitylation of proposed MuRF1 substrates techniques such as immunoprecipitation and mass spectrometry will validate its biological functions and substrate targeting specificity beyond correlation with mRNA levels.

Unravelling key protein substrates and modifications influencing substrate targeting specificity offers opportunities for therapeutic intervention beyond blunt transcriptional suppression.

Collectively, the proposed research is well-positioned to substantially further current understanding of molecular mechanisms underlying muscle wasting initiation and progression. Mechanistic insights into MuRF1's post-transcriptional governance of proteostasis may uncover alternative strategies for preserving precious lean tissue. This could involve selectively preserving myofibrillar structural integrity through interference with isoform-specific substrate recognition.

1.7 Aims of this Thesis.

The primary aim of this PhD thesis is to comprehensively investigate the molecular role of MuRF1 in skeletal muscle physiology. This overarching objective will be pursued through three specific aims:

Identification of Cooperating UBE2 Enzymes: The first objective is to elucidate the specific UBE2 enzymes that cooperate with MuRF1 in its ubiquitylation processes. By employing biochemical and proteomic techniques, this aim seeks to uncover the intricate network of UBE2 enzymes that directly interact with MuRF1 and contribute to its regulatory functions in skeletal muscle.

Characterization of Ubiquitin Chain Types Formed: The second objective is to characterize the types of ubiquitin chains formed by MuRF1 during the ubiquitylation process. By employing advanced techniques such as ubiquitin linkage-specific antibodies, ubiquitin chain purification, and mass spectrometry, this aim seeks to unravel the specific ubiquitin chain architectures generated by MuRF1. Understanding the types of ubiquitin linkages formed will contribute crucial insights into the regulatory mechanisms orchestrated by MuRF1 in skeletal muscle.

Identification of Direct Ubiquitylation Substrates: The third and final objective involves the systematic identification of direct substrates targeted by MuRF1-mediated

ubiquitylation. Through a combination of mass spectrometry, immunoprecipitation assays, and bioinformatics analyses, this aim aims to provide a comprehensive catalogue of proteins that undergo ubiquitylation by MuRF1, offering insights into the specific cellular pathways and proteins influenced by MuRF1 activity.

Collectively, achieving these aims will not only enhance our understanding of MuRF1's molecular role but also pave the way for novel therapeutic interventions targeting skeletal muscle disorders associated with dysregulated ubiquitylation processes.

1.8 References

1. Frontera WR, Ochala J. Skeletal Muscle: A Brief Review of Structure and Function. Calcif Tissue Int. 2015 Mar 8;96(3):183–95.

2. Baskin KK, Winders BR, Olson EN. Muscle as a “Mediator” of Systemic Metabolism. Cell Metab. 2015 Feb;21(2):237–48.

3. Bonaldo P, Sandri M. Cellular and molecular mechanisms of muscle atrophy. Dis Model Mech. 2013;6(1):25–39.

4. DeFronzo RA, Jacot E, Jequier E, Maeder E, Wahren J, Felber JP. The Effect of Insulin on the Disposal of Intravenous Glucose: Results from Indirect Calorimetry and Hepatic and Femoral Venous Catheterization. Diabetes. 1981 Dec 1;30(12):1000–7.

5. Rai M, Demontis F. Systemic Nutrient and Stress Signaling via Myokines and Myometabolites. Annu Rev Physiol. 2016 Feb 10;78(1):85–107.

6. Argilés JM, Campos N, Lopez-Pedrosa JM, Rueda R, Rodriguez-Mañas L. Skeletal Muscle Regulates Metabolism via Interorgan Crosstalk: Roles in Health and Disease. J Am Med Dir Assoc. 2016;17(9):789–96.

7. Meyer C, Dostou JM, Welle SL, Gerich JE. Role of human liver, kidney, and skeletal muscle in postprandial glucose homeostasis. American Journal of Physiology-Endocrinology and Metabolism. 2002 Feb 1;282(2):E419–27.

8. Sartori R, Romanello V, Sandri M. Mechanisms of muscle atrophy and hypertrophy: implications in health and disease. Nat Commun. 2021 Dec 1;12(1):1–12.

9. Nishimura Y, Musa I, Holm L, Lai YC. Recent advances in measuring and understanding the regulation of exercise-mediated protein degradation in skeletal muscle. American Journal of Physiology-Cell Physiology. 2021 Aug 1;321(2):C276–87.

10. Roubenoff R, Hughes VA. Sarcopenia: Current Concepts. J Gerontol A Biol Sci Med Sci. 2000 Dec 1;55(12):M716–24.

11. Fielding RA, Vellas B, Evans WJ, Bhasin S, Morley JE, Newman AB, et al. Sarcopenia: An Undiagnosed Condition in Older Adults. Current Consensus Definition: Prevalence, Etiology, and Consequences. International Working Group on Sarcopenia. J Am Med Dir Assoc. 2011 May;12(4):249–56.

12. Alajlouni DA, Bliuc D, Tran TS, Blank RD, Cawthon PM, Ensrud KE, et al. Muscle Strength and Physical Performance Are Associated With Risk of Postfracture Mortality But Not Subsequent Fracture in Men. Journal of Bone and Mineral Research. 2020 Dec 1;37(8):1571–9.

13. Alajlouni D, Bliuc D, Tran T, Eisman JA, Nguyen T V, Center JR. Decline in Muscle Strength and Performance Predicts Fracture Risk in Elderly Women and Men. J Clin Endocrinol Metab. 2020 Sep 1;105(9):e3363–73.

14. Cruz-Jentoft AJ, Baeyens JP, Bauer JM, Boirie Y, Cederholm T, Landi F, et al. Sarcopenia: European consensus on definition and diagnosis. Age Ageing. 2010 Jul 1;39(4):412–23.

15. Batsis JA, Villareal DT. Sarcopenic obesity in older adults: aetiology, epidemiology and treatment strategies. Nat Rev Endocrinol. 2018 Sep;14(9):513–37.

16. Beaudart C, Zaaria M, Pasleau F, Reginster JY, Bruyère O. Health Outcomes of Sarcopenia: A Systematic Review and Meta-Analysis. Wright JM, editor. PLoS One. 2017 Jan 17;12(1):e0169548.

17. Phillips T, Leeuwenburgh C. Muscle fiber-specific apoptosis and TNF-α signaling in sarcopenia are attenuated by life-long calorie restriction. The FASEB Journal. 2005 Apr 21;19(6):1–33.

18. Marzetti E, Calvani R, Tosato M, Cesari M, Di Bari M, Cherubini A, et al. Sarcopenia: an overview. Aging Clin Exp Res. 2017 Feb 2;29(1):11–7.

19. Beaudart C, Rolland Y, Cruz-Jentoft AJ, Bauer JM, Sieber C, Cooper C, et al. Assessment of Muscle Function and Physical Performance in Daily Clinical Practice. Calcif Tissue Int. 2019 Jul 10;105(1):1–14.

20. Dedeyne L, Dupont J, Koppo K, Verschueren S, Tournoy J, Gielen E. Exercise and Nutrition for Healthy AgeiNg (ENHANce) project – effects and mechanisms of action of combined anabolic interventions to improve physical functioning in sarcopenic older adults: study protocol of a triple blinded, randomized controlled trial. BMC Geriatr. 2020 Dec 10;20(1):532.

21. Meyer C, Dostou JM, Welle SL, Gerich JE. Role of human liver, kidney, and skeletal muscle in postprandial glucose homeostasis. American Journal of Physiology-Endocrinology and Metabolism [Internet]. 2002 Feb 1;282(2):E419–27. Available from: https://www.physiology.org/doi/10.1152/ajpendo.00032.2001

22. Cuthbertson D, Smith K, Babraj J, Leese G, Waddell T, Atherton P, et al. Anabolic signaling deficits underlie amino acid resistance of wasting, aging muscle. The FASEB Journal. 2005 Mar 13;19(3):1–22.

23. Volpi E, Nazemi R, Fujita S. Muscle tissue changes with aging. Curr Opin Clin Nutr Metab Care. 2004 Jul;7(4):405–10.

24. Volpi E, Sheffield-Moore M, Rasmussen BB, Wolfe RR. Basal Muscle Amino Acid Kinetics and Protein Synthesis in Healthy Young and Older Men. JAMA. 2001 Sep 12;286(10):1206.

25. Dickinson JM, Volpi E, Rasmussen BB. Exercise and Nutrition to Target Protein Synthesis Impairments in Aging Skeletal Muscle. Exerc Sport Sci Rev. 2013 Oct;41(4):216–23.

26. Argilés JM, Busquets S, Stemmler B, López-Soriano FJ. Cancer cachexia: understanding the molecular basis. Nat Rev Cancer. 2014 Nov 9;14(11):754–62.

27. Fearon KCH, Glass DJ, Guttridge DC. Cancer Cachexia: Mediators, Signaling, and Metabolic Pathways. Cell Metab. 2012 Aug;16(2):153–66.

28. Berardi E, Madaro L, Lozanoska-Ochser B, Adamo S, Thorrez L, Bouche M, et al. A Pound of Flesh: What Cachexia Is and What It Is Not. Diagnostics. 2021 Jan 12;11(1):116.

29. Dewys WD, Begg C, Lavin PT, Band PR, Bennett JM, Bertino JR, et al. Prognostic effect of weight loss prior tochemotherapy in cancer patients. Am J Med. 1980 Oct;69(4):491–7.

30. Fearon K, Strasser F, Anker SD, Bosaeus I, Bruera E, Fainsinger RL, et al. Definition and classification of cancer cachexia: an international consensus. Lancet Oncol. 2011 May;12(5):489–95.

31. Martin L, Birdsell L, MacDonald N, Reiman T, Clandinin MT, McCargar LJ, et al. Cancer Cachexia in the Age of Obesity: Skeletal Muscle Depletion Is a Powerful Prognostic Factor, Independent of Body Mass Index. Journal of Clinical Oncology. 2013 Apr 20;31(12):1539–47.

32. Argilés JM, Busquets S, Stemmler B, López-Soriano FJ. Cancer cachexia: understanding the molecular basis. Nat Rev Cancer. 2014 Nov 9;14(11):754–62.

33. Webster JM, Kempen LJAP, Hardy RS, Langen RCJ. Inflammation and Skeletal Muscle Wasting During Cachexia. Front Physiol. 2020 Nov 19;11.

34. Setiawan T, Sari IN, Wijaya YT, Julianto NM, Muhammad JA, Lee H, et al. Cancer cachexia: molecular mechanisms and treatment strategies. J Hematol Oncol. 2023 May 22;16(1):54.

35. Petruzzelli M, Wagner EF. Mechanisms of metabolic dysfunction in cancer-associated cachexia. Genes Dev. 2016 Mar 1;30(5):489–501.

36. Fearon KCH, Glass DJ, Guttridge DC. Cancer Cachexia: Mediators, Signaling, and Metabolic Pathways. Cell Metab. 2012 Aug;16(2):153–66.

37. Baracos VE, Martin L, Korc M, Guttridge DC, Fearon KCH. Cancer-associated cachexia. Nat Rev Dis Primers. 2018 Jan 18;4(1):17105.

38. Tipton KD, Hamilton DL, Gallagher IJ. Assessing the Role of Muscle Protein Breakdown in Response to Nutrition and Exercise in Humans. Vol. 48, Sports Medicine. 2018.

39. Mitch WE, Goldberg AL. Mechanisms of Muscle Wasting — The Role of the Ubiquitin–Proteasome Pathway. Epstein FH, editor. New England Journal of Medicine. 1996 Dec 19;335(25):1897–905.

40. Lecker SH, Jagoe RT, Gilbert A, Gomes M, Baracos V, Bailey J, et al. Multiple types of skeletal muscle atrophy involve a common program of changes in gene expression. The FASEB Journal. 2004;18(1):39–51.

41. Sandri M. Protein breakdown in muscle wasting: Role of autophagy-lysosome and ubiquitin-proteasome. International Journal of Biochemistry and Cell Biology. 2013;45(10):2121–9.

42. Hinde KL, O'Leary TJ, Greeves JP, Wardle SL. Measuring Protein Turnover in the Field: Implications for Military Research. Adv Nutr. 2021 Jun 1;12(3):887–96.

43. Cegielski J, Wilkinson DJ, Brook MS, Boereboom C, Phillips BE, Gladman JFR, et al. Combined in vivo muscle mass, muscle protein synthesis and muscle protein breakdown measurement: a 'Combined Oral Stable Isotope Assessment of Muscle (COSIAM)' approach. Geroscience. 2021 Dec 27;43(6):2653–65.

44. Elia M, Carter A, Bacon S, Winearls CG, Smith R. Clinical usefulness of urinary 3-methylhistidine excretion in indicating muscle protein breakdown. Br Med J (Clin Res Ed). 1981 Jan 31;282(6261):351–4.

45. Kochlik B, Gerbracht C, Grune T, Weber D. The Influence of Dietary Habits and Meat Consumption on Plasma 3-Methylhistidine—A Potential Marker for Muscle Protein Turnover. Mol Nutr Food Res. 2018 May 19;62(9).

46. Young VR, Munro HN. Ntau-methylhistidine (3-methylhistidine) and muscle protein turnover: an overview. Fed Proc. 1978 Jul;37(9):2291–300.

47. Ciechanover A, Orian A, Schwartz AL. Ubiquitin-mediated proteolysis: biological regulation via destruction. BioEssays. 2000 Apr 24;22(5):442–51.

48. Yang Q, Zhao J, Chen D, Wang Y. E3 ubiquitin ligases: styles, structures and functions. Molecular Biomedicine. 2021 Dec 30;2(1):23.

49. Sandri M, Sandri C, Gilbert A, Skurk C, Calabria E, Picard A, et al. Foxo Transcription Factors Induce the Atrophy-Related Ubiquitin Ligase Atrogin-1 and Cause Skeletal Muscle Atrophy. Cell. 2004 Apr;117(3):399–412.

50. Glass DJ. Skeletal muscle hypertrophy and atrophy signaling pathways. Int J Biochem Cell Biol. 2005 Oct;37(10):1974–84.

51. Mizushima N, Komatsu M. Autophagy: Renovation of Cells and Tissues. Cell. 2011 Nov;147(4):728–41.

52. Mizushima N, Levine B. Autophagy in mammalian development and differentiation. Nat Cell Biol. 2010 Sep;12(9):823–30.

53. Masiero E, Agatea L, Mammucari C, Blaauw B, Loro E, Komatsu M, et al. Autophagy Is Required to Maintain Muscle Mass. Cell Metab. 2009;10(6):507–15.

54. Kocaturk NM, Gozuacik D. Crosstalk Between Mammalian Autophagy and the Ubiquitin-Proteasome System. Front Cell Dev Biol. 2018 Oct 2;6.

55. Milan G, Romanello V, Pescatore F, Armani A, Paik JH, Frasson L, et al. Regulation of autophagy and the ubiquitin–proteasome system by the FoxO transcriptional network during muscle atrophy. Nat Commun. 2015 Apr 10;6(1):6670.

56. Hershko A, Ciechanover A. THE UBIQUITIN SYSTEM. Annu Rev Biochem. 1998 Jun;67(1):425–79.

57. Koepp DM. Cell Cycle Regulation by Protein Degradation. In 2014. p. 61–73.

58. Henry KW, Wyce A, Lo WS, Duggan LJ, Emre NCT, Kao CF, et al. Transcriptional activation via sequential histone H2B ubiquitylation and deubiquitylation, mediated by SAGA-associated Ubp8. Genes Dev. 2003 Nov 1;17(21):2648–63.

59. Goldberg AL. Protein degradation and protection against misfolded or damaged proteins. Nature. 2003 Dec;426(6968):895–9.

60. Duan S, Pagano M. Ubiquitin ligases in cancer: Functions and clinical potentials. Cell Chem Biol. 2021 Jul;28(7):918–33.

61. Rubinsztein DC. The roles of intracellular protein-degradation pathways in neurodegeneration. Nature. 2006 Oct 18;443(7113):780–6.

62. Lecker SH. Ubiquitin-protein ligases in muscle wasting: multiple parallel pathways? Curr Opin Clin Nutr Metab Care. 2003 May;6(3):271–5.

63. Hershko A, Ciechanover A, Heller H, Haas AL, Rose IA. Proposed role of ATP in protein breakdown: conjugation of protein with multiple chains of the polypeptide of ATP-dependent proteolysis. Proceedings of the National Academy of Sciences. 1980 Apr;77(4):1783–6.

64. Hershko A, Heller H, Elias S, Ciechanover A. Components of ubiquitin-protein ligase system. Resolution, affinity purification, and role in protein breakdown. J Biol Chem. 1983 Jul 10;258(13):8206–14.

65. Joazeiro CAP, Weissman AM. RING Finger Proteins. Cell. 2000 Sep;102(5):549–52.

66. Pickart CM, Eddins MJ. Ubiquitin: structures, functions, mechanisms. Biochimica et Biophysica Acta (BBA) - Molecular Cell Research. 2004 Nov;1695(1–3):55–72.

67. Ikeda F, Dikic I. Atypical ubiquitin chains: New molecular signals. “Protein Modifications: Beyond the Usual Suspects” Review Series. Vol. 9, EMBO Reports. 2008. p. 536–42.

68. Komander D, Rape M. The Ubiquitin Code. Annu Rev Biochem. 2012 Jul 7;81(1):203–29.

69. Kulathu Y, Komander D. Atypical ubiquitylation — the unexplored world of polyubiquitin beyond Lys48 and Lys63 linkages. Nat Rev Mol Cell Biol. 2012 Aug 23;13(8):508–23.

70. Heride C, Urbé S, Clague MJ. Ubiquitin code assembly and disassembly. Current Biology. 2014 Mar;24(6):R215–20.

71. McDowell GS, Philpott A. Non-canonical ubiquitylation: Mechanisms and consequences. Int J Biochem Cell Biol. 2013 Aug;45(8):1833–42.

72. Li X, Han M, Zhang H, Liu F, Pan Y, Zhu J, et al. Structures and biological functions of zinc finger proteins and their roles in hepatocellular carcinoma. Biomark Res. 2022 Dec 9;10(1):2.

73. Husnjak K, Dikic I. Ubiquitin-Binding Proteins: Decoders of Ubiquitin-Mediated Cellular Functions. Annu Rev Biochem. 2012 Jul 7;81(1):291–322.

74. Ciechanover A. The ubiquitin-proteasome proteolytic pathway. Cell. 1994 Oct;79(1):13–21.

75. Smith DM, Chang SC, Park S, Finley D, Cheng Y, Goldberg AL. Docking of the Proteasomal ATPases' Carboxyl Termini in the 20S Proteasome's α Ring Opens the Gate for Substrate Entry. Mol Cell. 2007 Sep;27(5):731–44.

76. Finley D. Recognition and Processing of Ubiquitin-Protein Conjugates by the Proteasome. Annu Rev Biochem. 2009 Jun 1;78(1):477–513.

77. Groll M, Ditzel L, Löwe J, Stock D, Bochtler M, Bartunik HD, et al. Structure of 20S proteasome from yeast at 2.4Å resolution. Nature. 1997 Apr;386(6624):463–71.

78. Haas AL, Rose IA. The mechanism of ubiquitin activating enzyme. A kinetic and equilibrium analysis. J Biol Chem. 1982 Sep 10;257(17):10329–37.

79. Schulman BA, Wade Harper J. Ubiquitin-like protein activation by E1 enzymes: the apex for downstream signalling pathways. Nat Rev Mol Cell Biol. 2009 May 8;10(5):319–31.

80. Henneberg LT, Schulman BA. Decoding the messaging of the ubiquitin system using chemical and protein probes. Cell Chem Biol. 2021 Jul;28(7):889–902.

81. Nandi D, Tahiliani P, Kumar A, Chandu D. The ubiquitin-proteasome system. J Biosci. 2006 Mar 1;31(1):137–55.

82. Michelle C, Vourc'h P, Mignon L, Andres CR. What Was the Set of Ubiquitin and Ubiquitin-Like Conjugating Enzymes in the Eukaryote Common Ancestor? J Mol Evol. 2009 Jun 19;68(6):616–28.

83. Deshaies RJ, Joazeiro CAP. RING Domain E3 Ubiquitin Ligases. Annu Rev Biochem. 2009 Jun 1;78(1):399–434.

84. Rotin D, Kumar S. Physiological functions of the HECT family of ubiquitin ligases. Nat Rev Mol Cell Biol. 2009 Jun 13;10(6):398–409.

85. Freemont PS. Ubiquitination: RING for destruction? Current Biology. 2000;10(2):84–7.

86. Lorick KL, Jensen JP, Fang S, Ong AM, Hatakeyama S, Weissman AM. RING fingers mediate ubiquitin-conjugating enzyme (E2)-dependent ubiquitination. Proceedings of the National Academy of Sciences. 1999 Sep 28;96(20):11364–9.

87. Aravind L, Koonin E V. The U box is a modified RING finger — a common domain in ubiquitination. Current Biology. 2000 Feb;10(4):R132–4.

88. Breckel CA, Hochstrasser M. Ubiquitin Ligase Redundancy and Nuclear-Cytoplasmic Localization in Yeast Protein Quality Control. Biomolecules. 2021 Dec 3;11(12):1821.

89. Wenzel DM, Lissounov A, Brzovic PS, Klevit RE. UBCH7 reactivity profile reveals parkin and HHARI to be RING/HECT hybrids. Nature. 2011 Jun 1;474(7349):105–8.

90. Cornelissen T, Vilain S, Vints K, Gounko N, Verstreken P, Vandenberghe W. Deficiency of parkin and PINK1 impairs age-dependent mitophagy in Drosophila. Elife. 2018 May 29;7.

91. Centner T, Yano J, Kimura E, McElhinny AS, Pelin K, Witt CC, et al. Identification of muscle specific ring finger proteins as potential regulators of the titin kinase domain. J Mol Biol. 2001;306(4):717–26.

92. Centner T, Yano J, Kimura E, McElhinny AS, Pelin K, Witt CC, et al. Identification of muscle specific ring finger proteins as potential regulators of the titin kinase domain. J Mol Biol. 2001;306(4):717–26.

93. Bodine SC, Latres E, Baumhueter S, Lai VKM, Nunez L, Clarke BA, et al. Identification of ubiquitin ligases required for skeletal Muscle Atrophy. Science (1979). 2001;294(5547):1704–8.

94. McElhinny AS, Kakinuma K, Sorimachi H, Labeit S, Gregorio CC. Muscle-specific RING finger-1 interacts with titin to regulate sarcomeric M-line and thick filament structure and may have nuclear functions via its interaction with glucocorticoid modulatory element binding protein-1. Journal of Cell Biology. 2002;157(1):125–36.

95. Clarke BA, Drujan D, Willis MS, Murphy LO, Corpina RA, Burova E, et al. The E3 Ligase MuRF1 Degrades Myosin Heavy Chain Protein in Dexamethasone-Treated Skeletal Muscle. Cell Metab. 2007;6(5):376–85.

96. Bodine SC, Latres E, Baumhueter S, Lai VKM, Nunez L, Clarke BA, et al. Identification of ubiquitin ligases required for skeletal Muscle Atrophy. Science (1979). 2001;294(5547):1704–8.

97. Labeit S, Kohl CH, Witt CC, Labeit D, Jung J, Granzier H. Modulation of muscle atrophy, fatigue and MLC phosphorylation by MuRF1 as indicated by hindlimb suspension studies on MuRF1-KO mice. J Biomed Biotechnol. 2010;

98. Baehr LM, Furlow JD, Bodine SC. Muscle sparing in muscle RING finger 1 null mice: Response to synthetic glucocorticoids. Journal of Physiology. 2011;589(19):4759–76.

99. Hwee DT, Baehr LM, Philp A, Baar K, Bodine SC. Maintenance of muscle mass and load-induced growth in Muscle RING Finger 1 null mice with age. Aging Cell. 2014;13(1):92–101.

100. Cohen S, Brault JJ, Gygi SP, Glass DJ, Valenzuela DM, Gartner C, et al. During muscle atrophy, thick, but not thin, filament components are degraded by MuRF1-dependent ubiquitylation. Journal of Cell Biology. 2009;185(6):1083–95.

101. Hirner S, Krohne C, Schuster A, Hoffmann S, Witt S, Erber R, et al. MuRF1-dependent Regulation of Systemic Carbohydrate Metabolism as Revealed from Transgenic Mouse Studies. J Mol Biol. 2008 Jun;379(4):666–77.

102. Willis MS, Schisler JC, Li L, Rodríguez JE, Hilliard EG, Charles PC, et al. Cardiac Muscle Ring Finger-1 Increases Susceptibility to Heart Failure In Vivo. Circ Res. 2009 Jul 2;105(1):80–8.

103. Chen SN, Czernuszewicz G, Tan Y, Lombardi R, Jin J, Willerson JT, et al. Human molecular genetic and functional studies identify TRIM63, encoding muscle RING finger protein 1, as a novel gene for human hypertrophic cardiomyopathy. Circ Res. 2012;111(7):907–19.

104. Jokela M, Baumann P, Huovinen S, Penttilä S, Udd B. Homozygous Nonsense Mutation p.Q274X in TRIM63 (MuRF1) in a Patient with Mild Skeletal Myopathy and Cardiac Hypertrophy. J Neuromuscul Dis. 2019 Jan 30;6(1):143–6.

105. Salazar-Mendiguchía J, Ochoa JP, Palomino-Doza J, Domínguez F, Díez-López C, Akhtar M, et al. Mutations in TRIM63 cause an autosomal-recessive form of hypertrophic cardiomyopathy. Heart. 2020 Sep;106(17):1342–8.

106. Bodine SC, Baehr LM. Skeletal muscle atrophy and the E3 ubiquitin ligases MuRF1 and MAFbx/atrogin-1. Am J Physiol Endocrinol Metab. 2014;307(6):E469–84.

107. Stewart MD, Ritterhoff T, Klevit RE, Brzovic PS. E2 enzymes: More than just middle men. Cell Res. 2016;26(4):423–40.

108. Polge C, Cabantous S, Deval C, Claustre A, Hauvette A, Bouchenot C, et al. A muscle-specific MuRF1-E2 network requires stabilization of MuRF1-E2 complexes by telethonin, a newly identified substrate. J Cachexia Sarcopenia Muscle. 2018;9(1):129–45.

109. Jackman RW, Kandarian SC. The molecular basis of skeletal muscle atrophy. American Journal of Physiology-Cell Physiology. 2004 Oct;287(4):C834–43.

110. Mrosek M, Labeit D, Witt S, Heerklotz H, von Castelmur E, Labeit S, et al. Molecular determinants for the recruitment of the ubiquitin-ligase MuRF-1 onto M-line titin. The FASEB Journal. 2007;21(7):1383–92.

111. Mrosek M, Meier S, Ucurum-Fotiadis Z, Von Castelmur E, Hedbom E, Lustig A, et al. Structural analysis of B-box 2 from MuRF1: Identification of a novel self-association pattern in a RING-like fold. Biochemistry. 2008;47(40):10722–30.

112. Higashikuse Y, Mittal N, Arimura T, Yoon SH, Oda M, Enomoto H, et al. Perturbation of the titin/MURF1 signaling complex is associated with hypertrophic cardiomyopathy in a fish model and in human patients. DMM Disease Models and Mechanisms. 2019;12(11).

113. Bowen TS, Adams V, Werner S, Fischer T, Vinke P, Brogger MN, et al. Small-molecule inhibition of MuRF1 attenuates skeletal muscle atrophy and dysfunction in cardiac cachexia. J Cachexia Sarcopenia Muscle. 2017 Dec;8(6):939–53.

114. Bogomolovas J, Fleming JR, Franke B, Manso B, Simon B, Gasch A, et al. Titin kinase ubiquitination aligns autophagy receptors with mechanical signals in the sarcomere. EMBO Rep. 2021;22(10):1–14.

115. Scalabrin M, Adams V, Labeit S, Bowen TS. Emerging strategies targeting catabolic muscle stress relief. Int J Mol Sci. 2020;21(13):1–18.

Chapter 2

Methods

2.1 Western Blotting

Cell lysates were prepared in 1xNuPAGE LDS sample buffer (Invitrogen; NP0008) containing 2-mercaptoethanol (final concentration 1.25%) and allowed to denature overnight at room temperature. The prepared cell lysates were loaded onto 8% or 10% Bis/Tris gels for subsequent sodium dodecyl sulphate-polyacrylamide gel electrophoresis (SDS-PAGE). Gels were run in 1x MOPS buffer for 10 minutes at 100 V and then approximately 60 minutes at 140 V. Proteins were transferred onto 0.2-μm polyvinylidene fluoride (PVDF) membranes (Millipore, Watford, UK) for 1 hour at 100 V. Following the transfer, membranes were blocked in 5% milk diluted in Tris-buffered saline-Tween 20 (TBS-T): 137 mM sodium chloride, 20 mM Tris-base pH 7.5, 0.1% Tween 20 for 1 hour. After blocking, membranes underwent three 10-minute washes in TBS-T before overnight incubation at 4°C with the appropriate primary antibodies. Membranes were washed three times for 10 minutes in TBS-T before incubation in horseradish peroxidase-conjugated secondary antibodies at room temperature for 1 hour. Subsequently, membranes were washed another three times in TBS-T before antibody detection using an enhanced chemiluminescence horseradish peroxidase substrate detection kit (Millipore, Watford, UK). Imaging was performed with a G:BOX Chemi-XR5 (Syngene, Cambridge, UK).

Name	Catalogue Number	Manufacturer	Dilution
Anti-MBP	E8038S	New England Biolabs	1:60,000
6xHis	631212	Clontech	1:10,000
Anti-MYLPF	MF-5	Developmental Studies Hybridoma Bank	1:1000
Desmin	5332	Cell Signalling Technology	1:1000
Anti-ubiquitylated proteins FK2	04-263	Merck-Millipore	1:1000
Anti-ubiquitin P4D1	646302	Biolegend	1:1000
Anti-K48-Specific Ubiquitin	05-1307	Merck-Millipore	1:1000
Anti-Ubiquitin K63-Specific	05-1313	Merck-Millipore	1:1000

Table 2.1. Antibodies used for Western Blotting

2.2 Mutagenesis

Mutagenesis was conducted following the protocol outlined by Liu and Naismith, 2008 (1). Primers were meticulously designed with a 5' overlapping sequence encompassing the targeted nucleotides for mutation and a non-overlapping 3' sequence (see table 2.2). These primers were employed in a 50 µL end-point PCR reaction utilizing Q5 High-Fidelity DNA Polymerase (New England Biolabs, USA) according to the manufacturer's instructions. After PCR amplification, 0.5 µL of DPN1 was added directly to the reaction mixture to remove parent (non-mutant) plasmids; incubated at 37 °C for 2 hours and a subsequent step at 80 °C for 20 minutes.

DH5a competent cells were thawed, and 2 µL of the PCR product was added per 50 µL of cells. After a 30-minute incubation on ice, the cells underwent heat shock at 42°C for 45 seconds, followed by an additional 5-minute incubation on ice. The transformed bacteria were then plated on LB agar plates treated with the necessary antibiotic and incubated overnight at 37°C to facilitate colony formation. As a control, a second plate was streaked with un-transformed DH5a, expected to exhibit no colony growth.

Single colonies were transferred to 4 mL of antibiotic-treated LB media and incubated overnight at 37°C with agitation at 180 RPM to propagate E. coli containing the target plasmid. The subsequent morning, the culture was harvested, and DNA was extracted using a Spin Miniprep Kit (Qiagen). The extracted DNA was either stored at -20°C or sent for sequencing.

Name	Sequence
Titin A168-A170 102KTLE105-AAAA FWD	AACTCTTGCAGGCATGGGAGCAGTTCATGCTCTCCG
Titin A168-A170 102KTLE105-AAAA REV	CATGCCTGCAAGAGTTTTAGGTAAGTGTATCTTAGCTGGAACTTCC
Titin A168-A170 K316R FWD	ATAACCAGAGAAGATAAGACCAGAGCTATGAACTATGATG
Titin A168-A170 K316R REV	TATCTTCTCTGGTTATGGTTGGTTCTGAAGGCTCTGAA

Table 2.2. Primers used for Mutagenesis

2.3 Protein Expression

Plasmids (MBP-MuRF1, HIS-UBE1, HIS-UBE2s obtained from MRC PPU Reagents and Services; HIS-Titin A168-A170 obtained from Olga Mayans) underwent transformation into competent BL21 E. Coli and were incubated overnight at 37°C. A single colony of each plasmid was chosen and inoculated in LB media at 37°C, expanding to a 2000 mL culture. Bacteria were grown to an OD 600 of 0.6, measured using a FluoStar Omega microplate reader (BMG Labtech, Aylesbury, UK). Protein expression was induced by the addition of 250 µM IPTG and the cultures were left to express overnight at 18°C. The cultures were centrifuged, and the resulting pellets were resuspended in lysis buffer. For HIS-tagged proteins, the buffer comprised 50 mM Tris-HCL pH 8.0, 150 mM NaCl, 50 mM Imidazole, 0.5 mM TCEP, and 1 mM PMSF. On the other hand, MBP-MuRF1 utilized a buffer of 50 mM Tris-HCL pH 7.5, 150 mM NaCl, 5% Glycerol, 1 mM TCEP, and 1 mM PMSF. The cell lysis was accomplished using an Emulsiflex C3 Cell Disruptor (Avestin Europe, Mannheim, Germany).

Purification of the recombinant proteins was carried out following the manufacturer's instructions, utilizing either HIS-trap (GE Healthcare) or Amylose resin (New England Biosciences). The protein concentrations were determined by nanodrop, and the final products were stored at -80°C.

2.4 Co-Precipitation Assay of MBP- and HIS-Tagged Proteins

10 µl of prewashed Ni-NTA Agarose (Qiagen) or Amylose (New England Biolabs) bead slurry, previously washed twice with 500 µl ice-cold dilution buffer (20 mM HEPES pH 7.4; 0.5 mM TCEP), was utilized. Subsequently, 6 µg of recombinant proteins were pipetted onto the beads and left on a tube rotator at 4°C for 2 hours. Following this incubation, beads were pelleted for 1 minute at 4°C at 3500 rpm, and the supernatant was carefully removed. The beads underwent washing with a buffer containing 150 mM NaCl and 0.5% Triton to eliminate non-specifically bound proteins, a process repeated three times. The beads were then resuspended in 400 µl of dilution buffer and transferred to a spin column and collection tube.

To the beads, 50 µL of 1x LDS was added before incubating and shaking at 1400 RPM at 37°C. Columns were centrifuged for 1 minute at 13000 RPM (4°C) before removing the filter column and adding 2-mercaptoethanol up to 1.25%.

2.5 Mass Spectrometry

Nano-liquid chromatography (nanoLC) was conducted using the Ultimate 3000 RSCLnano system (Dionex) at 40 °C, employing an Acclaim PepMap 300 µm i.d. x 5 mm, 5 µm, 100 Å µ-precolumn cartridge and an Acclaim PepMap RSLC 75 µm i.d. x 50 cm, 2 µm, 100 Å analytical column (Thermo Scientific). Peptides underwent separation through a gradient with Mobile Phase A (100% H2O, 0.1% Formic Acid) and Mobile Phase B (100% Acetonitrile, 0.1% Formic Acid). Elution was performed using a gradient ranging from 4% to 6% B to 25% to 35% B over 32 minutes, followed by a 90% B wash (3 min) and re-equilibration at 4% B (5 mins). The column flow rate was set to 250 nL/min, and the column temperature was maintained at 40 °C.

Peptides eluted from the nanoLC system underwent electrospray ionization for gas-phase conversion before analysis using a Thermo Orbitrap Fusion mass spectrometer (ThermoFisher Scientific). Instrument parameters were configured as follows: Ion Transfer Tube temperature: 275 °C; RF lens: 60%; MS1 Orbitrap mass analyser resolution: 120,000; Automatic Gain Control (AGC): 200,000; Maximum Injection Time: 150 ms; Scan Range: 375-1575 m/z. For MS/MS analysis, Precursor Ion Quadrupole Isolation was set to 1.2 m/z and subjected to Higher Energy Collision Dissociation (HCD) with normalized HCD energy set to 33%. Dynamic Exclusion was implemented for 25 s, and MS/MS spectra were acquired in the Ion Trap mass analyser with the following parameters: Scan Rate: Rapid, Monoisotopic Precursor Ion Selection (MIPS): Peptide, AGC: 5000, Maximum Injection Time: 200 ms.

Xcalibur 4.1.31.9 was used for manual validation of all RAW files, and subsequent analysis was conducted utilizing MaxQuant 1.5.5.1 with the Andromeda search engine. Searches were executed against the Homo sapiens FASTA File (Taxonomy: 9606, generated September 2019), with the following parameters: Digestion enzyme: Trypsin; Modifications: Oxidation (M), Acetyl (Protein N-Terminus), Phosphorylation (STY), Carbamidomethyl (C); Quantification: LFQ; PSM FDR: 1%; Protein FDR: 1%. All other MaxQuant parameters were maintained at default settings.

2.6 References

[1] Liu, H., Naismith, J.H. An efficient one-step site-directed deletion, insertion, single and multiple-site plasmid mutagenesis protocol. *BMC Biotechnol* **8**, 91 (2008). https://doi.org/10.1186/1472-6750-8-91.

Chapter 3 Uncovering the Mechanisms of MuRF1 Ubiquitylation

Title: Uncovering the mechanisms of MuRF1-induced ubiquitylation and revealing similarities with MuRF2 and MuRF3

Journal submission: Biochemical and Biophysical Research Communications, March 2024.

Authorship: Samuel O. Lord [a,*], Peter W.J. Dawson [a,b,*], Jitpisute Chunthorng-Orn [a], Leslie Baehr [c], David Hughes [c], Pooja Sridhar [d], Timothy Knowles [d], Sue Bodine [c] and Yu-Chiang Lai [a,b]

*Samuel O. Lord and Peter W.J. Dawson contributed equally to this work

Affiliations:

[a] School of Sport, Exercise and Rehabilitation Sciences, University of Birmingham, Birmingham, UK

[b] MRC Versus Arthritis Centre for Musculoskeletal Ageing Research, University of Birmingham, Birmingham, UK.

[c] Department of Internal Medicine, Division of Endocrinology and Metabolism, Carver College of Medicine, University of Iowa, Iowa City, USA

[d] School of Biosciences, University of Birmingham, Birmingham, UK

Corresponding Author:

Dr Yu-Chiang Lai [a,b]

3.1 Abstract

MuRF1 (Muscle-specific RING finger protein 1; gene name TRIM63) is a ubiquitin E3 ligase, associated with the progression of muscle atrophy. As a RING (Really Interesting New Gene) type E3 ligase, its unique activity of ubiquitylation is driven by a specific interaction with a UBE2 (ubiquitin conjugating enzyme). Our understanding of MuRF1 function remains unclear as candidate UBE2s have not been fully elucidated. In the present study, we screened human ubiquitin dependent UBE2s *in-vitro* and found that MuRF1 engages in ubiquitylation with UBE2D, UBE2E, UBE2N/V families and UBE2W. MuRF1 can cause mono-ubiquitylation, K48- and K63-linked polyubiquitin chains in a UBE2 dependent manner. Moreover, we identified a two-step UBE2 dependent mechanism by which UBE2W allows MuRF1 to monoubiquitylate which then acts as an anchor for UBE2N/V to generate polyubiquitin chains. With the *in-vitro* UBE2 ubiquitylation assay, we also found that MuRF2 and MuRF3 not only share the same UBE2 partners as MuRF1 but can also directly ubiquitylate the same substrates: Titin (A168-A170), Desmin, and MYLPF (Myosin Light Chain, Phosphorylatable, Fast Skeletal Muscle; also called Myosin Light Regulatory Chain 2). In summary, our work presents new insights into the mechanisms that underpin MuRF1 activity and reveals overlap in MuRF-induced ubiquitylation which could explain their partial redundancy *in-vivo*.

Key words: RING E3 Ligase, Ubiquitin Conjugating Enzyme (UBE2), Ubiquitin, autoubiquitylation, *In-vitro*, Muscle Atrophy

Abbreviations: ELISA, enzyme-linked immunosorbent assay; HIS, Histidine; IPTG, Isopropyl β- d-1-thiogalactopyranoside; LB, Lysogeny Broth; MBP, Maltose Binding Protein; MuRF1, Muscle-specific RING finger protein 1; MuRF2, Muscle-specific RING finger protein 2; MuRF3, Muscle-specific RING finger protein 3; MYLPF, Myosin Light Chain Phosphorylatable Fast Skeletal Muscle Protein; RING, Really Interesting New Gene; SUMO, Small Ubiquitin-like Modifier; SPR, Surface Plasmon Resonance; TBS-T, Tris-buffered saline Tween-20; TRIM, Tripartite Motif-Containing; UBE1, E1 ubiquitin activating enzyme; UBE2, E2 ubiquitin-conjugating enzyme; VCP, Valosin-containing protein.

Funding: S.L. was supported by the Biotechnology and Biological Sciences Research Council (BBSRC) and University of Birmingham-funded Midlands Integrative Biosciences Training Partnership (MIBTP) (BB/T00746X/1). P.D. was supported by MRC Versus Arthritis Centre for Musculoskeletal Aging Research (MR/ P021220/1). J.C-O. was supported by Ministry of Higher Education, Science, Research and Innovation, Thailand and Department of Applied Thai Traditional Medicine, Faculty of Medicine, Thammasat University, Thailand. Y-C.L. was supported by MRC Versus Arthritis Centre for Musculoskeletal Aging Research (MR/ P021220/1).

3.2 Introduction

MuRF1, a muscle-specific RING finger protein, plays a critical role in skeletal muscle atrophy. Many studies in humans and rodents, demonstrate that MuRF1 gene (TRIM63) and protein expression increase following numerous atrophy models including disuse, denervation, cancer, renal failure, heart failure, burn injury, fasting, diabetes, corticosteroid treatment and cytokine exposure [1]–[7]. Importantly, suppression of MuRF1 expression perturbs atrophy induced by denervation, glucocorticoid treatment, limb unloading, and lung injury [2], [8]–[10]. These earlier studies have established MuRF1 as a key regulator of skeletal muscle mass. Nonetheless, insight into the molecular mechanisms of MuRF1-induced muscle atrophy is unclear, slowing the development of therapeutics that target MuRF1-induced muscle atrophy.

MuRF1 is an E3 ligase, which functions to target proteins for ubiquitylation. The process of protein ubiquitylation is a coordinated sequence of three enzymatic actions: by an E1 ubiquitin-activating enzyme (UBE1), an E2 ubiquitin-conjugating enzyme (UBE2), and finally an E3 ubiquitin-ligase. The UBE1 enzyme hydrolyses ATP to adenylate ubiquitin, which is transferred to an UBE2 active site. As MuRF1 is a RING-type (Really Interesting New Gene) E3 ligase, with no catalytic activity, it requires the interaction of a UBE2 to directly transfer ubiquitin to the substrate(s) [11]. UBE2s are responsible for the type of ubiquitylation (mono-, multi-mono-, or poly-ubiquitylation) and the structure of ubiquitin chains based on ubiquitin-ubiquitin

attachment residue [12], [13]. There are eight different polyubiquitin chain types (M1, K6, K11, K27, K29, K33, K48 and K63) and the topology of ubiquitin chain types ultimately determine the fate of the target protein, such as degradation, localisation, or other signalling events [14]. Therefore, to understand the functional role of MuRF1 ubiquitylation onto its substrate, one must identify the UBE2 that partners with MuRF1. Identifying MuRF1 partnering UBE2s would also provide a tool to directly explore substrates of MuRF1 *in-vitro* and characterise their specific form of ubiquitylation.

Previous studies have attempted to identify UBE2s that interact with MuRF1. Polge et al [15] applied yeast two-hybrid screen and SPR (surface plasmon resonance) technologies and identified several UBE2s, including UBE2E1, UBE2G1, UBE2J1, UBE2J2, and UBE2L3, as interacting with MuRF1. However, these two methods only measure protein-protein interaction without detecting ubiquitin E3 ligase activity of MuRF1. When MuRF1-UBE2 ubiquitylation activity has been studied using ELISA based methods, only 11 UBE2s have been explored [16]. Due to limited characterisation of MuRF1-UBE2 partners, studies have often used UBE2D (UBCH5) family when investigating MuRF1 substrates [17]–[20]. While this offers some insights into MuRF1-UBE2D ubiquitylation activity, it is worth noting that the UBE2D family may be promiscuous and can interact and produce ubiquitylation activity with most RING type E3 ligases [13]. Therefore, the current literature offers limited understanding of MuRF1-UBE2 partners and how they relate to MuRF1 ubiquitylation

function. A study of all human UBE2s with MuRF1 is necessary to further understand the mechanism of MuRF1-mediated ubiquitylation.

MuRF1 shares high homology with two other TRIM family members, MuRF2 (TRIM55) and MuRF3 (TRIM54). Sequence alignment shows MuRF1 displays 62% and 77% overlap with MuRF2 and MuRF3 respectively [21]. Given their similar sequence it is possible that they share overlapping roles, a concept supported by genetic mouse models which highlight the redundancy of MuRF E3 ligases. For example, removal of MuRF1 has no detrimental effect on mice phenotype [2], [20], [22]. However, when MuRF2 or MuRF3 are also removed this causes severe detrimental effects on skeletal and cardiac muscle size and function. Double knockout (dKO) of MuRF1 and MuRF2 causes hypertrophic cardiomyopathy that resulted in the death of ~75% of mice in their first few weeks [23], [24]. MuRF1 and MuRF3 dKO mice experience skeletal muscle myopathy and hypertrophic cardiomyopathy [20]. Similar features were observed in human patients with mutations in MuRF1 (homozygous) and MuRF3 (heterozygous) [25]. These findings suggest that the loss of MuRF1 can be somewhat compensated by the presence of MuRF2 or MuRF3. Given the lack of molecular understanding surrounding MuRF-induced ubiquitylation, there is no comprehensive explanation for this response. Therefore, a study directly comparing MuRF1, MuRF2 and MuRF3 ubiquitylation is needed.

In the present study a full human UBE2 library (excluding ubiquitin-like UBE2s; see table S1) were screened using a standard *in-vitro* ubiquitylation assay. This revealed

that UBE2D, UBE2E, UBE2N/V families and UBE2W partner with MuRF1 during ubiquitylation. We found that MuRF1 partners with UBE2W and UBE2N/V in a sequential two-step fashion, forming K63-linked ubiquitin chains. Moreover, we showed that MuRF2 and MuRF3 also function with these UBE2s during ubiquitylation and can target the same set of substrates as MuRF1 (Titin, Desmin and MYLPF), providing a molecular explanation for their functional redundancy *in-vivo*.

3.3 Methods

Constructs

Ubiquitin, HIS-UBE1 and the full library of human E2s were sourced from the Medical Research Council - Protein, Phosphorylation and Ubiquitylation Unit (MRC PPU) Reagents and Services (https://mrcppureagents.dundee.ac.uk/). Plasmids for HIS-Titin were provided by Prof. Olga Mayans (University of Konstanz). Titin was cloned into a pMEX3Cb vector to express His-Titin. Recombinant Desmin (A60041) and His-SUMO-MYLPF (A225264) were bought from antibodies.com.

Expression and Purification of Proteins

Plasmids were transformed into BL21 competent Escherichia Coli (E. Coli) cells. A single colony was selected and inoculated in Ampicillin-treated LB media expanding to 1 Litre (For MBP-MuRF1, MBP-MuRF2 and MBP-MuRF3 expression 200 μM $ZnSO_4$ was also added prior to IPTG induction) at 37°C 180 rpm. Bacteria were grown to OD 600 of 0.6 before the addition of 250 μM IPTG to induce protein expression. Growth was inhibited by reducing the temperature down to 18°C left overnight to continue protein expression. The cells were pelleted by centrifugation at 5000 xg at 4°C for 15 minutes. Pellets were resuspended in lysis buffer (HIS tag: 50 mM Tris-HCl pH 8.0, 150 mM NaCl, 50 mM Imidazole, 0.5 mM TCEP, 1 mM PMSF. MBP tag: 50 mM Tris-HCl pH 7.5, 150 mM NaCl, 5% Glycerol, 1 mM TCEP, 1 mM PMSF) and lysed using an Emulsiflex C3 Cell Disruptor (Avestin Europe, Mannheim, Germany). Lysate was cleared at 5000 xg 4°C for 2 hours and filtered using a 0.45 μm filter to remove any remaining cell debris. Recombinant proteins were purified

using His-Trap (GE Healthcare) or Amylose resin (New England Biosciences) as per manufacturer's protocol. Briefly, protein bound to beads overnight 4°C and flow-through was collected. Protein purity was confirmed using a Coomassie blue stain and protein concentration was determined using a nanodrop. Protein samples were concentrated using 50K centrifugal filters (Amicon, Merck) and stored at -80 °C. The removal of the HIS-tag was achieved by incubating with TEV protease overnight at room temperature in a buffer containing 25 mM Tris (pH 8), 50 mM NaCl, and 5 mM DTT.

In-vitro ubiquitylation assay

In-vitro reaction (50 µl) contained 50 mM HEPES pH 7.5, 1 mM DTT, 10 mM MgCl2, 1 mM ATP, 50 µg ubiquitin, 0.2 µg HIS-UBE1, 0.6 µg UBE2 and 2.5 µg MBP-MuRF1, MBP-MuRF2 or MBP-MuRF3. For experiments involving substrates (His-Titin fragment (A168-A170), Desmin or His-SUMO-MYLPF), 0.5 µg of substrate was included alongside 0.5 µg of MBP-MuRF1, MBP-MuRF2 or MBP-MuRF3. Reactions were performed at 37°C for 1 hour at 1000 rpm on the Thermoshaker (Eppendorf) and terminated with the addition of 4x LDS sample buffer (Thermo Scientific) containing 5% β-mercaptoethanol to final concentration 1x and 1.25% respectively. Samples were left overnight at room temperature to denature.

Western blotting

Samples were loaded on 4-12% Bis-Tris gels and separated using SDS-PAGE gel electrophoresis. Gels were run in 1x MOPS buffer for approximately 90 minutes at 140V. Proteins were transferred onto PVDF membranes (Millipore, Hertfordshire, UK) for 2.5h at 30V based on an optimised protocol for detecting polyubiquitin chains [26]. Membranes were blocked in 5% BSA diluted in Tris-buffered saline Tween-20 (TBS-T) and incubated overnight at 4°C with the appropriate primary antibody: Anti-MBP (E8038S, 1:60,000) from New England Biolabs, 6xHis (631212, 1:10,000) from Clontech, Anti-MYLPF (MF-5, 1:1000) from Developmental Studies Hybridoma Bank, Desmin (5332, 1:1000) from Cell Signalling Technology, Anti-ubiquitylated proteins FK2 (04-263, 1:1000), Anti-ubiquitin P4D1 (646302, 1:1000), Anti-K48-Specific Ubiquitin (05-1307, 1:1000) and Anti-Ubiquitin K63-Specific (05-1313, 1:1000) from

Merck-Millipore. Membranes were washed in TBS-T three times prior to 1h incubation at room temperature in horseradish peroxidase-conjugated secondary antibodies from Cell Signalling Technology (1:10,000). Membranes were washed a further three times in TBS-T prior to antibody detection using enhanced chemiluminescence horseradish peroxidase substrate detection kit (Millipore, Hertfordshire, UK). Imaging was undertaken using a G:BOX Chemi-XR5 (Syngene, Cambridgeshire, UK).

RNA Isolation and qPCR

RNA was isolated from frozen gastrocnemius muscle powder using RNAzol RT reagent (Sigma-Aldrich, St Louis, MO) in accordance with the manufacturer's instructions. cDNA was synthesised using the iScript Reverse Transcription Supermix kit (BioRad, Hercules, CA) from 1 µg of total RNA. PCR reactions (10 µL) were set up as: 2 µL of cDNA, 0.5 µL (10 µM stock) forward and reverse primers, 5 µL of Power SYBR Green master mix (Thermo Fisher Scientific) and 2 µL of RNA/DNA free water. Gene expression analysis was then performed by quantitative PCR on a Quantstudio 6 Flex Real-time PCR System (Applied Biosystems, Foster City, CA). PCR cycling: hold at 50 °C for 5 min, 10 min hold at 95 °C, before 40 PCR cycles of 95 °C for 15 s followed by 59 °C for 30 s and 72 °C for 30 s. Melt curve analysis at the end of the PCR cycling protocol yielded a single peak. As a result of reference gene instability, gene expression was normalised to tissue weight and subsequently reported as the fold change relative to control muscles, as described previously [27], [28]. The mouse primers used in this study are shown in Table S2.

Statistical Analysis

Data presented as ± SEM. The statistical analyses were performed using Prism (GraphPad Software). One-way ANOVA was performed with Tukey's post hoc test and p values < 0.05 were considered statistically significant.

3.4 Results

MuRF1 interacts with UBE2D, E, N/V families, and UBE2W to induce ubiquitylation.

To investigate which UBE2s interact with MuRF1, a full screen of 28 recombinant human UBE2s was undertaken to determine which catalyse MuRF1-dependent ubiquitylation *in-vitro*. The results showed that MBP-MuRF1 interacts with UBE2D family (D1, D2, D3 and D4), UBE2E family (E1, E2, and E3), UBE2N/V1 and UBE2N/V2 by forming polyubiquitin chains (Fig 3.1). We found that UBE2W monoubiquitylates MuRF1, illustrated by the single band ~90 kilodaltons (Fig 3.1). This demonstrates MuRF1 produces distinct ubiquitylation in a UBE2 dependent manner.

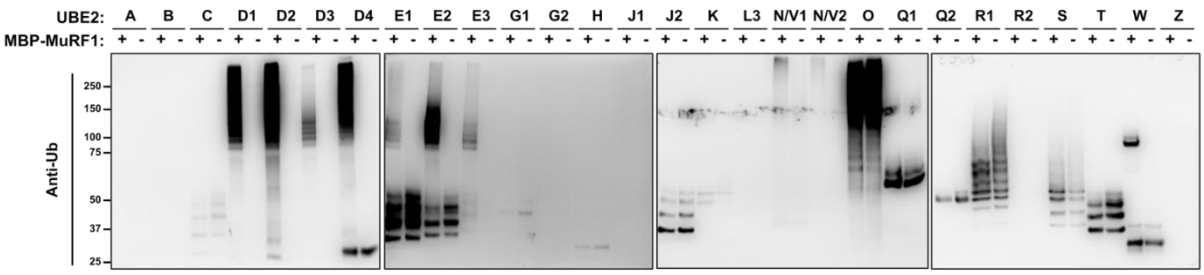

Figure 3. 1 - MuRF1-UBE2 Screening

In-vitro ubiquitylation assay shows UBE2D, UBE2E, UBE2N/V, and UBE2W family members partnering with MuRF1 to form conjugated ubiquitin (mono- or poly-ubiquitin). A library of 28 human ubiquitin E2s (with exception to non-classical Ubiquitin E2s - listed in Table S1) were incubated with or without MBP-MuRF1 for 1 hour during an *in-vitro* ubiquitylation assay. Samples were subject to SDS-PAGE gel electrophoresis before western blot imaging to detect MuRF1-dependent ubiquitylation using anti-ubiquitylated proteins antibody.

MuRF1 autoubiquitylates by a sequential interaction with UBE2W then UBE2N/V family to form K63-linked polyubiquitin chains.

Previous research has shown other TRIM E3 ligases, TRIM5α and TRIM21, partner with UBE2W to form monoubiquitin as an anchor to attach additional polyubiquitin chains [29], [30]. As such, we proceeded to explore whether this mechanism also occurs with MuRF1. First, we determined which UBE2s were capable of attaching ubiquitin onto MuRF1 itself (autoubiquitylation). We found that unlike the other MuRF1 partnering UBE2s, UBE2N/V1 and UBE2N/V2 generated polyubiquitin chains unbound to MBP-MuRF1 (Fig S3.1). Therefore, we hypothesised that the UBE2N/V family requires UBE2W to form anchored polyubiquitin chains. To test this hypothesis, we examined the ubiquitin chains formed by each MuRF1-interacting UBE2 in the presence or absence of UBE2W. We found that the combination of UBE2N/V1 or N/V2 with UBE2W causes polyubiquitylation of MBP-MuRF1 (Fig 3.2A). This indicates that monoubiquitin is an anchor on MuRF1 to allow further polyubiquitin chains, generated by UBE2N/V1 or N/V2, to attach. Furthermore, probing for specific polyubiquitin chain types demonstrated that UBE2N/V1 and N/V2 can generate K63-linked, but not K48-linked, polyubiquitin chains (Fig 3.2C and D). Consistent with previous experiments, UBE2D2 was able to form polyubiquitin chains on MBP-MuRF1 (Fig 3.2A and B). UBE2D families are able to generate all eight different linkage types of polyubiquitin chains [31]. In similar fashion UBE2D2 was able to generate K48- and K63-linked polyubiquitin chains (Fig 3.2C and 3D).

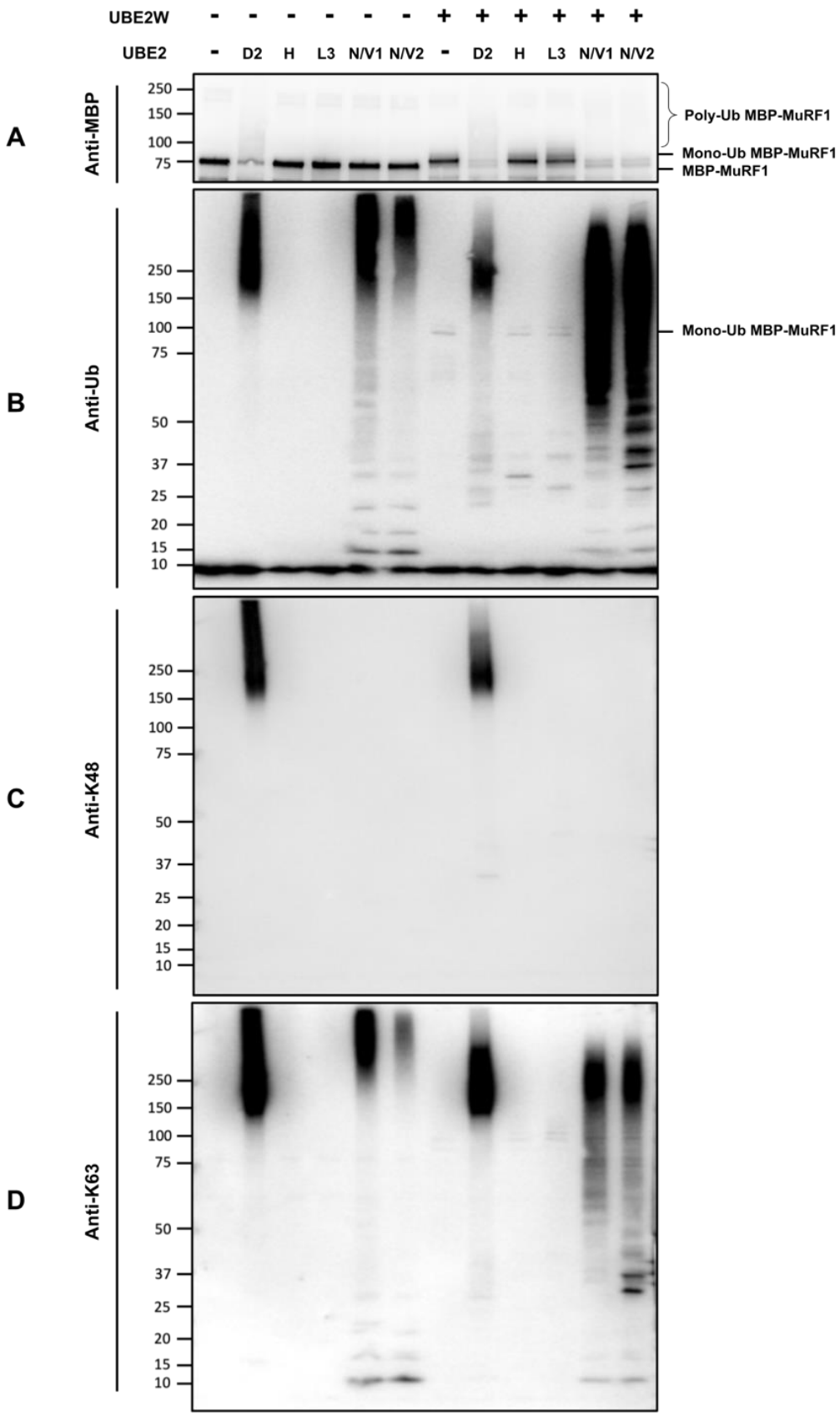
UBE2W - - - - - - + + + + + +
UBE2 - D2 H L3 N/V1 N/V2 - D2 H L3 N/V1 N/V2
A
Anti-MBP
250
150
100
75
Poly-Ub MBP-MuRF1
Mono-Ub MBP-MuRF1
MBP-MuRF1
B
Anti-Ub
250
150
100
75
50
37
25
20
15
10
Mono-Ub MBP-MuRF1
C
Anti-K48
250
150
100
75
50
37
25
20
15
10
D
Anti-K63
250
150
100
75
50
37
25
20
15
10

Figure 3. 2 - MuRF1-E2 + UBE2W Screening

Combination of UBE2W with other MuRF1-interacting UBE2s shows that UBE2W and UBE2N/V cooperate to generate MuRF1-anchored K63 polyubiquitin chains. *In-vitro* ubiquitylation assay of MuRF1-interacting E2s: UBE2D2, N/V1 and N/V2, were incubated in the presence or absence of UBE2W. UBE2H and UBE2L3 were used as negative controls. The reaction mixtures were separated by SDS-PAGE and proteins detected by anti-MBP (A), anti-ubiquitin (B), anti-lysine 48 ubiquitin chains (C) and anti-lysine 63 ubiquitin chains (D).

MuRF2 and MuRF3 partner with the same UBE2s as MuRF1 to execute protein ubiquitylation.

Sequencing of each MuRF E3 ligase shows over 80% alignment across their N-terminal residues, including the UBE2-binding RING finger domain [21]. Therefore, we hypothesised that MuRF1, MuRF2 and MuRF3 would share UBE2 partners. To investigate this, we screened MuRF2 and MuRF3 with 28 UBE2s to determine whether they partner with the same UBE2s as MuRF1. We found that as with MuRF1, MuRF2 and MuRF3 also function with the UBE2D, UBE2E, UBE2N/V and UBE2W family (Fig 3.3). As expected, UBE2W attached a single ubiquitin molecule to MBP-MuRF2 and MBP-MuRF3, whereas UBE2D, UBE2E, and UBE2N/V produced polyubiquitin chains.

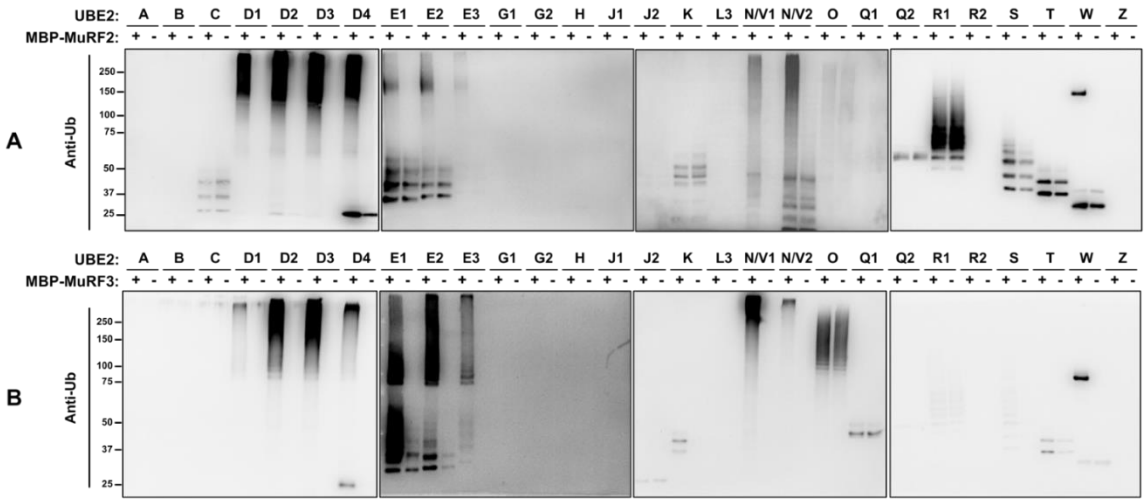

Figure 3. 3 – MuRF2- and MuRF3-UBE2 Screening

In-vitro ubiquitylation assay shows UBE2D, UBE2E, UBE2 N/V, and UBE2W family members partnering with MuRF2 and MuRF3 to form conjugated ubiquitin (mono- or polyubiquitin). 28 different UBE2s were incubated with or without a) MBP-MuRF2 or b) MBP-MuRF3 for 1 hour during an *in-vitro* ubiquitylation assay. Samples were subject to SDS-PAGE gel electrophoresis before western blot imaging to detect MuRF2- and MuRF3-dependent ubiquitylation using anti-ubiquitylated proteins antibody.

MuRF E3 ligases directly ubiquitylates Titin, MYLPF and Desmin *in-vitro*

To provide further evidence for MuRF overlap during ubiquitylation, we next explored whether MuRF1, 2 and 3 can ubiquitylate the same substrates *in-vitro*. The first substrate tested was Titin (A168-170) which is well established as a site of MuRF1 translocation and interaction [21], [32]–[34], and more recently a binding site for MuRF2 and MuRF3 [35]. Additionally, we included MYLPF and Desmin as *in-vitro* substrates, previously identified as potential MuRF1 substrates [36]–[38]. The ubiquitylation assays revealed that MuRF1, MuRF2 and MuRF3 partner with UBE2W to ubiquitylate His-Titin (A168-A170) (Fig 4A), His-SUMO-MYLPF (Fig 3.4C) and Desmin (Fig 3.4E), confirming them to be direct substrates of all MuRF E3 ligases. The two-step mechanism of UBE2W and UBE2N/V2 that had been identified during MuRF autoubiquitylation, is also seen with substrate ubiquitylation whereby UBE2N/V2 can only polyubiquitylated substrates once they have been monoubiquitylated by UBE2W (Figure 3.4B, D and F). To confirm that the labelled bands in the His blots were in fact ubiquitylated Titin and MYLPF and not other His-tagged proteins present in the reaction e.g., UBE2s, we also blotted for the ubiquitin and MYLPF respectively. These western blots showed the bands above His-Titin (A168-A170) and His-SUMO-MYLPF, confirming that these bands are the ubiquitylated substrates (Fig S3.2 and S3.3). To ensure that our model of substrate ubiquitylation was valid, we wanted to confirm that substrate ubiquitylation doesn't occur just because of their close proximity to ubiquitin and ubiquitin-regulating enzymes. Using our model, we also tested Valosin-containing protein (VCP) - another potential MuRF1 substrate [38], and found that it is not directly ubiquitylated by

MuRF1 (Fig S3.4). Therefore, our model does not cause all proteins to be ubiquitylated and so we can take more confidence that Titin, MYLPF and Desmin are direct substrates of MuRF1, MuRF2 and MuRF3.

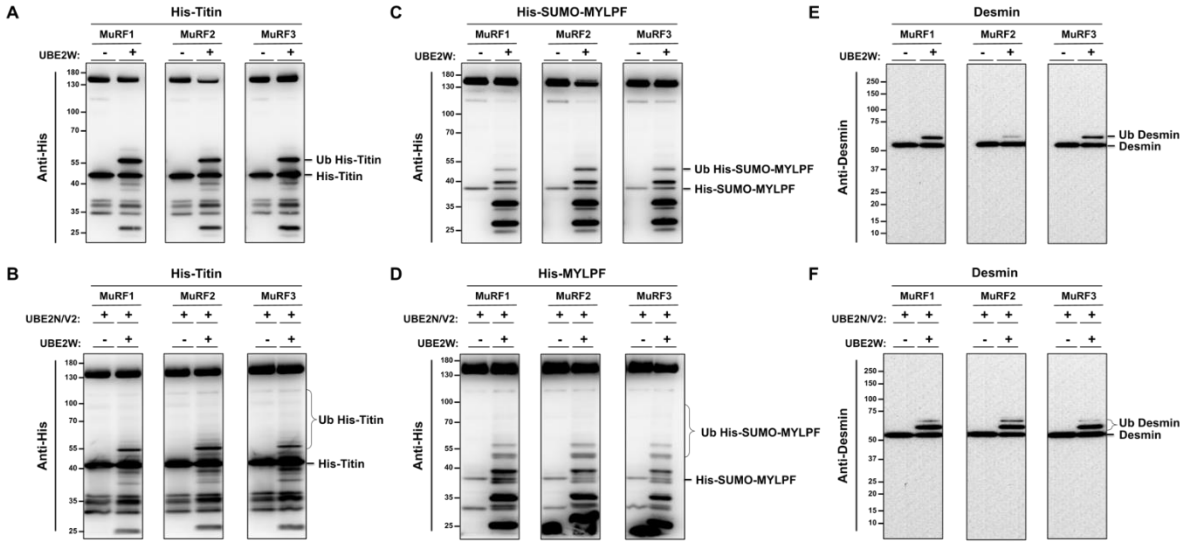

Figure 3. 4 – MuRF1, 2 and 3 Substrate Ubiquitylation Assay

A-B) His-Titin (A168-A170), C-D) His-SUMO-MYLPF and E-F) Desmin were incubated with MBP-MuRF1, MBP-MuRF2 or MBP-MuRF3 with or without UBE2s (W and N/V2) for 1 hour during an *in-vitro* ubiquitylation assay. Samples were subject to SDS-PAGE gel electrophoresis before western blot imaging. Anti-His antibody was used to detect His-Titin and His-SUMO-MYLPF and Anti-Desmin antibody was used to detect Desmin.

UBE2N, W, and V2 gene expression increases following denervation of mouse skeletal muscle.

Having identified MuRF E3 ligases cooperating with UBE2W and UBE2N/V during autoubiquitylation and substrate ubiquitylation, we wanted to investigate the importance of these UBE2s in skeletal muscle. MuRF1 is best known for its increased expression during different atrophic conditions, therefore we were interested to see if UBE2W and UBE2N/V followed a similar pattern. Using denervated mouse muscle that experienced muscle atrophy and increased MuRF1 mRNA expression [39], we measured the mRNA expression of UBE2W, UBE2N, UBE2V1 and UBE2V2. We confirmed the presence of all these UBE2's in muscle and found that UBE2W, UBE2N and UBE2V2 are upregulated following 14 days of denervation (Fig 3.5A, B and D). Therefore, the two-step mechanism of UBE2W and UBE2N/V could play an important role in regulating the function of MuRF1 during denervation-induced muscle atrophy.

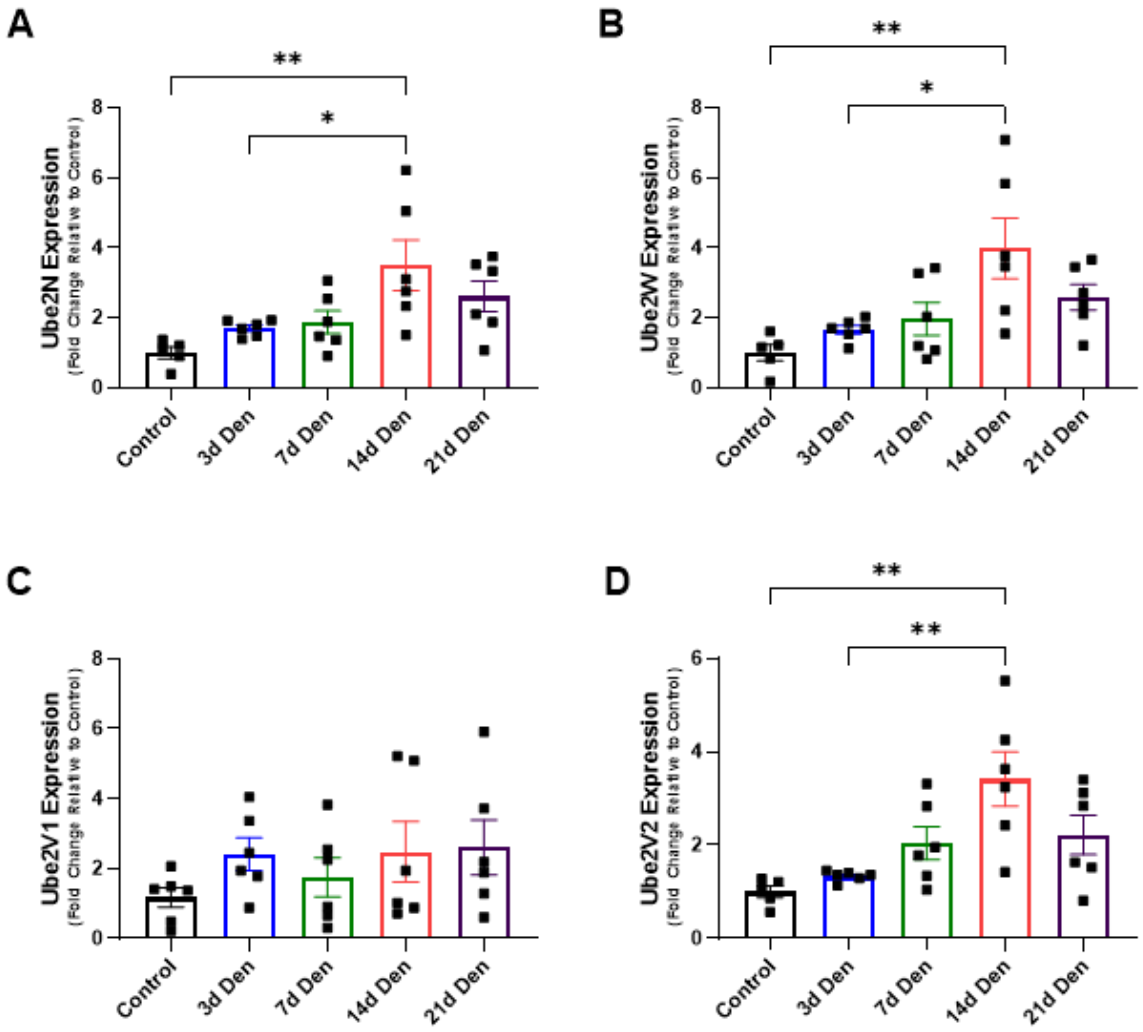

Figure 3. 5 – mRNA Expression of UBE2N, W, and V1/2 during denervation in mice.

UBE2N, UBE2W, UBE2V2, but not UBE2V1, mRNA expression increases following denervation of gastrocnemius complex muscle in mice. C57BL/6 mice were grown for 3-4 months and then had their right leg denervated through surgical ablation of the sciatic nerve. Mice were sacrificed (at days 3, 7, 14, and 21) and their gastrocnemius UBE2 mRNA expression was measured by rt-qPCR. P-values were calculated using a one-way ANOVA with Tukey's post hoc test, *P <.05; **P < .01. Data presented as means ± SEM (n = 6).

3.5 Discussion

The *in-vitro* assay allows us to demonstrate a direct reaction/interaction among the molecules presented in the test tubes. With this assay, we identified a list of UBE2s that can partner with MuRF1 during ubiquitylation processes. Further, we showed that MuRF1 partners with different UBE2s to form multiple chain types, including K48- and K63-linked polyubiquitin chains. We identified that MuRF1 can partner with UBE2W to monoubiquitylate itself (autoubiquitylation), which can then serve as an anchor for K63-linked polyubiquitylation. This two-step mechanism allows MuRF1 to directly ubiquitylate Titin (A168-A170), MYLPF and Desmin. Utilising this *in-vitro* method, we also found that MuRF2 and MuRF3 share the same UBE2 partners as MuRF1 and can target the same substrates, providing a molecular explanation for their functional redundancy *in-vivo*.

We identified that MuRF1 was able to partner with all the UBE2D and UBE2E members to form polyubiquitin chains. Previous research has already shown the capacity for MuRF1 to partner with UBE2D and E families to form polyubiquitin chains [16], [19], [20], [40]. The mechanisms by which MuRF1 function with the UBE2D family are disputed, with yeast-two hybrid methods showing no physical interaction with UBE2D2 [41]. However, it is possible that UBE2 binding properties are altered when bound to ubiquitin, which is not included during these interaction-based methods. Therefore, it is important not to directly compare the findings of *in-vitro* ubiquitylation studies to interaction-based studies. Our data highlights MuRF1 ubiquitylation activity through direct cooperation with the UBE2D and E family of

enzymes and therefore aligns with the current literature. These two families of UBE2s make up a quarter of the ubiquitin-conjugating enzymes in humans, offering a substantial number of partners to facilitate MuRF1 activity.

Our data demonstrates a common familial function of MuRF1 with fellow TRIM E3s, TRIM21 and TRIM5α. Like these E3 Ligases, MuRF1 can form K63-linked polyubiquitin chains in a two-step fashion by partnering with UBE2N/V1, or V2 and UBE2W to form an anchor on the substrate [29], [30]. It is crucial to understand the diversity of ubiquitin chain types generated by this mechanism, since chain types determine the fate of substrates. We were able to confirm that K48-linked polyubiquitin chains were not formed, however future work would benefit from screening all ubiquitin chain types. Having shown overlap of MuRF1-UBE2 partners with other TRIM E3 ligases, we hypothesised that this could occur with MuRF2 and MuRF3. Previous work using ELISA-based methods found MuRF1, MuRF2 and MuRF3 display autoubiquitylation activity with some individual UBE2s [16], here we demonstrated that MuRF1, MuRF2 and MuRF3 function with all the same UBE2 enzymes (UBE2Ds, Es, Ns/Vs and W) during *in-vitro* ubiquitylation.

Our *in-vitro* data demonstrates that a fragment of Titin (A168-A170), MYLPF and Desmin are direct substrates of all MuRF E3 ligases. We further showed that substrate ubiquitylation can occur by a two-step ubiquitylation with UBE2W and UBE2N/V enzymes. This offers a mechanistic link to previous work showing that

MuRF E3 ligases regulate K63-linked ubiquitin chains on Titin to signal for the degradation via autophagy [35]. A recent study reported that MuRF1 ubiquitylation of Titin resulted in recruitment of NBR1 and P62, proteins that facilitate the autophagy of large protein cargo [42]. MuRF2 also interacts with NBR1/P62 on Titin [43]. These data build a causal chain of events that end with Titin autophagy by p62 and NBR1, mediated by K63-linked chains, instigated by the MuRF-UBE2 partners that we have elucidated. Studies have shown that MYLPF is degraded by MuRF1 after denervation-induced atrophy [37] and is reduced following 14 days of MuRF1 overexpression [38]. We found that MuRF1 directly ubiquitylates MYLPF, supporting the hypothesis that degradation of MuRF1 substrates is caused by direct ubiquitylation. By revealing that MuRF2 and MuRF3 can also ubiquitylate MYLPF, it will be interesting to see if the same response occurs during atrophy and whether they can compensate for the loss of MuRF1. Desmin has been previously shown to be degraded during fasting-induced atrophy in a TRIM32 dependent manner [44]. Their study showed that TRIM32 expression did not change by fasting-induced atrophy, whereas MuRF1 expression increased. Since revealing Desmin as a direct substrate of MuRF1, this raises the question whether both MuRF1 and TRIM32 are required to contribute to Desmin ubiquitylation, facilitating its degradation. Furthermore, proteomic approaches have revealed 10 different ubiquitylation sites on Desmin [45]. Future work could investigate whether any of these sites are ubiquitylated by all MuRF E3 ligase.

Given the role of MuRF1 during muscle atrophy, we wanted to test whether the UBE2's they function with are also upregulated during muscle atrophy. In dexamethasone treated mice, UBE2E1 knockdown exacerbated muscle atrophy [46]. Furthermore, transcriptomics of mice treated with dexamethasone for 14 days have shown increased expression of UBE2D2, D3, N, V1, and V2 [47]. Following denervation-induced atrophy in mice, we found that mRNA expression of UBE2N, W, and V2 transiently increased at 14 days post-denervation. However, the peak mRNA expression of these UBE2 enzymes occurs later than MuRF1 mRNA, which occurs 3-7 days post denervation [39]. The loss of muscle mass is significantly greater after 14 days denervation when compared to 3-7 days, which could suggest that these UBE2's only increase in response to more severe muscle wasting. The delayed transient expression of UBE2s shown in our work highlights the importance of screening multiple time points of atrophy when studying UBE2s.

3.6 Conclusion

The data presented here offers molecular insight into MuRF-induced ubiquitylation. We show that MuRF1 can interact with the UBE2D, E, N/V families and UBE2W during ubiquitylation. MuRF1 forms monoubiquitylation and creates K48- and K63-linked polyubiquitin chains in a UBE2 dependent manner. We provide evidence of direct substrates of MuRF1 ubiquitylation, namely Titin, MYLPF, and Desmin. Additionally, we show that these mechanisms are not specific to MuRF1, but also occur with MuRF2 and MuRF3. We propose that these findings are important for partial MuRF functional redundancy *in-vivo*. Therefore, we have put forward a working hypothesis that MuRF1, MuRF2 and MuRF3 are co-ordinately involved in the ubiquitylation of certain substrates to ensure that individual loss of MuRF E3 ligase function does not impair the function of skeletal muscle (Fig 3.6).

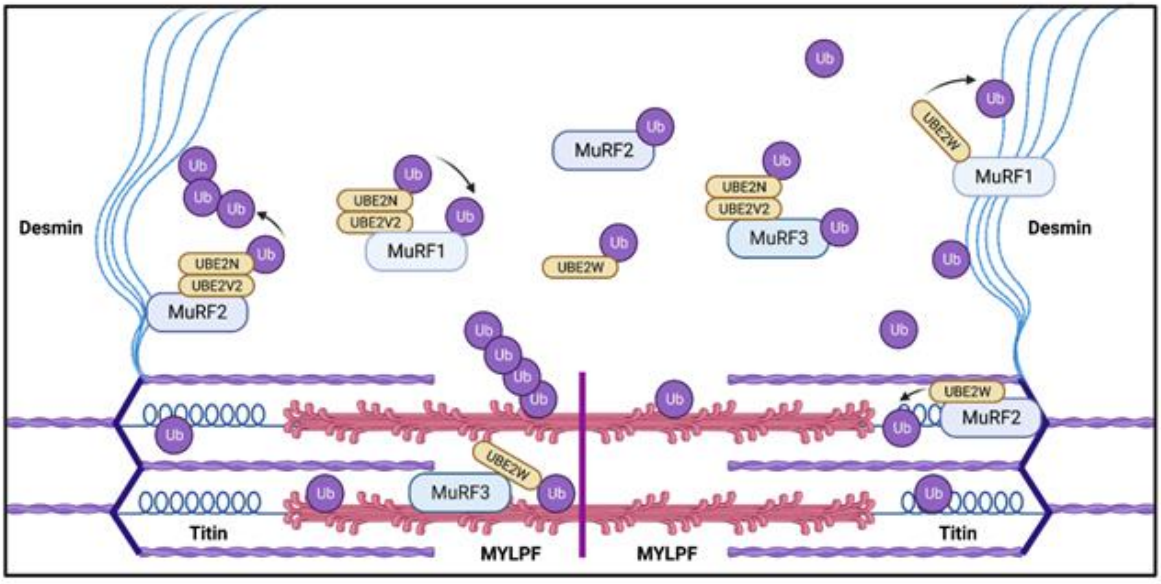

Figure 3. 6 - Schematic of proposed explanation for MuRF E3 ligase functional redundancy.

MuRF E3 ligases operate with UBE2W and UBE2N/V2 to ubiquitylate Titin, MYLPF and Desmin. Both monoubiquitin and polyubiquitin chains can be formed depending on which UBE2 is involved. Created with BioRender.com.

Acknowledgements: The authors gratefully acknowledge the Dr Axel Knebel and MRC protein phosphorylation and ubiquitylation unit, University of Dundee for providing numerous recombinant proteins required for *in-vitro* ubiquitylation assays. We also thank Prof. Olga Mayans (University of Konstanz) for providing the His-Titin plasmid.

3.7 Supplementary Figures

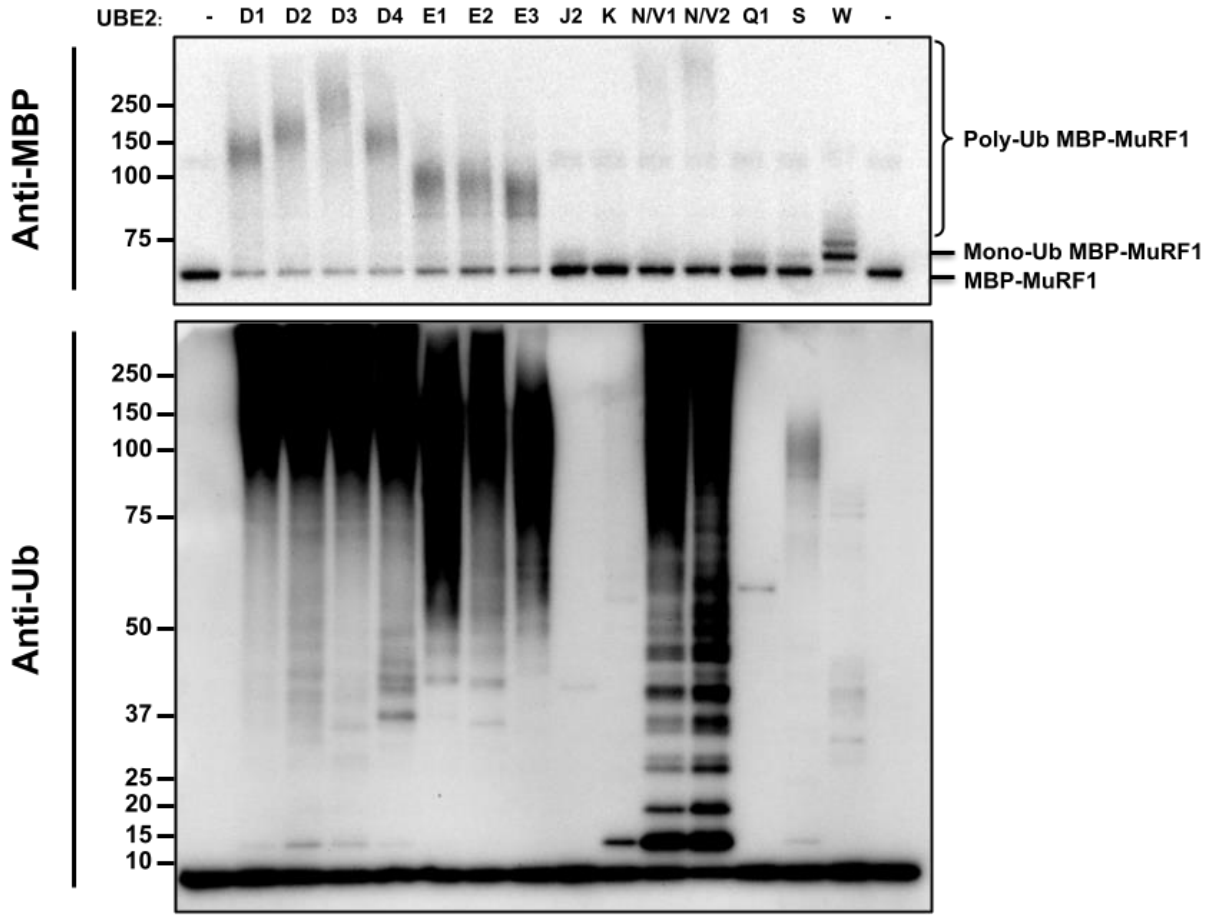

Supplementary Figure S3. 1 – MBP-MuRF1-UBE2 Ubiquitylation Screening

UBE2D, E and W family partner with MuRF1 to form auto-ubiquitylation, whereas UBE2N/V forms unanchored ubiquitin chains. Ten selected UBE2s identified as MuRF1 partners (Fig 1) and four non-partners (UBE2J2, K, Q1, and S) as negative controls, were incubated with MBP-MuRF1 for 1 hour during an *in-vitro* ubiquitylation assay. Samples were subject to SDS-PAGE gel electrophoresis before western blot imaging. Anti-MBP antibody was used to detect MBP-MuRF1 auto-ubiquitylation (A). Anti-ubiquitin antibody was used to detect ubiquitin chain formation (B).

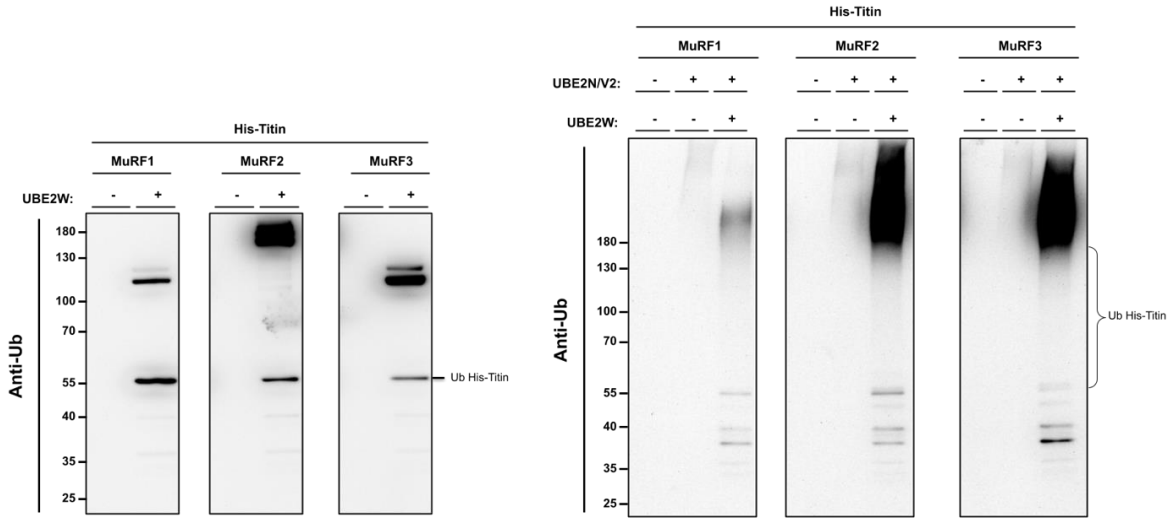

Supplementary Figure S3. 2 – Ubiquitylation Assay of His-Titin A168-A170 by MuRF1, 2, and 3.

Anti-ubiquitin blot confirms Titin ubiquitylation by each MuRF E3 ligase. His-Titin (A168-A170) was incubated with MBP-MuRF1, MBP-MuRF2 or MBP-MuRF3 with or without UBE2s (or N/V2) for 1 hour during an *in-vitro* ubiquitylation assay. Samples were subject to SDS-PAGE gel electrophoresis before western blot imaging. Anti-ubiquitylated proteins antibody was used to detect Titin monoubiquitylation (A) and Titin polyubiquitylation (B). The strong bands at the top of the membrane are auto-ubiquitylated MBP-tagged MuRF E3 ligases.

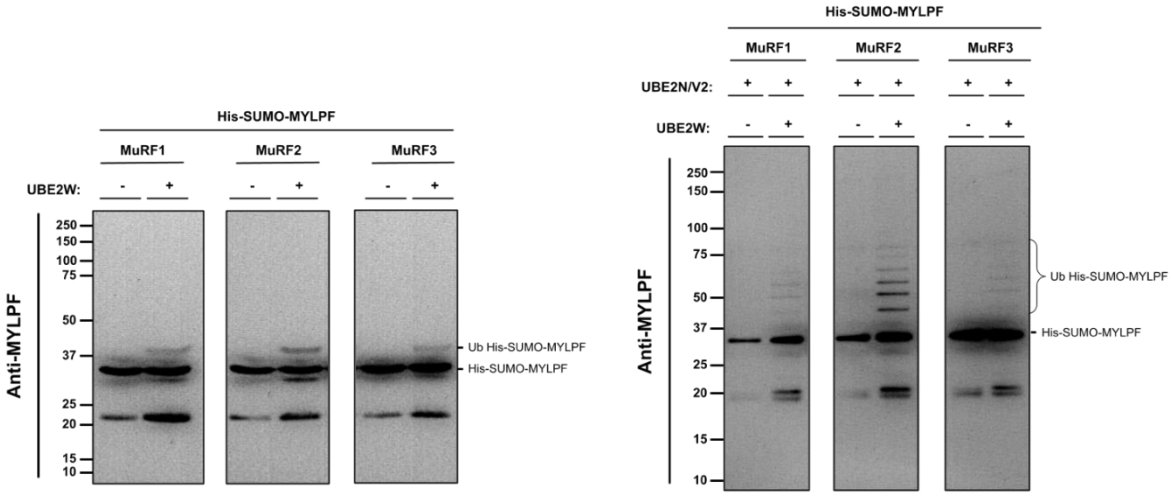

Supplementary Figure S3. 3 - Ubiquitylation Assay of HIS-SUMO-MYLPF by MuRF1, 2, and 3.

Anti-MYLP blot confirms MYLP ubiquitination by each MuRF3 ligase. His-SUMO-MYLP was incubated with MBP-MurF1, MBP-MurF2 or MBP-MurF3 with or without UBE2W (N or V2) for 1 hour during an *in-vitro* ubiquitination assay. Samples were subject to SDS-PAGE gel electrophoresis before western blot imaging. Anti-MYLP antibody was used to detect MYLP monoubiquitination (A) and MYLP polyubiquitination (B).

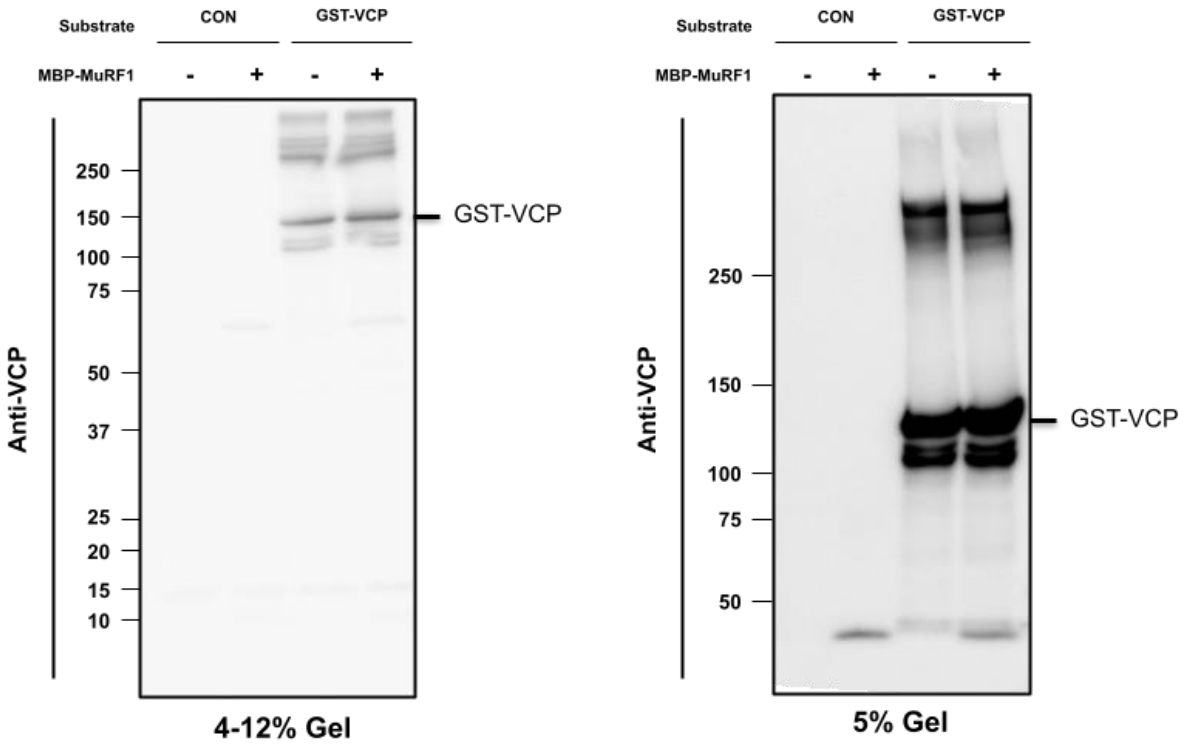

Supplementary Figure S3. 4 - Ubiquitylation Assay of GST-VCP by MuRF1.

MuRF1 does not directly ubiquitinate VCP. GST-VCP was incubated with or without MBP-MurF1 for 1 hour during an *in-vitro* ubiquitination assay using UBE2W. Samples were subject to 4-12% acrylamide (A) or 5% acrylamide (B) SDS-PAGE gel electrophoresis before western blot imaging. Anti-VCP antibody was used to detect presence or absence of monoubiquitylated GST-VCP.

3.8 Supplementary Tables

Potential UBE2	Reason for exclusion
UBE2F	NEDD8-conjugating E2
UBE2I	SUMO-conjugating E2
UBE2L6	ISG15-conjugating E2
UBE2M	NEDD8-conjugating E2
UBE2QL	Only a probable E2
BIRC6	Chimeric E2/E3
UBE2U	Only expressed in Testis

Table 3. Supplementary - UBE2s excluded from *in-vitro* screening.

Primers	Sequence (5'-3')	Accession Number
Trim63 (MuRF1)-F	GCTGGTGGAAAACATCATTGACA T	NM_001039048.2
Trim63 (MuRF1)-R	CATCGGGTGGCTGCCTTT	NM_001039048.2
UBE2N-F	CCAATGGCAGCACCTAAAGTACG	NM_080560.3
UBE2N-R	GGATTGATAGCAGAACTGTGCGG	NM_080560.3
UBE2W-F	CGATACCCTTTTGACTCTCCTCA	NM_001271016.3
UBE2W-R	TGCTGAGACAGACTGACTGCAC	NM_001271016.3
UBE2V1-F	GATAGAGTGTGGGCCTAAGTACC	NM_001311131.1
UBE2V1-R	GAGTTCTGCCACTTTGCCAGCA	NM_001311131.1
UBE2V2-F	TACCCAGAAGCTCCTCCATCAG	NM_023585.4
UBE2V2-R	GCTAATACTGGTATGCTCCGTGC	NM_023585.4

Table 4. Supplementary – Primers used for qPCR.

Table 5 Supplementary - **List of plasmids used for generating recombinant proteins.**

Plasmid	Protein name	Identity (DU number)
pFastBac HTb 6His TEV UBE1	UBE1	DU32888
pGEX6P-3-GST-UBE2A	UBE2A	DU4203
pET156P-1 6His UBE2B	UBE2B	DU32555
pET156P 6His UBE2C	UBE2C	DU32146
pET28a(+) 6His-UBE2D1 (UBCH5a)	UBE2D1	DU4315
pET28- 6His-UBE2D2	UBE2D2	DU20184
pET156P 6His 3C UBCH5c	UBE2D3	DU15703
pET28a 6His-UBE2D4	UBE2D4	DU8232
pET156P 6His-UBCH6	UBE2E1	DU12803
pET28a 6His-UBE2E2	UBE2E2	DU12394
pET28a(+)6His-UBE2E3	UBE2E3	DU14049
pET28a(+)6His-UBE2G1	UBE2G1	DU14055
pET28a 6His-UBE2G2	UBE2G2	DU20174
pET156P 6His-UBE2H	UBE2H	DU32149
pET28a 6His-UBE2J1 1-282	UBE2J1	DU20686
pET28a 6His-UBE2J2 1-226	UBE2J2	DU20695
pET156P 6His-UBC1	UBE2K	DU20018
pET156P 6His-3C-UBCH7	UBE2L3	DU12798
pET15b 6His-3C-UBC13	UBE2N	DU15705

pET28a 6His-UBE2V1	UBE2V1	DU20179
pET15b 6His-C3-UBE2V2	UBE2V2	DU12415
pET156P 6His-UBE20	UBE2O	DU32152
pET28 6His-UBE2Q1	UBE2Q1	DU20176
pET15b 6His-3C-UBE2Q2	UBE2Q2	DU12801
pET28a(+) 6His-CDC34	UBE2R1	DU4317
pGEX6P-1-GST-UBE2R2	UBE2R2	DU4616
pET28-6His-UBE2S	UBE2S	DU20175
pET15b6P 6His-UBE2T	UBE2T	DU12416
pET28a-6His-UBE2W isoform 1	UBE2W	DU20190
pET15b 6HIS C3 6His-UBE2Z	UBE2Z	DU20121
pMEX3Cb MBP 3C-TEV-TRIM63	MBP-MuRF1	DU58528
pMEX3Cb MBP-TRIM54	MBP-MuRF3	DU49175
pMEX3Cb MBP-TRIM55	MBP-MuRF2*	uncatalogued
pET24 Ubiquitin	Ubiquitin	uncatalogued

Plasmids obtained from Medical Research Council – Protein Phosphorylation and Ubiquitylation Unit Reagents and Services (https://mrcppureagents.dundee.ac.uk) are listed, while others are detailed in the Methods.

*TRIM55 gene (pcDNA3.1) was purchased from GenScript (Clone ID OHu29713) and then shuttled into pMEX3Cb MBP-tag vector

3.9 Supplementary Raw Figures

“Ubiquitin for Fig 3.1”

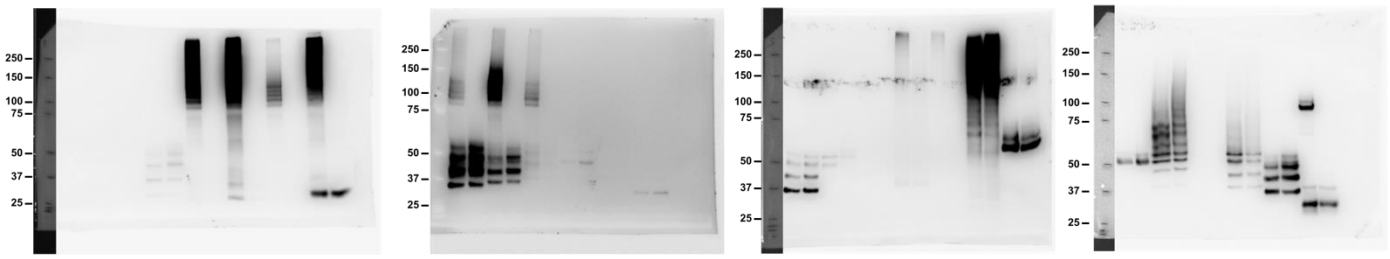

“MBP for Fig 3.2A”

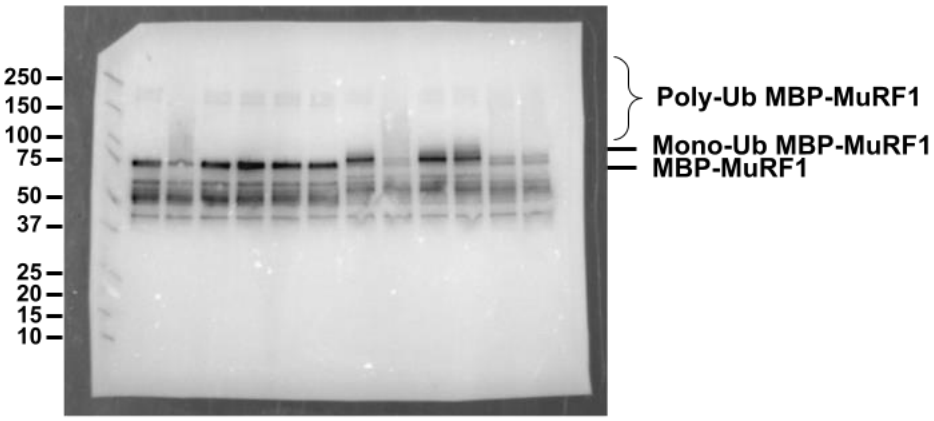

“Ubiquitin for Fig 3.2B”

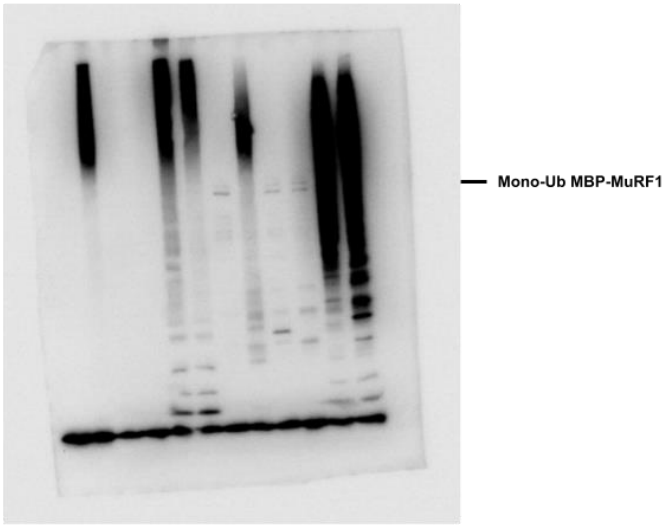

“K48 for Fig 3.2C”

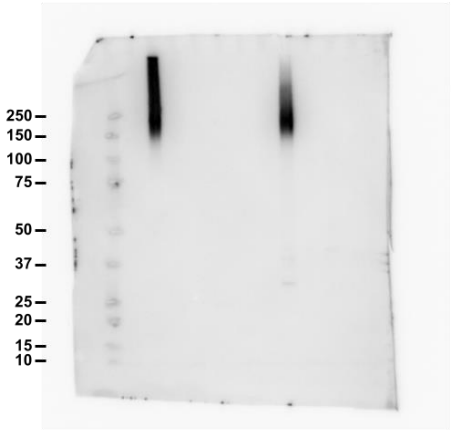

“K63 for Fig 3.2C”

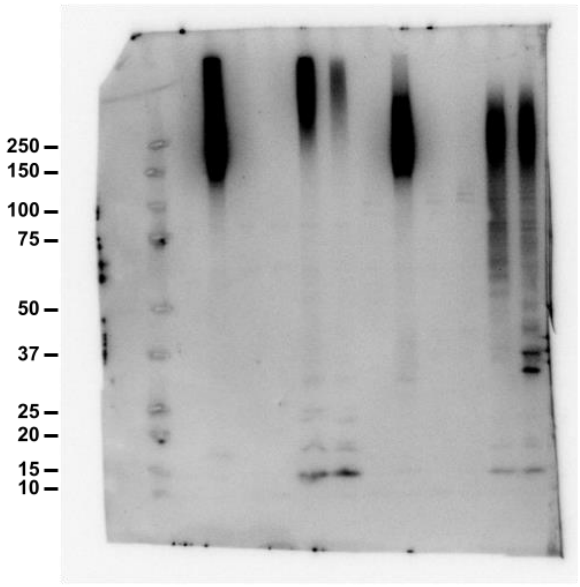

“Ubiquitin for Fig 3.3A”

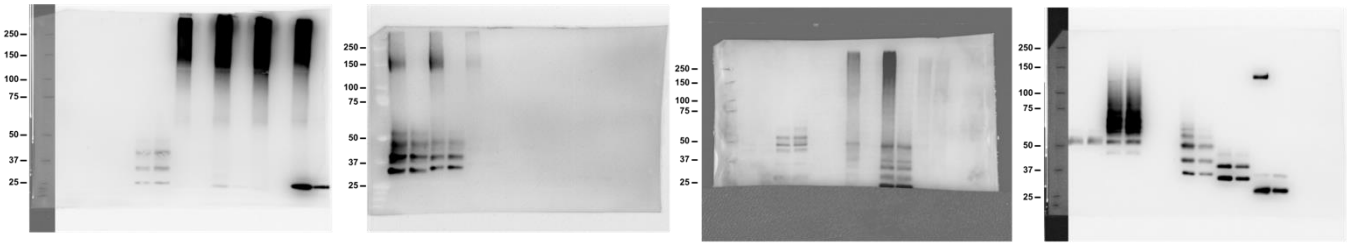

“Ubiquitin for Fig 3.3B”

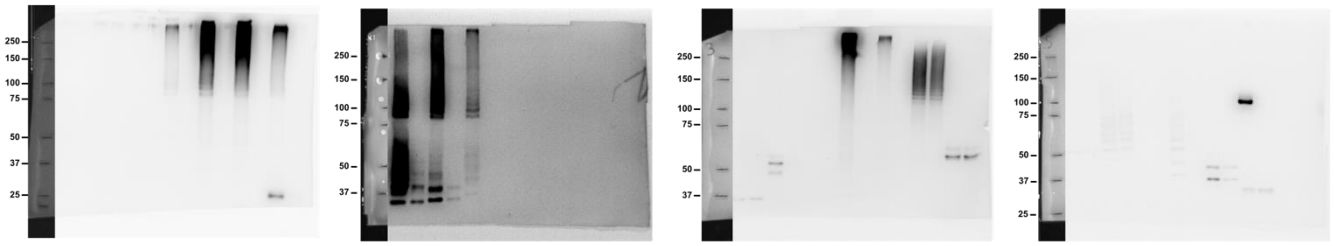

“His for Fig 3.4A”

Note: Fig 3.4A splits the image for each MuRF protein

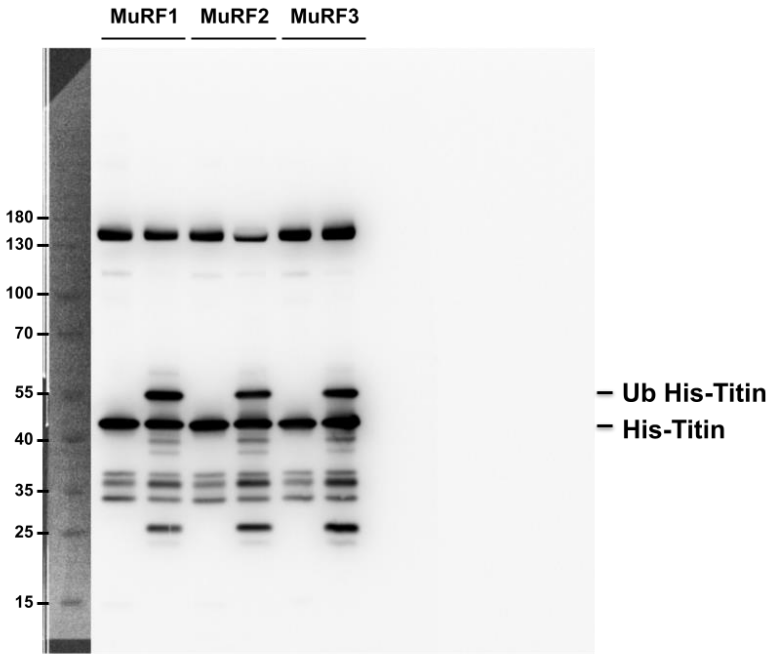

“His for Fig 3.4B”

Note: Fig 3.4B splits the image for each MuRF protein

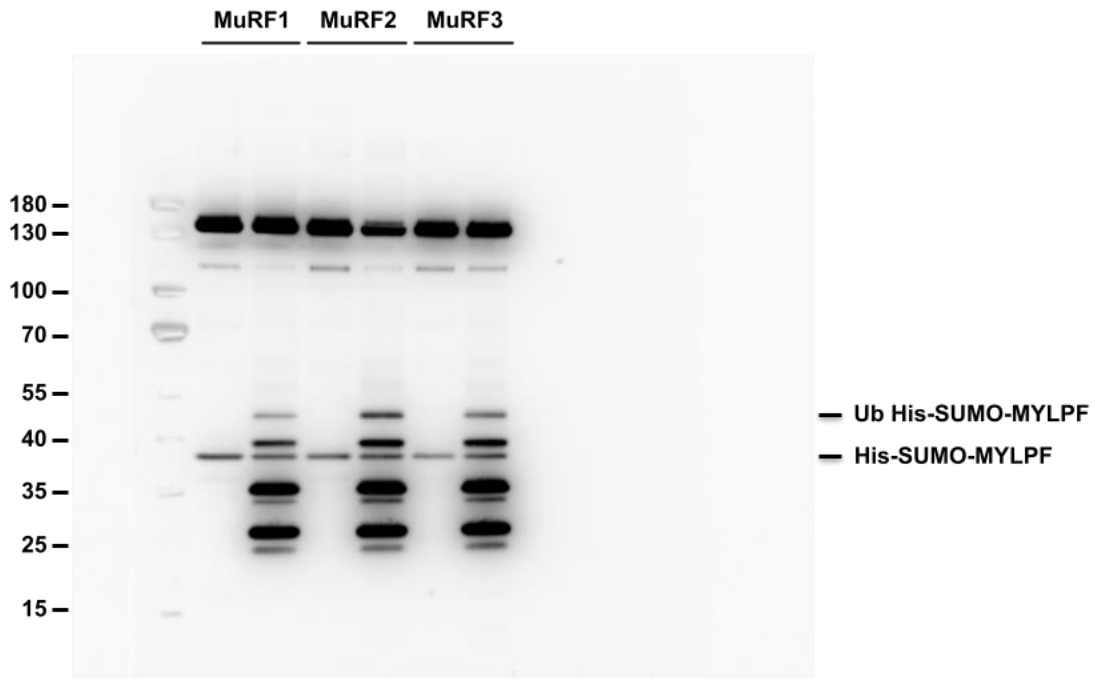

“Desmin for Fig 3.4C and Fig 3.4F”

Note: Fig 3.4C and Fig 3.4F splits the image for each MuRF protein

Also only Lanes “-“ and “W” are used for Fig 4C and only Lanes “ N/V2” and “W+N/V2” used for Fig 4F. Lane “D2” not used in figures

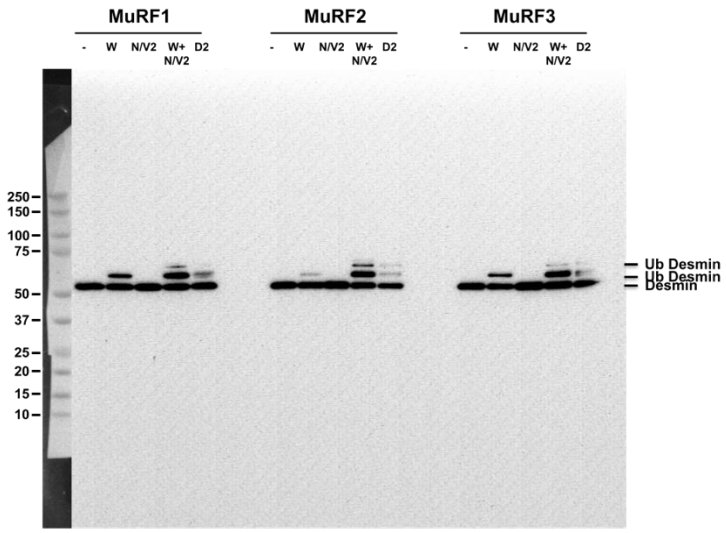

“His for Fig 3.4D”

Note: Fig 3.4B splits the image for each MuRF protein

Also, Lanes “-” not used in figures

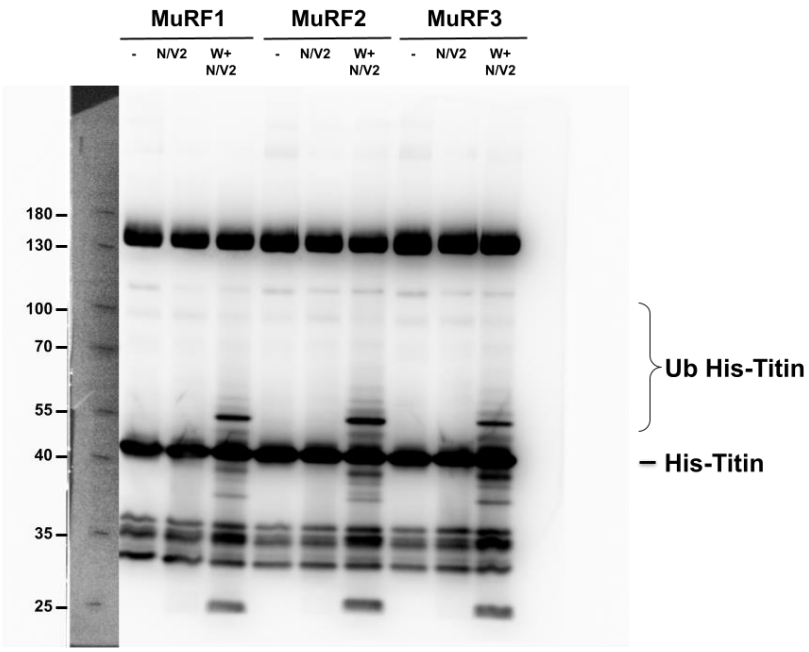

“His for Fig 3.4E”

Note: Lanes “-” not used in figures

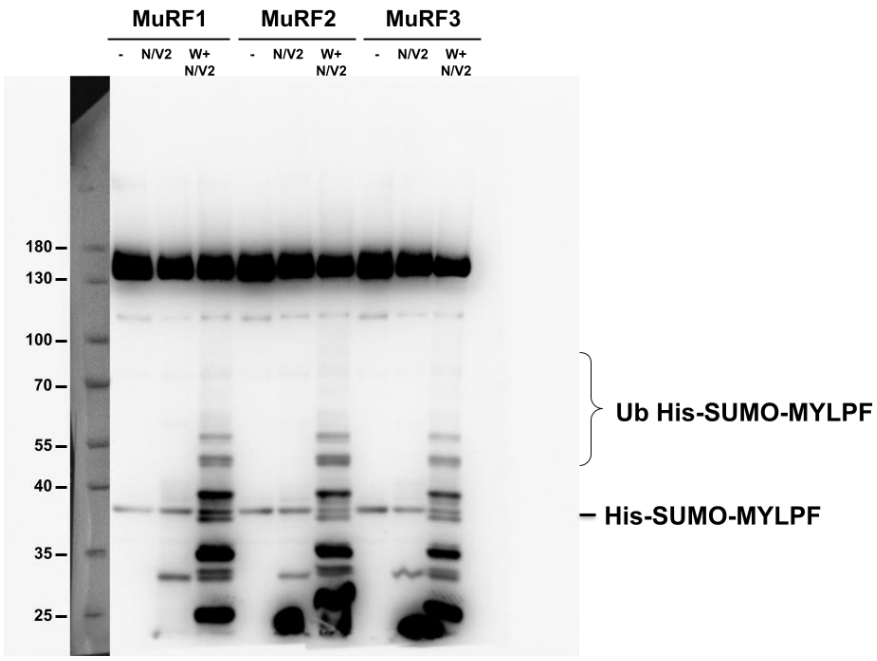

“MBP for Fig S3.1”

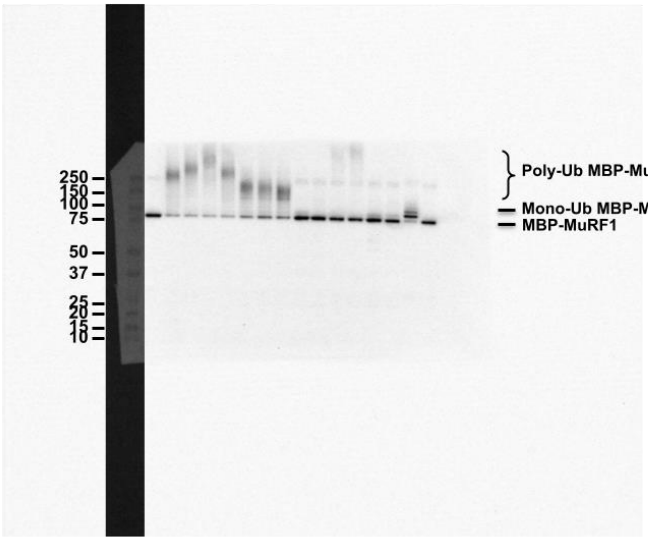

“Ubiquitin for Fig S3.1”

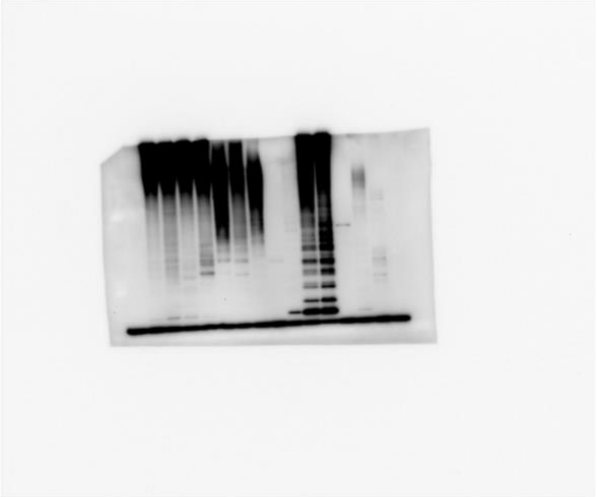

“Ubiquitin for Fig S3.2A”

Note: Fig S2 splits the image for each MuRF protein

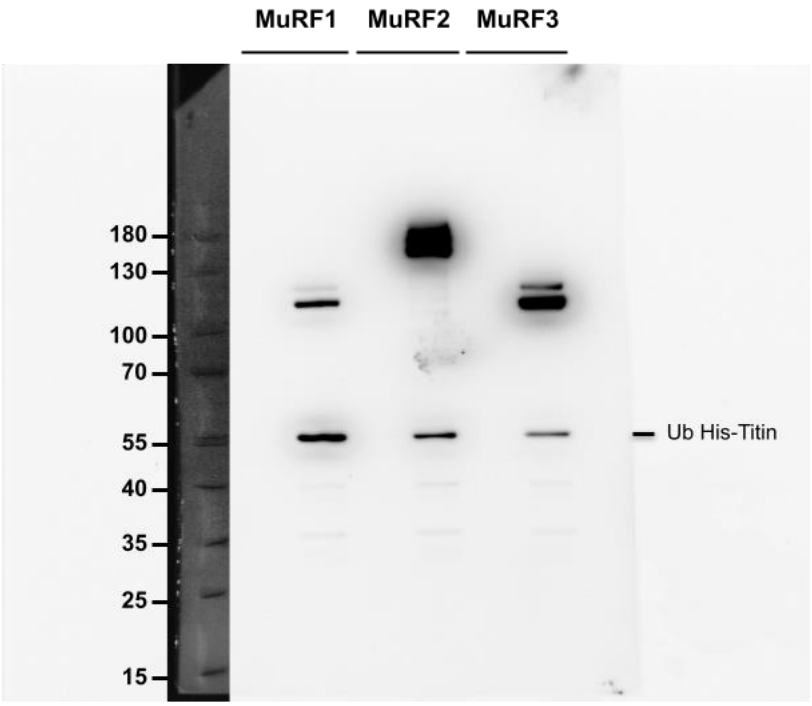

“Ubiquitin for Fig S3.2B”

Note: Fig S3.2B splits the image for each MuRF protein

Also, Lanes “-” not used in figures

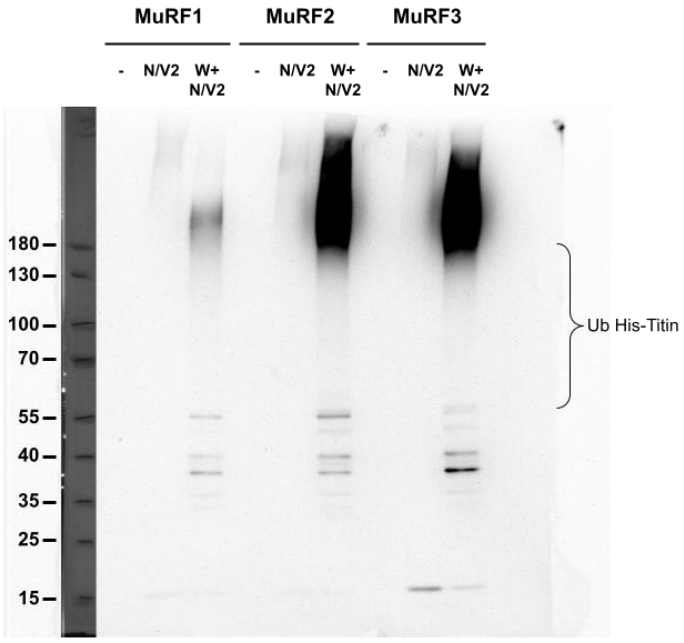

“MYLPF for Fig S3.3A”

Note: Fig S3.3A splits the image for each MuRF protein

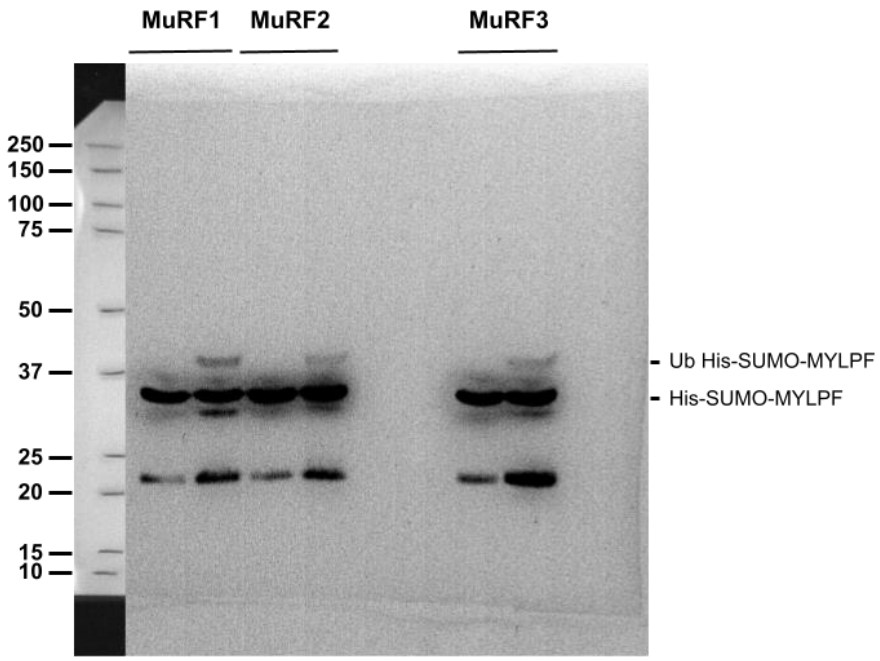

“Ubiquitin for Fig S3.3B”

Note: Fig S3.3B splits the image for each MuRF protein

Also, Lanes “-” not used in figures

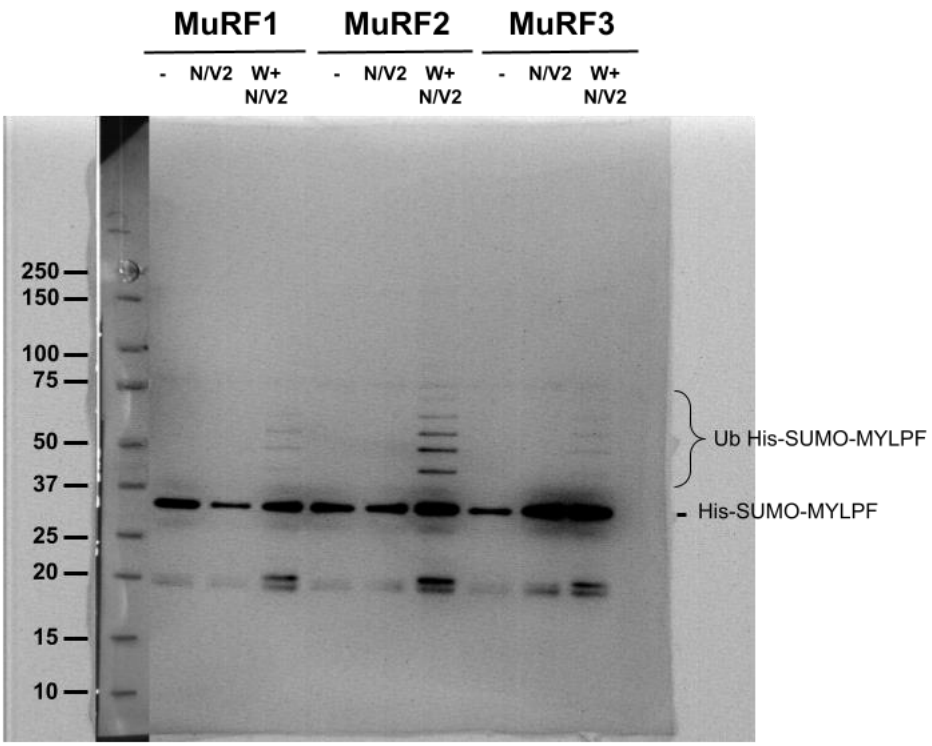

“VCP for Fig S3.4A”

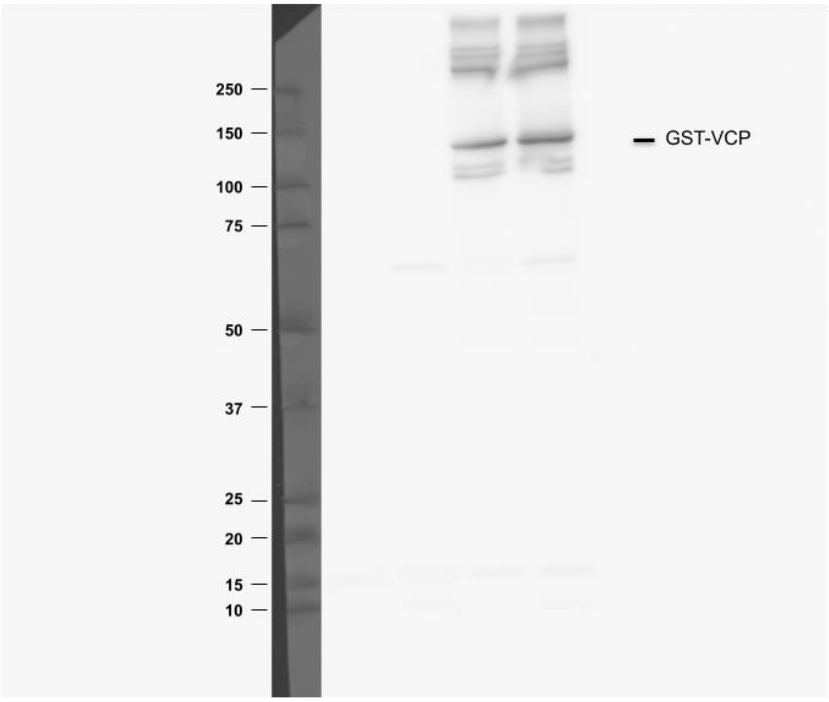

“VCP for Fig S3.4B”

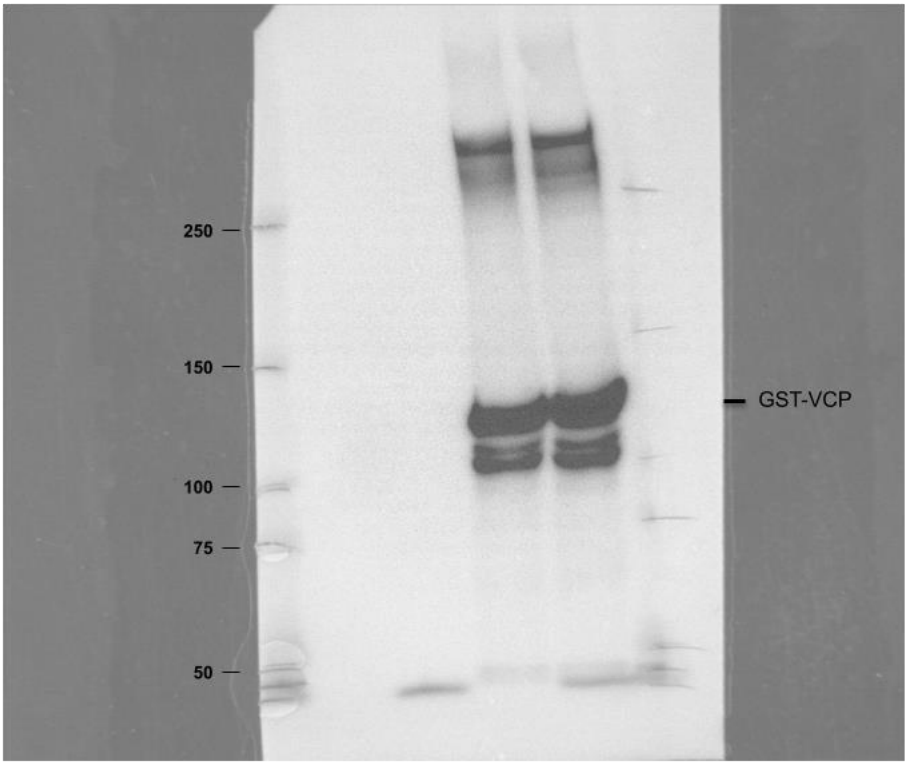

3.9 References

[1] S. W. Jones, R. J. Hill, P. A. Krasney, B. O. Conner, N. Peirce, and P. L. Greenhaff, “Disuse atrophy and exercise rehabilitation in humans profoundly affects the expression of genes associated with the regulation of skeletal muscle mass,” *FASEB J.*, vol. 27, no. 4, pp. 1–27, 2004.

[2] S. C. Bodine *et al.*, “Identification of Ubiquitin Ligases Required for Skeletal Muscle Atrophy,” 2001. Accessed: Apr. 01, 2019. [Online]. Available: https://www-jstor-org.ezproxye.bham.ac.uk/stable/pdf/3085298.pdf?refreqid=excelsior%3Aaf00ba1aeb2f31bef1633084dffca959.

[3] J. Aniort *et al.*, “Muscle wasting in patients with end-stage renal disease or early-stage lung cancer: common mechanisms at work,” *J. Cachexia. Sarcopenia Muscle*, vol. 10, no. 2, pp. 323–337, 2019, doi: 10.1002/jcsm.12376.

[4] R. F. Carvalho *et al.*, “Heart failure increases atrogin-1 and MuRF1 gene expression in skeletal muscle with fiber type-specific atrophy,” *J. Mol. Histol.*, vol. 41, no. 1, pp. 81–87, 2010, doi: 10.1007/s10735-010-9262-x.

[5] E. K. Merritt, A. Thalacker-Mercer, J. M. Cross, S. T. Windham, S. J. Thomas, and M. M. Bamman, “Increased expression of atrogenes and TWEAK family members after severe burn injury in nonburned human skeletal muscle,” *J. Burn Care Res.*, vol. 34, no. 5, pp. 5–8, 2013, doi: 10.1097/BCR.0b013e31827a2a9c.

[6] B. A. Clarke *et al.*, “The E3 Ligase MuRF1 Degrades Myosin Heavy Chain Protein in Dexamethasone-Treated Skeletal Muscle,” *Cell Metab.*, vol. 6, no. 5, pp. 376–385, 2007, doi: 10.1016/j.cmet.2007.09.009.

[7] O. Schakman *et al.*, “Role of IGF-I and the TNFα/NF-κB pathway in the induction of muscle atrogenes by acute inflammation,” *Am. J. Physiol. - Endocrinol. Metab.*, vol. 303, no. 6, 2012, doi: 10.1152/ajpendo.00060.2012.

[8] L. M. Baehr, J. D. Furlow, and S. C. Bodine, “Muscle sparing in muscle RING finger 1 null mice: Response to synthetic glucocorticoids,” *J. Physiol.*, vol. 589, no. 19, pp. 4759–4776, 2011, doi: 10.1113/jphysiol.2011.212845.

[9] S. Labeit, C. H. Kohl, C. C. Witt, D. Labeit, J. Jung, and H. Granzier, “Modulation of muscle atrophy, fatigue and MLC phosphorylation by MuRF1 as indicated by hindlimb suspension studies on MuRF1-KO mice,” *J. Biomed. Biotechnol.*, vol. 2010, 2010, doi: 10.1155/2010/693741.

[10] D. C. Files *et al.*, “A critical role for muscle ring finger-1 in acute lung injury-associated skeletal muscle wasting,” *Am. J. Respir. Crit. Care Med.*, vol. 185, no. 8, pp. 825–834, 2012, doi: 10.1164/rccm.201106-1150OC.

[11] R. Budhidarmo, Y. Nakatani, and C. L. Day, “RINGs hold the key to ubiquitin transfer,” *Trends Biochem. Sci.*, vol. 37, no. 2, pp. 58–65, 2012, doi: 10.1016/j.tibs.2011.11.001.

[12] Y. Ye and M. Rape, “Building ubiquitin chains: E2 enzymes at work,” *Nat. Rev. Mol. Cell Biol.*, vol. 10, no. 11, pp. 755–764, 2009, doi: 10.1038/nrm2780.

[13] M. D. Stewart, T. Ritterhoff, R. E. Klevit, and P. S. Brzovic, “E2 enzymes : more than just middle men,” *Nat. Publ. Gr.*, vol. 26, no. 4, pp. 423–440, 2016, doi: 10.1038/cr.2016.35.

[14] D. Komander and M. Rape, “The Ubiquitin Code,” *Annu. Rev. Biochem.*, vol. 81, no. 1, pp. 203–229, 2012, doi: 10.1146/annurev-biochem-060310-170328.

[15] C. Polge *et al.*, “A muscle-specific MuRF1-E2 network requires stabilization of MuRF1-E2 complexes by telethonin, a newly identified substrate,” *J. Cachexia. Sarcopenia Muscle*, vol. 9, no. 1, pp. 129–145, 2018, doi: 10.1002/jcsm.12249.

[16] J. G. Marblestone *et al.*, “Comprehensive Ubiquitin E2 Profiling of Ten Ubiquitin E3 Ligases,” *Cell Biochem. Biophys.*, vol. 67, no. 1, pp. 161–167, 2013, doi: 10.1007/s12013-013-9627-3.

[17] Y. Maejima *et al.*, “Muscle-specific RING finger 1 negatively regulates pathological cardiac hypertrophy through downregulation of calcineurin A,” *Circ. Hear. Fail.*, vol. 7, no. 3, pp. 479–490, 2014, doi: 10.1161/CIRCHEARTFAILURE.113.000713.

[18] V. Kedar, H. McDonough, R. Arya, H. H. Li, H. A. Rockman, and C. Patterson, “Muscle-specific RING finger 1 is a bona fide ubiquitin ligase that degrades cardiac troponin I,” *Proc. Natl. Acad. Sci. U. S. A.*, vol. 101, no. 52, pp. 18135–18140, 2004, doi: 10.1073/pnas.0404341102.

[19] C. Polge *et al.*, “ Muscle actin is polyubiquitinylated in vitro and in vivo and targeted for breakdown by the E3 ligase MuRF1 ,” *FASEB J.*, vol. 25, no. 11, pp. 3790–3802, 2011, doi: 10.1096/fj.11-180968.

[20] J. Fielitz *et al.*, “Myosin accumulation and striated muscle myopathy result from the loss of muscle RING finger 1 and 3,” *J. Clin. Invest.*, vol. 117, no. 9, pp. 2486–2495, 2007, doi: 10.1172/JCI32827.

[21] T. Centner *et al.*, “Identification of muscle specific ring finger proteins as potential regulators of the titin kinase domain,” *J. Mol. Biol.*, vol. 306, no. 4, pp. 717–726, 2001, doi: 10.1006/jmbi.2001.4448.

[22] M. S. Willis, C. Ike, L. Li, D. Z. Wang, D. J. Glass, and C. Patterson, “Muscle ring finger 1, but not muscle ring finger 2, regulates cardiac hypertrophy in vivo,” *Circ. Res.*, vol. 100, no. 4, pp. 456–459, 2007, doi: 10.1161/01.RES.0000259559.48597.32.

[23] M. S. Willis *et al.*, “Muscle ring finger 1 and muscle ring finger 2 are necessary but functionally redundant during developmental cardiac growth and regulate E2F1-

mediated gene expression in vivo," *Cell Biochem. Funct.*, vol. 32, no. 1, pp. 39–50, 2014, doi: 10.1002/cbf.2969.

[24] C. C. Witt, S. H. Witt, S. Lerche, D. Labeit, W. Back, and S. Labeit, "Cooperative control of striated muscle mass and metabolism by MuRF1 and MuRF2," *EMBO J.*, vol. 27, no. 2, pp. 350–360, 2008, doi: 10.1038/sj.emboj.7601952.

[25] M. Olivé *et al.*, "New cardiac and skeletal protein aggregate myopathy associated with combined MuRF1 and MuRF3 mutations," *Hum. Mol. Genet.*, vol. 24, no. 13, pp. 3638–3650, 2015, doi: 10.1093/hmg/ddv108.

[26] C. H. Emmerich and P. Cohen, "Optimising methods for the preservation, capture and identification of ubiquitin chains and ubiquitylated proteins by immunoblotting," *Biochem. Biophys. Res. Commun.*, vol. 466, no. 1, pp. 1–14, 2015, doi: 10.1016/j.bbrc.2015.08.109.

[27] D. C. Hughes *et al.*, "Alterations in the muscle force transfer apparatus in aged rats during unloading and reloading: impact of microRNA-31," *J. Physiol.*, vol. 596, no. 14, pp. 2883–2900, 2018, doi: 10.1113/JP275833.

[28] L. M. Baehr *et al.*, "Age-related deficits in skeletal muscle recovery following disuse are associated with neuromuscular junction instability and ER stress, not impaired protein synthesis," *Aging (Albany. NY).*, vol. 8, no. 1, pp. 127–146, 2016, doi: 10.18632/aging.100879.

[29] A. J. Fletcher, D. L. Mallery, R. E. Watkinson, C. F. Dickson, L. C. James, and J. Luban, "Sequential ubiquitination and deubiquitination enzymes synchronize the dual sensor and effector functions of TRIM21," *Proc. Natl. Acad. Sci. U. S. A.*, vol. 112, no. 32, pp. 10014–10019, 2015, doi: 10.1073/pnas.1507534112.

[30] A. J. Fletcher *et al.*, " TRIM 5α requires Ube2W to anchor Lys63-linked ubiquitin chains and restrict reverse transcription ," *EMBO J.*, vol. 34, no. 15, pp. 2078–2095, 2015, doi: 10.15252/embj.201490361.

[31] P. S. Brzovic and R. E. Klevit, "Ubiquitin transfer from the E2 perspective: Why is UbcH5 so promiscuous?," *Cell Cycle*, vol. 5, no. 24, pp. 2867–2873, 2006, doi: 10.4161/cc.5.24.3592.

[32] A. S. McElhinny, K. Kakinuma, H. Sorimachi, S. Labeit, and C. C. Gregorio, "Muscle-specific RING finger-1 interacts with titin to regulate sarcomeric M-line and thick filament structure and may have nuclear functions via its interaction with glucocorticoid modulatory element binding protein-1," *J. Cell Biol.*, vol. 157, no. 1, pp. 125–136, 2002, doi: 10.1083/jcb.200108089.

[33] C. C. Gregorio, C. N. Perry, and A. S. Mcelhinny, "Functional properties of the titin/connectin-associated proteins, the muscle-specific RING finger proteins (MURFs), in striated muscle," *J. Muscle Res. Cell Motil.*, vol. 26, no. 6–8, pp. 389–400, 2005, doi: 10.1007/s10974-005-9021-x.

[34] M. Mrosek *et al.*, “Molecular determinants for the recruitment of the ubiquitin-ligase MuRF-1 onto M-line titin,” *FASEB J.*, vol. 21, no. 7, pp. 1383–1392, 2007, doi: 10.1096/fj.06-7644com.

[35] E. Müller, S. Salcan, S. Bongardt, D. M. Barbosa, M. Krüger, and S. Kötter, “E3-ligase knock down revealed differential titin degradation by autopagy and the ubiquitin proteasome system,” *Sci. Rep.*, vol. 11, no. 1, pp. 1–13, 2021, doi: 10.1038/s41598-021-00618-7.

[36] S. H. Witt, H. Granzier, C. C. Witt, and S. Labeit, “MURF-1 and MURF-2 Target a Specific Subset of Myofibrillar Proteins Redundantly: Towards Under-standing MURF-dependent Muscle Ubiquitination,” 2005, doi: 10.1016/j.jmb.2005.05.021.

[37] S. Cohen *et al.*, “During muscle atrophy, thick, but not thin, filament components are degraded by MuRF1-dependent ubiquitylation,” *J. Cell Biol.*, vol. 185, no. 6, pp. 1083–1095, 2009, doi: 10.1083/jcb.200901052.

[38] L. M. Baehr *et al.*, “Identification of the MuRF1 skeletal muscle ubiquitylome through quantitative proteomics,” *Am. Physiol. Soc. - Funct.*, vol. 2, no. May, pp. 14–27, 2021.

[39] D. C. Hughes, L. M. Baehr, J. R. Driscoll, S. A. Lynch, D. S. Waddell, and S. C. Bodine, “Identification and characterization of Fbxl22, a novel skeletal muscle atrophy-promoting E3 ubiquitin ligase,” *Am. J. Physiol. - Cell Physiol.*, vol. 319, no. 4, pp. C700–C719, 2020, doi: 10.1152/ajpcell.00253.2020.

[40] T. K. Hyoung *et al.*, “Certain pairs of ubiquitin-conjugating enzymes (E2s) and ubiquitin-protein ligases (E3s) synthesize nondegradable forked ubiquitin chains containing all possible isopeptide linkages,” *J. Biol. Chem.*, vol. 282, no. 24, pp. 17375–17386, 2007, doi: 10.1074/jbc.M609659200.

[41] C. Polge *et al.*, “UBE2D2 is not involved in MuRF1-dependent muscle wasting during hindlimb suspension,” *Int. J. Biochem. Cell Biol.*, vol. 79, pp. 488–493, 2016, doi: 10.1016/j.biocel.2016.06.019.

[42] J. Bogomolovas *et al.*, “Titin kinase ubiquitination aligns autophagy receptors with mechanical signals in the sarcomere,” *EMBO Rep.*, vol. 22, no. 10, pp. 1–14, 2021, doi: 10.15252/embr.201948018.

[43] S. Lange *et al.*, “The Kinase Domain of Titin,” *Science (80-.).*, vol. 308, no. June, pp. 1599–1603, 2005.

[44] S. Cohen, B. Zhai, S. P. Gygi, and A. L. Goldberg, “Ubiquitylation by Trim32 causes coupled loss of desmin, Z-bands, and thin filaments in muscle atrophy,” *J. Cell Biol.*, vol. 198, no. 4, pp. 575–589, 2012, doi: 10.1083/jcb.201110067.

[45] G. Agnetti, H. Herrmann, and S. Cohen, “New roles for desmin in the maintenance of muscle homeostasis,” *FEBS J.*, vol. 289, no. 10, pp. 2755–2770, 2022, doi: 10.1111/febs.15864.

[46] P. Cécile *et al.*, “UBE2E1 is preferentially expressed in the cytoplasm of slow-twitch fibers and protects skeletal muscles from exacerbated atrophy upon dexamethasone treatment,” *Cells*, vol. 7, no. 11, 2018, doi: 10.3390/cells7110214.

[47] L. C. Hunt *et al.*, “Integrated genomic and proteomic analyses identify stimulus-dependent molecular changes associated with distinct modes of skeletal muscle atrophy,” *Cell Rep.*, vol. 37, no. 6, p. 109971, 2021, doi: 10.1016/j.celrep.2021.109971.

Chapter 4

Method Development – Perturbation of MuRF1 Ubiquitylation

4.1 Background

The overarching aim of this thesis is to establish MuRF1's mechanistic role to provide targets for future anti-atrophy therapies (50,93). Having characterized its ubiquitylation mechanisms, the next objective was to identify potential methods to perturb MuRF1 activity. The exploration focused on three methods: 1) assessing the importance of substrate attachment in the process of MuRF1-mediated ubiquitylation, 2) pinpointing the specific amino acids on substrates that are marked for ubiquitylation, and 3) examining whether a confirmed MuRF1 inhibitor can obstruct the ubiquitylation process in a controlled, in-vitro setting.

Titin A168-A170 was selected as a suitable substrate, which has been well-characterized structurally as a MuRF1 interactor and substrate (91,94,110–112). Titin's identified MuRF1 binding domain and prior use as a substrate in development of a MuRF1 inhibitor provide avenues to explore perturbing MuRF1's substrate ubiquitylation activity (113). Histidine-tagged Titin A168-A170 has been purified to homogeneity and binding to MuRF1 assessed by isothermal titration calorimetry and NMR, identifying key interacting residues (110). In cell models MuRF1 has been shown to co-precipitate with Titin A168-Titin Kinase Region (Just beyond A168) and is necessary for the ubiquitylation of this Titin fragment (114). Furthermore, ubiquitylation of Titin with wildtype versus a validated MuRF1 inhibitor was assessed in-vitro (113). Together, characterizing the MuRF1-Titin interaction and inhibitor effects on MuRF1 activity establishes foundations for future studies on substrate targeting and inhibitor mechanisms which could inform therapy development (115).

4.2 Experiment 1 – Does Mutation of the MuRF1 Binding site on Titin A168-A170 Impair MuRF1 Ubiquitylation Activity?

4.2.1 Introduction

Mrosek et al. published the first crystal structure of the Titin A168-A170 segment in 2007(110). Using recombinant proteins containing amino acids 168-170 from the Titin A-domain, they were able to crystallize the fragment and solve its structure to high resolution of 2.2 angstroms using X-ray crystallography.

The structure revealed the A168-A170 region forms a compact three-helix bundle conformation stabilized by hydrophobic interactions between residues on each helix. This globular structure represented a small subdomain within the larger mostly alpha-helical Titin A-domain. In silico protein-protein docking with the known coil-coil domain structure of MuRF1 allowed the authors to computationally model its interaction. The modelling predicted a stable complex could form between Titin's second helix containing residues 102KTLE105 and a groove on MuRF1's coil-coil domain composed of hydrophobic patches.

This putative interaction interface indicated these sequences were critical for the Titin-MuRF1 association. A quadruple alanine substitution was generated (102KTLE105→AAAA) in recombinant Titin A168-A170 to disrupt potential coil-coil interactions. Co-precipitation assays were then utilized to assess binding, which

showed that MuRF1 coil-coil domain was unable to be co-precipitated with Titin A168-A170 with the AAAA mutation.

The aim is to build on this knowledge by co-precipitating Titin A168-A170 with the 102KTLE105 to AAAA mutation, with a full-length MuRF1 protein. This will be followed by an *in-vitro* ubiquitylation assay to explore its impact on MuRF1 ubiquitylation activity.

4.2.2 Assessing the MuRF1 and Titin A168-A170 Interaction After Mutation of Binding Site 102KTLE105 of Titin A168-A170.

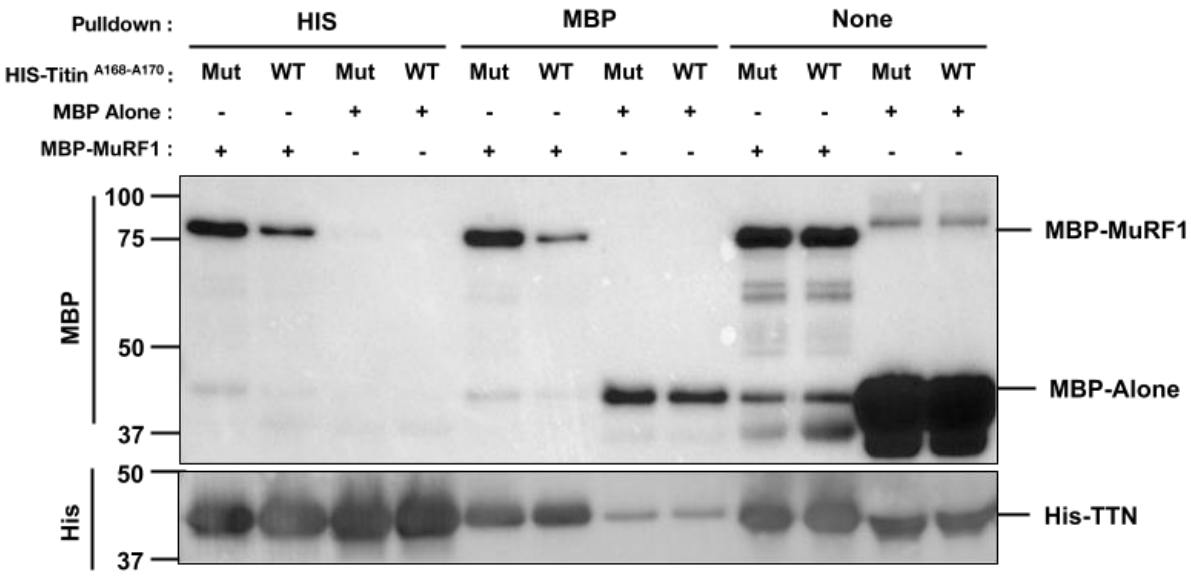

Figure 4. 1 - Mutation of HIS-titin(A168-A170) 102KTLE105 to AAAA does not stop interaction with MuRF1.

Recombinant HIS-Titin A168-A170 and MBP-MuRF1/MBP were co-incubated and subjected to pulldown with Ni-Sepharose or Amylose beads to isolate HIS and MBP tags, respectively. Samples were washed on a spin column and prepared for western blot analysis with LDS buffer and MBP or HIS antibodies.

When HIS was pulled down (lanes 1-4), HIS-Titin A168-A170 was detected alongside MBP-MuRF1, which was co-precipitated with WT and mutant HIS-Titin. MBP alone was not present after His pull-down, confirming there was no unwanted MBP precipitation.

For MBP pulldowns (lanes 5-8), MBP-MuRF1 (Lanes 5-6) and MBP (Lanes 7-8) were

detected as expected. Interestingly, MBP-alone pulldown resulted in a small amount of HIS-Titin A168-A170 (WT and Mutant) were co-precipitated; MBP-MuRF1 co-precipitated a greater amount of HIS-Titin A168-A170 than MBP-Alone. Input protein controls lacking pulldown are in lanes 9-12.

This data demonstrates that regardless of mutation, Titin and MuRF1 co-precipitated upon pulldown of either protein. This suggests the proposed binding site is not solely responsible for the interaction, as mutation did not reduce or block co-precipitation. In summary, MuRF1 and Titin A168-A170 interact in-vitro independent of the binding site 102KTLE105.

4.2.3 In-Vitro Ubiquitylation Assay of Titin A168-A170, With and Without Binding Site Mutation, by MuRF1.

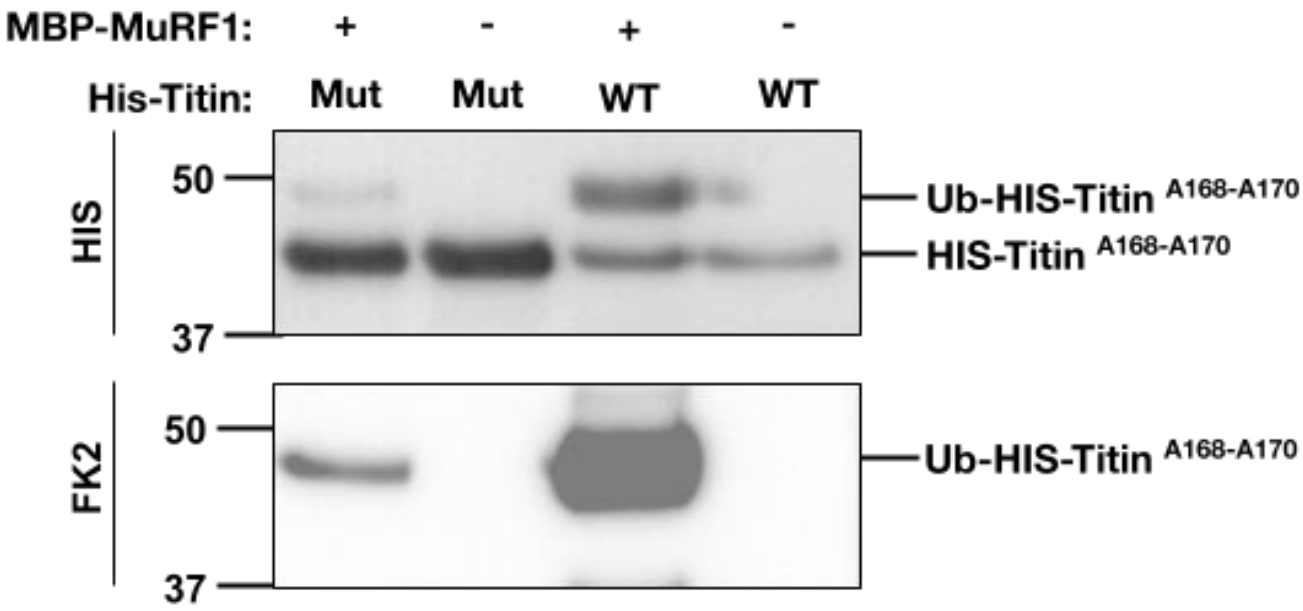

Figure 4. 2 - Mutation of HIS-titin A168-A170 102KTLE105 to AAAA does not stop ubiquitylation by MBP-MuRF1 *in-vitro*.

Wildtype or mutant (102KTLE105→AAAA) HIS-Titin A168-A170 were incubated with or without MBP-MuRF1 for 1 hour.

Samples were separated by SDS-PAGE and proteins visualized by immunoblotting with anti-HIS (top panel) and anti-ubiquitin FK2 antibodies (bottom panel).

Mutation of the 102KTLE105 sequence to AAAA reduced mono-ubiquitylation of Titin A168-A170 by the MuRF1-UBE2W system. While mutant HIS-Titin could still be mono-ubiquitylated, the stoichiometry was greatly decreased relative to wildtype.

The results validate the 102KTLE105 sequence as important for the MuRF1-Titin interaction mediating ubiquitylation.

Though mutant HIS-Titin (A168-A170) AAAA could still be mono-ubiquitylated by MuRF1, as shown by immunoblotting (Figure 4.2, Upper Panel), the stoichiometry was greatly reduced compared to wildtype, as seen in (Figure 4.2, Lower Panel). Therefore, mutating the 102KTLE105 sequence impairs ubiquitylation as expected based on the known binding interface but does not observably inhibit MuRF1-Titin interaction. This suggests this motif is not solely responsible for their interaction and subsequent ubiquitylation, which appears to involve additional contacts beyond the predicted residues.

4.3 Experiment 2 – Identifying the ubiquitylation residue of Titin A168-A170.

4.3.1 Mass Spectrometry

Having detected mono-ubiquitylation of Titin A168-A170 with MuRF1-E2 cooperation, mass spectrometry was employed to identify the specific ubiquitylated residue(s). The *in-vitro* ubiquitylation assay was performed as previously, followed by SDS-PAGE. The mono-ubiquitylated Titin A168-A170 band was excised and submitted for proteomic analysis as outlined in the methods section.

Mass spectrometry revealed five ubiquitylation sites, including three methionine and two lysine residues (Fig 4.4). One site was on the HIS-tag and another at K316 of Titin A168-A170. The use of mass spectrometry proteomics successfully identified candidate ubiquitylation sites on Titin after detecting its modification by MuRF1 and an E2 *in-vitro*. This advanced the understanding of how MuRF1 may directly modify substrates at the amino acid level.

MKHHHHHHPMSDYDIPTTENLYFQGAMAPHFKEELRNLNVRYQSNATLVCKVTGHPKPIVKWYRQ GKEIIADGLKYRIQEFKGGYHQLIIASVTDDDATVYQVRATNQGGSVSGTASLEVEVPAKIHLPKTLEG MGAVHALRGEVVSIKIPFSGKPDPVITWQKGQDLIDNNGHYQVIVTRSFTSLVFPNGVERKDAGFYVV CAKNRFGIDQKTVELDVADVPDPPRGVKVSDVSRDSVNLTWTEPASDGGSKITNYIVEKCATTAERWL RVGQARETRYTVINLFGKTSYQFRVIAENKFGLSKPSEPSEPTITKEDKTRAMNYDEEV

Figure 4. 3 - Amino Acid Structure of HIS-Titin A168-A170.

Amino acid sequence mapping the HIS-Titin A168-A170 used in this thesis. Blue represents the HIS-tag, red highlights the TEV protease cleavage site, and grey is the Titin A168-A170 sequence.

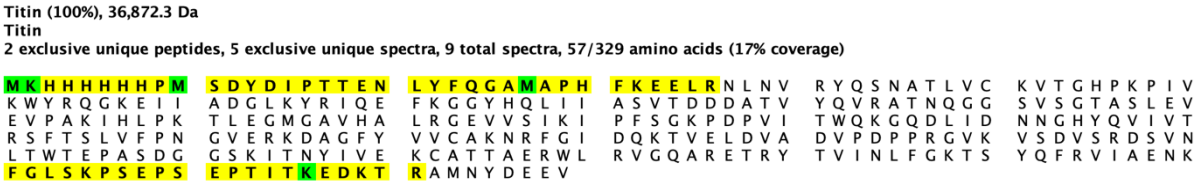

Figure 4. 4 - The amino acid sequence of ubiquitylated titin, with mass spectrometry predictions of the peptides ubiquitylated.

The mass spectrometry results highlighted regions in yellow indicating peptides predicted to be ubiquitylated, with the methionine and lysines in those peptides highlighted in green as potential residues for ubiquitylation. As only N-Terminal methionine can be ubiquitylated, M1 is the only methionine available to be ubiquitylated; however, N-terminal methionine is a universal target for ubiquitylation of all proteins, i.e. its ubiquitylation in this instance doesn't provide any insights about the characteristics of Titin, specifically. The lysines highlighted (K2 and K316) could be eliminated to just lysine 316 (K316) as a discreet Titin residue for MuRF1 ubiquitylation, as it was within the Titin A168-A170 sequence instead of the non-native HIS tag.

4.3.2. In-Vitro Ubiquitylation Assay Evaluation of the predicted ubiquitylation residues on Titin A168-A170

This discovery prompted exploration of whether K316 exclusively served as the ubiquitylation site. The K316R mutant gene was created, expressed, and purified using established protocols in section 2.2.

To discern the targeted residue, in-vitro ubiquitylation assays were conducted with MuRF1 and UBE2W using: wildtype control, K316R mutant, wildtype without HIS, and K316R HIS-Titin A168-A170 without HIS. These were analysed by SDS-PAGE to determine the specific ubiquitylation site without ambiguities arising from the HIS-tag. This targeted mutagenesis approach aimed to validate K316 as the residue singly modified by MuRF1.

The K136R mutation in His-Titin (A168-A170) exhibits no significant impact on MuRF1-mediated mono-ubiquitylation, as illustrated in Figure 4.5. Nevertheless, eliminating the HIS-tag leads to a reduction in the stoichiometry of MuRF1-mediated ubiquitylation, irrespective of the presence of K316R mutants. These results strongly indicate that MuRF1-mediated mono-ubiquitylation predominantly occurs within the HIS-Tag region, hinting at a potential promiscuous capability of MuRF1 to ubiquitylate its substrate on various accessible amino acids.

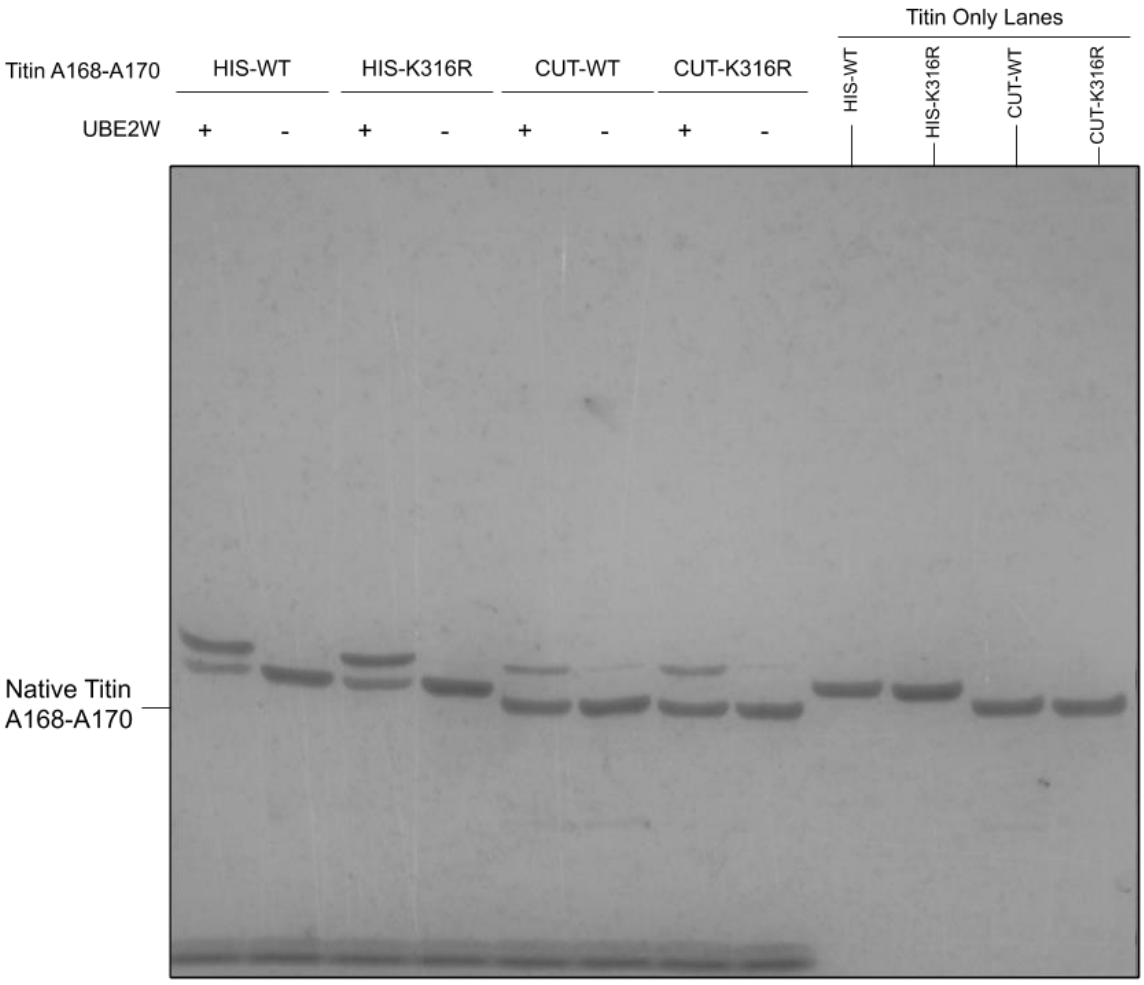

Figure 4. 5 - Examination of the potential ubiquitylation sites of Titin A168-A170, with removal of the HIS-tag and mutation of K316.

HIS-tagged Titin (A168-A170) with combination of K316R mutation and HIS-tag cleavage were incubated with or without UBE2W and MBP-MuRF1 for 1 hr. Proteins were separated by SDS-PAGE and detected by Coomassie blue stain.

4.4 Experiment 3 - Assessing the impact of a known MuRF1 inhibitor on Auto- and Substrate-ubiquitylation *in-vitro*.

4.4.1 Identification of a validated MuRF1 inhibitor in the current literature.

A search of the literature identified a potential MuRF1 inhibitor; Bowen et al performed a high-throughput screen of 130,000 compounds identified compounds that inhibited the interaction between MuRF1 and its substrate titin. One compound, ID#704946, was selected based on potency, specificity, and low toxicity (113).

In cell, 704946 attenuated MuRF1 expression and myotube atrophy induced by dexamethasone in C2C12 myotubes. In mice, monocrotaline treatment induced cardiac cachexia characterized by weight loss, muscle wasting and contractile dysfunction. Mice treated with monocrotaline and treated with 704946 were protected from skeletal muscle wasting, particularly in the tibialis anterior muscle. Contractile dysfunction was also prevented (113).

Proteomic and biochemical analyses suggested 704946 stabilized protein translation and suppressed apoptosis. MuRF1 expression and ubiquitylation/degradation of its substrate titin were also reduced.

This data suggests that inhibiting the MuRF1-titin interaction with a small molecule protected against muscle wasting and contractile dysfunction in a mouse model of cardiac cachexia.

4.4.2 Does a Validated MuRF1 Inhibitor Prevent the Ubiquitylation of Titin A168-A170 *In-Vitro.*

A concentration of 40μM was used as this was the initial concentration used by Bowen 2014 (113) when screening for MuRF1-Titin inhibitors; 10μM of inhibitor 704946 was shown to be effective at perturbing atrophy in-vivo.

In-vitro ubiquitylation assays were performed, as previously described, with the addition of inhibitor 704946 and use of HIS-SUMO-MuRF1. Proteins were denatured using LDS, separated by SDS-PAGE, and stained using InstantBlue (Abcam, Cambridge UK). UBE2W and UBE2D2 were used to explore both mono-ubiquitylation and poly-ubiquitylation of MuRF1.

Control (No UBE2) showed the protein abundance in the reaction without ubiquitylation (Fig 4.6). UBE2W and UBE2D2 were able to ubiquitylate HIS-Titin A168-A170, as shown by the addition of an upper band and decrease in the native HIS-Titin A168-A170 band; the addition of inhibitor 704946 did not produce any change in the stoichiometry of ubiquitylated HIS-Titin A168-A170. To add further confidence to this result HIS-SUMO-MuRF1 was subject to equal levels of ubiquitylation, independent of UBE2 or Inhibitor 704946 (Figure 4.6). This result was confirmed by western blotting for HIS-tag (Fig 4.7), where the interaction of MuRF1 with UBE2W causes mono-ubiquitylation – demonstrated by the additional band appearing above both HIS-SUMO-MuRF1 and HIS-Titin (A168-A170); the interaction of MuRF1 and UBE2D2 generates polyubiquitylation of HIS-SUMO-MuRF1 and HIS-

Titin (A168-A170) demonstrated by the lower stoichiometry of the native protein, and presence of an upper smear in both HIS and Ubiquitin antibody blots (Fig 4.7). . The addition of inhibitor 704946 did not cause a visible change in the ubiquitylation of either MuRF1 or Titin (A168-A170, indicating that there was no difference between reactions run with or without the inhibitor 704946.

To confirm this result was due to ubiquitylation and that it was on the HIS-Titin A168-A170 and HIS-SUMO-MuRF1, western blots were performed with HIS and Ubiquitin antibodies. This confirmed no ubiquitylation occurs when UBE2 are not present and the addition of mono-ubiquitylation bands for HIS-SUMO-MuRF1 and HIS-Titin A168-A170 are present when incubated with UBE2W. Poly-ubiquitin chains were formed in cooperation with UBE2D2 as shown in the ubiquitin antibody panel. Neither mono nor poly-ubiquitylation were perturbed by inhibitor 704946.

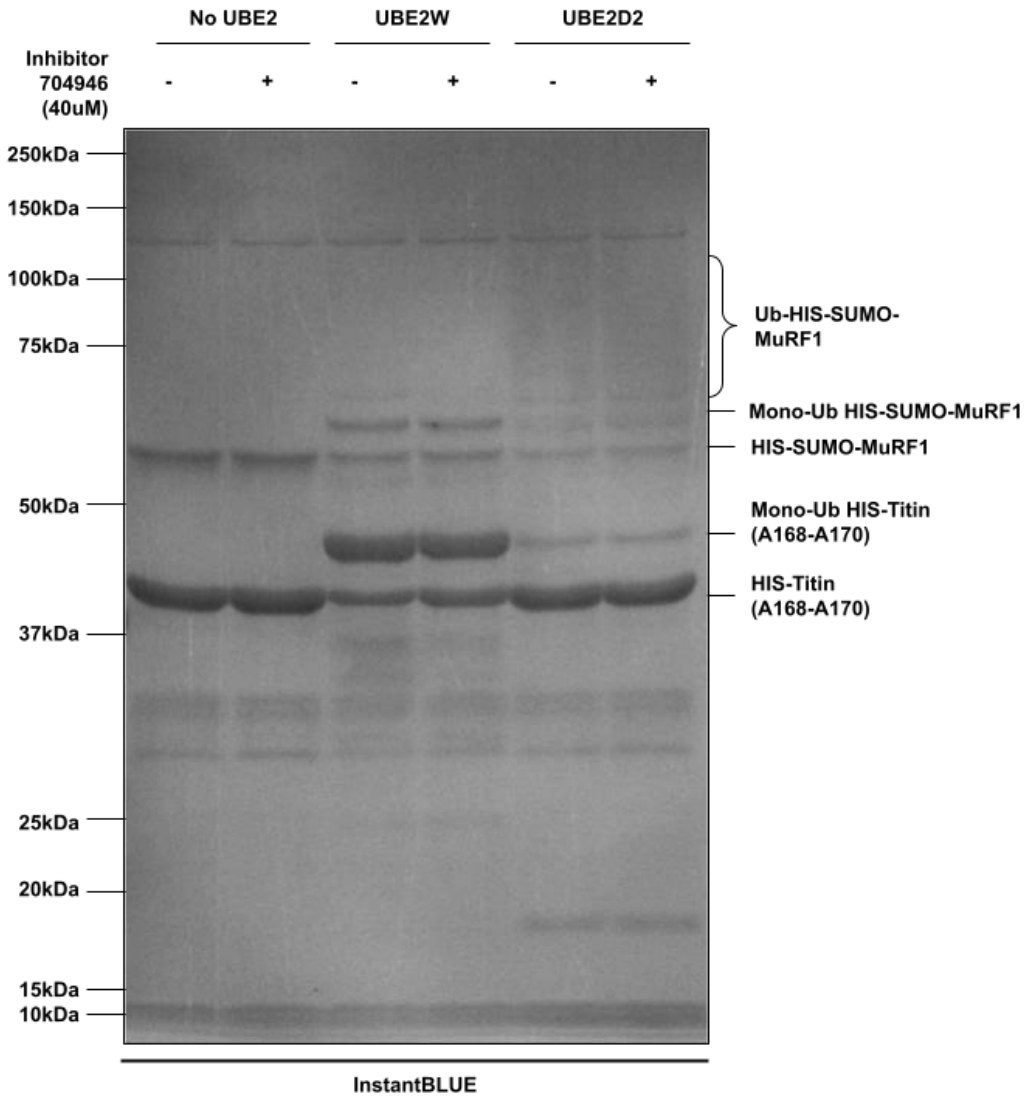

Figure 4. 6 - Staining of *in-vitro* Reaction of MuRF1 with HIS-Titin A168-A170, with and without Inhibitor 704946.

HIS-tagged Titin (A168-A170) and HIS-SUMO-MuRF1 were incubated alone, with UBE2W, and UBE2D2 for 1 hr. Proteins were separated by SDS-PAGE and detected by staining.

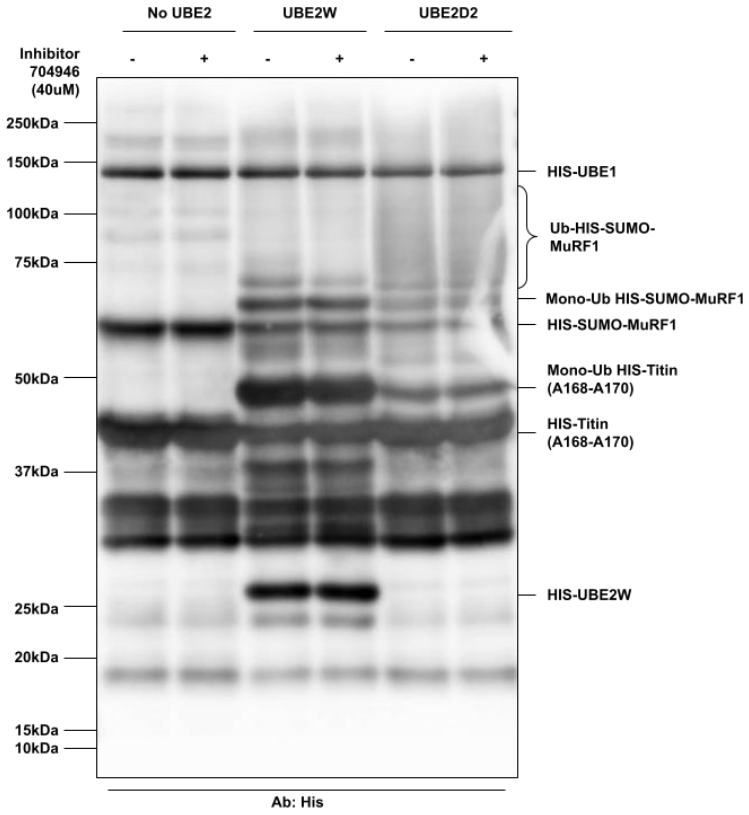
No UBE2
UBE2W
UBE2D2
Inhibitor 704946 (40uM)
- + - + - +
250kDa
150kDa
100kDa
75kDa
50kDa
37kDa
25kDa
20kDa
15kDa
10kDa
HIS-UBE1
Ub-HIS-SUMO-MuRF1
Mono-Ub HIS-SUMO-MuRF1
HIS-SUMO-MuRF1
Mono-Ub HIS-Titin (A168-A170)
HIS-Titin (A168-A170)
HIS-UBE2W
Ab: His

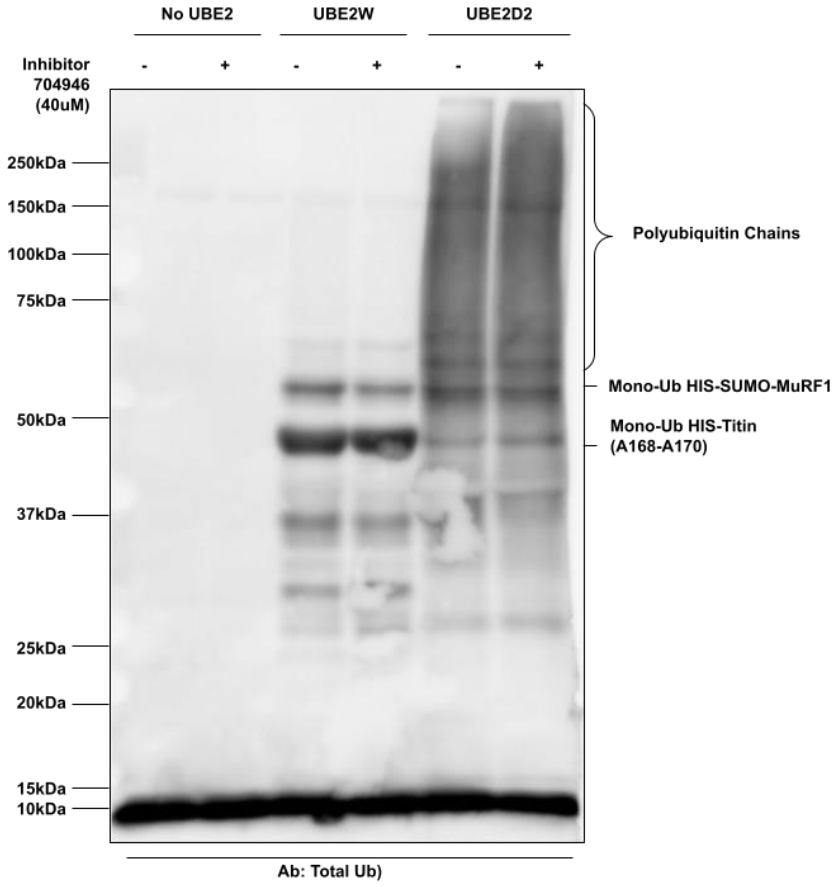
No UBE2
UBE2W
UBE2D2
Inhibitor 704946 (40uM)
- + - + - +
250kDa
150kDa
100kDa
75kDa
50kDa
37kDa
25kDa
20kDa
15kDa
10kDa
Polyubiquitin Chains
Mono-Ub HIS-SUMO-MuRF1
Mono-Ub HIS-Titin (A168-A170)
Ab: Total Ub)

Figure 4. 7 - Western Blot of *in-vitro* Reaction of MuRF1 with HIS-Titin A168-A170, with and without Inhibitor 704946.

HIS-tagged Titin (A168-A170) and HIS-SUMO-MuRF1 were incubated alone, with UBE2W, and UBE2D2 for 1 hr. Proteins were separated by SDS-PAGE and detected by western blot using HIS and Total Ubiquitin antibodies.

4.5 Discussion

This chapter presents experimental investigations into the mechanisms of MuRF1-mediated ubiquitylation and potential disruption techniques, contributing to our knowledge of MuRF1's molecular function and its association with muscle atrophy. The research also underscores the intricacies of devising targeted interventions.

The first experiment elucidates the vital role of the 102KTLE105 sequence in the MuRF1-Titin ubiquitylation, which was did not appear to be driven by interaction. Residual ubiquitylation upon mutation indicates other contributing contacts. This necessitates additional studies to fully understand the MuRF1-Titin interaction and its ubiquitylation consequences. Further work would need to be conducted to establish the reason why the interaction does not appear impaired, but MuRF1 activity is. As SDS-PAGE and Western Blot are more quantitative, than qualitative assay, it would be useful to examine the physical structure of the MuRF1-Titin interaction post-mutation of the binding site. This would establish if the spatial relationship to MuRF1 was altered in such a way to influence Titin’s proclivity to be ubiquitylated.

Mass spectrometry analysis in the second experiment demonstrates MuRF1's broad ubiquitylation capacity across various accessible amino acids on HIS-Titin A168-A170; the ubiquitylation of the HIS-Tag region is of particular interest as this is not a native structure, merely present as an artifact of the protein purification process, and therefore MuRF1 has not evolved in parallel with the HIS tag. This promiscuous ubiquitylation poses challenges for pinpointing specific ubiquitylation sites, suggesting a sophisticated mechanism in which the ability of MuRF1 to interact with a substrate is

the limiting factor to its ability to ubiquitylate, and not its preference of a discreet lysine residue. This warrants further investigation into its structural ubiquitylation tendencies and regulatory implications of this activity.

The third experiment's evaluation of a known MuRF1 inhibitor, compound 704946, in *in-vitro* ubiquitylation assays, contrasts with its reported efficacy in cellular and *in-vivo* muscle atrophy models, showing negligible inhibition *in-vitro*. This discrepancy could arise from experimental condition variances, additional regulatory components in more complex biological systems, or limitations inherent to *in-vitro* assays, emphasizing the necessity for thorough inhibitor efficacy validation in diverse models.

In summary, the research underscores the sophisticated nature of MuRF1's ubiquitylation operations and the hurdles in creating specific muscle atrophy treatments. Although the experiments advance our molecular understanding of MuRF1's functionalities, they also highlight the imperative for continued research to unravel MuRF1-mediated ubiquitylation and discover effective perturbation strategies. Future studies integrating structural, biochemical, and cellular methodologies promise to enhance our grasp of MuRF1's role in muscle atrophy and lead to novel therapeutic avenues for this debilitating ailment.

4.6 References

1. Frontera WR, Ochala J. Skeletal Muscle: A Brief Review of Structure and Function. Calcif Tissue Int. 2015 Mar 8;96(3):183–95.

2. Baskin KK, Winders BR, Olson EN. Muscle as a “Mediator” of Systemic Metabolism. Cell Metab. 2015 Feb;21(2):237–48.

3. Bonaldo P, Sandri M. Cellular and molecular mechanisms of muscle atrophy. Dis Model Mech. 2013;6(1):25–39.

4. DeFronzo RA, Jacot E, Jequier E, Maeder E, Wahren J, Felber JP. The Effect of Insulin on the Disposal of Intravenous Glucose: Results from Indirect Calorimetry and Hepatic and Femoral Venous Catheterization. Diabetes. 1981 Dec 1;30(12):1000–7.

5. Rai M, Demontis F. Systemic Nutrient and Stress Signaling via Myokines and Myometabolites. Annu Rev Physiol. 2016 Feb 10;78(1):85–107.

6. Argilés JM, Campos N, Lopez-Pedrosa JM, Rueda R, Rodriguez-Mañas L. Skeletal Muscle Regulates Metabolism via Interorgan Crosstalk: Roles in Health and Disease. J Am Med Dir Assoc. 2016;17(9):789–96.

7. Meyer C, Dostou JM, Welle SL, Gerich JE. Role of human liver, kidney, and skeletal muscle in postprandial glucose homeostasis. American Journal of Physiology-Endocrinology and Metabolism. 2002 Feb 1;282(2):E419–27.

8. Sartori R, Romanello V, Sandri M. Mechanisms of muscle atrophy and hypertrophy: implications in health and disease. Nat Commun. 2021 Dec 1;12(1):1–12.

9. Nishimura Y, Musa I, Holm L, Lai YC. Recent advances in measuring and understanding the regulation of exercise-mediated protein degradation in skeletal muscle. American Journal of Physiology-Cell Physiology. 2021 Aug 1;321(2):C276–87.

10. Roubenoff R, Hughes VA. Sarcopenia: Current Concepts. J Gerontol A Biol Sci Med Sci. 2000 Dec 1;55(12):M716–24.

11. Fielding RA, Vellas B, Evans WJ, Bhasin S, Morley JE, Newman AB, et al. Sarcopenia: An Undiagnosed Condition in Older Adults. Current Consensus Definition: Prevalence, Etiology, and Consequences. International Working Group on Sarcopenia. J Am Med Dir Assoc. 2011 May;12(4):249–56.

12. Alajlouni DA, Bliuc D, Tran TS, Blank RD, Cawthon PM, Ensrud KE, et al. Muscle Strength and Physical Performance Are Associated With Risk of Postfracture Mortality But Not Subsequent Fracture in Men. Journal of Bone and Mineral Research. 2020 Dec 1;37(8):1571–9.

13. Alajlouni D, Bliuc D, Tran T, Eisman JA, Nguyen T V, Center JR. Decline in Muscle Strength and Performance Predicts Fracture Risk in Elderly Women and Men. J Clin Endocrinol Metab. 2020 Sep 1;105(9):e3363–73.

14. Cruz-Jentoft AJ, Baeyens JP, Bauer JM, Boirie Y, Cederholm T, Landi F, et al. Sarcopenia: European consensus on definition and diagnosis. Age Ageing. 2010 Jul 1;39(4):412–23.

15. Batsis JA, Villareal DT. Sarcopenic obesity in older adults: aetiology, epidemiology and treatment strategies. Nat Rev Endocrinol. 2018 Sep;14(9):513–37.

16. Beaudart C, Zaaria M, Pasleau F, Reginster JY, Bruyère O. Health Outcomes of Sarcopenia: A Systematic Review and Meta-Analysis. Wright JM, editor. PLoS One. 2017 Jan 17;12(1):e0169548.

17. Phillips T, Leeuwenburgh C. Muscle fiber-specific apoptosis and TNF-α signaling in sarcopenia are attenuated by life-long calorie restriction. The FASEB Journal. 2005 Apr 21;19(6):1–33.

18. Marzetti E, Calvani R, Tosato M, Cesari M, Di Bari M, Cherubini A, et al. Sarcopenia: an overview. Aging Clin Exp Res. 2017 Feb 2;29(1):11–7.

19. Beaudart C, Rolland Y, Cruz-Jentoft AJ, Bauer JM, Sieber C, Cooper C, et al. Assessment of Muscle Function and Physical Performance in Daily Clinical Practice. Calcif Tissue Int. 2019 Jul 10;105(1):1–14.

20. Dedeyne L, Dupont J, Koppo K, Verschueren S, Tournoy J, Gielen E. Exercise and Nutrition for Healthy AgeiNg (ENHANce) project – effects and mechanisms of action of combined anabolic interventions to improve physical functioning in sarcopenic older adults: study protocol of a triple blinded, randomized controlled trial. BMC Geriatr. 2020 Dec 10;20(1):532.

21. Meyer C, Dostou JM, Welle SL, Gerich JE. Role of human liver, kidney, and skeletal muscle in postprandial glucose homeostasis. American Journal of Physiology-Endocrinology and Metabolism [Internet]. 2002 Feb 1;282(2):E419–27. Available from: https://www.physiology.org/doi/10.1152/ajpendo.00032.2001

22. Cuthbertson D, Smith K, Babraj J, Leese G, Waddell T, Atherton P, et al. Anabolic signaling deficits underlie amino acid resistance of wasting, aging muscle. The FASEB Journal. 2005 Mar 13;19(3):1–22.

23. Volpi E, Nazemi R, Fujita S. Muscle tissue changes with aging. Curr Opin Clin Nutr Metab Care. 2004 Jul;7(4):405–10.

24. Volpi E, Sheffield-Moore M, Rasmussen BB, Wolfe RR. Basal Muscle Amino Acid Kinetics and Protein Synthesis in Healthy Young and Older Men. JAMA. 2001 Sep 12;286(10):1206.

25. Dickinson JM, Volpi E, Rasmussen BB. Exercise and Nutrition to Target Protein Synthesis Impairments in Aging Skeletal Muscle. Exerc Sport Sci Rev. 2013 Oct;41(4):216–23.

26. Argilés JM, Busquets S, Stemmler B, López-Soriano FJ. Cancer cachexia: understanding the molecular basis. Nat Rev Cancer. 2014 Nov 9;14(11):754–62.

27. Fearon KCH, Glass DJ, Guttridge DC. Cancer Cachexia: Mediators, Signaling, and Metabolic Pathways. Cell Metab. 2012 Aug;16(2):153–66.

28. Berardi E, Madaro L, Lozanoska-Ochser B, Adamo S, Thorrez L, Bouche M, et al. A Pound of Flesh: What Cachexia Is and What It Is Not. Diagnostics. 2021 Jan 12;11(1):116.

29. Dewys WD, Begg C, Lavin PT, Band PR, Bennett JM, Bertino JR, et al. Prognostic effect of weight loss prior tochemotherapy in cancer patients. Am J Med. 1980 Oct;69(4):491–7.

30. Fearon K, Strasser F, Anker SD, Bosaeus I, Bruera E, Fainsinger RL, et al. Definition and classification of cancer cachexia: an international consensus. Lancet Oncol. 2011 May;12(5):489–95.

31. Martin L, Birdsell L, MacDonald N, Reiman T, Clandinin MT, McCargar LJ, et al. Cancer Cachexia in the Age of Obesity: Skeletal Muscle Depletion Is a Powerful Prognostic Factor, Independent of Body Mass Index. Journal of Clinical Oncology. 2013 Apr 20;31(12):1539–47.

32. Argilés JM, Busquets S, Stemmler B, López-Soriano FJ. Cancer cachexia: understanding the molecular basis. Nat Rev Cancer. 2014 Nov 9;14(11):754–62.

33. Webster JM, Kempen LJAP, Hardy RS, Langen RCJ. Inflammation and Skeletal Muscle Wasting During Cachexia. Front Physiol. 2020 Nov 19;11.

34. Setiawan T, Sari IN, Wijaya YT, Julianto NM, Muhammad JA, Lee H, et al. Cancer cachexia: molecular mechanisms and treatment strategies. J Hematol Oncol. 2023 May 22;16(1):54.

35. Petruzzelli M, Wagner EF. Mechanisms of metabolic dysfunction in cancer-associated cachexia. Genes Dev. 2016 Mar 1;30(5):489–501.

36. Fearon KCH, Glass DJ, Guttridge DC. Cancer Cachexia: Mediators, Signaling, and Metabolic Pathways. Cell Metab. 2012 Aug;16(2):153–66.

37. Baracos VE, Martin L, Korc M, Guttridge DC, Fearon KCH. Cancer-associated cachexia. Nat Rev Dis Primers. 2018 Jan 18;4(1):17105.

38. Tipton KD, Hamilton DL, Gallagher IJ. Assessing the Role of Muscle Protein Breakdown in Response to Nutrition and Exercise in Humans. Vol. 48, Sports Medicine. 2018.

39. Mitch WE, Goldberg AL. Mechanisms of Muscle Wasting — The Role of the Ubiquitin–Proteasome Pathway. Epstein FH, editor. New England Journal of Medicine. 1996 Dec 19;335(25):1897–905.

40. Lecker SH, Jagoe RT, Gilbert A, Gomes M, Baracos V, Bailey J, et al. Multiple types of skeletal muscle atrophy involve a common program of changes in gene expression. The FASEB Journal. 2004;18(1):39–51.

41. Sandri M. Protein breakdown in muscle wasting: Role of autophagy-lysosome and ubiquitin-proteasome. International Journal of Biochemistry and Cell Biology. 2013;45(10):2121–9.

42. Hinde KL, O'Leary TJ, Greeves JP, Wardle SL. Measuring Protein Turnover in the Field: Implications for Military Research. Adv Nutr. 2021 Jun 1;12(3):887–96.

43. Cegielski J, Wilkinson DJ, Brook MS, Boereboom C, Phillips BE, Gladman JFR, et al. Combined in vivo muscle mass, muscle protein synthesis and muscle protein breakdown measurement: a 'Combined Oral Stable Isotope Assessment of Muscle (COSIAM)' approach. Geroscience. 2021 Dec 27;43(6):2653–65.

44. Elia M, Carter A, Bacon S, Winearls CG, Smith R. Clinical usefulness of urinary 3-methylhistidine excretion in indicating muscle protein breakdown. Br Med J (Clin Res Ed). 1981 Jan 31;282(6261):351–4.

45. Kochlik B, Gerbracht C, Grune T, Weber D. The Influence of Dietary Habits and Meat Consumption on Plasma 3-Methylhistidine—A Potential Marker for Muscle Protein Turnover. Mol Nutr Food Res. 2018 May 19;62(9).

46. Young VR, Munro HN. Ntau-methylhistidine (3-methylhistidine) and muscle protein turnover: an overview. Fed Proc. 1978 Jul;37(9):2291–300.

47. Ciechanover A, Orian A, Schwartz AL. Ubiquitin-mediated proteolysis: biological regulation via destruction. BioEssays. 2000 Apr 24;22(5):442–51.

48. Yang Q, Zhao J, Chen D, Wang Y. E3 ubiquitin ligases: styles, structures and functions. Molecular Biomedicine. 2021 Dec 30;2(1):23.

49. Sandri M, Sandri C, Gilbert A, Skurk C, Calabria E, Picard A, et al. Foxo Transcription Factors Induce the Atrophy-Related Ubiquitin Ligase Atrogin-1 and Cause Skeletal Muscle Atrophy. Cell. 2004 Apr;117(3):399–412.

50. Glass DJ. Skeletal muscle hypertrophy and atrophy signaling pathways. Int J Biochem Cell Biol. 2005 Oct;37(10):1974–84.

51. Mizushima N, Komatsu M. Autophagy: Renovation of Cells and Tissues. Cell. 2011 Nov;147(4):728–41.

52. Mizushima N, Levine B. Autophagy in mammalian development and differentiation. Nat Cell Biol. 2010 Sep;12(9):823–30.

53. Masiero E, Agatea L, Mammucari C, Blaauw B, Loro E, Komatsu M, et al. Autophagy Is Required to Maintain Muscle Mass. Cell Metab. 2009;10(6):507–15.

54. Kocaturk NM, Gozuacik D. Crosstalk Between Mammalian Autophagy and the Ubiquitin-Proteasome System. Front Cell Dev Biol. 2018 Oct 2;6.

55. Milan G, Romanello V, Pescatore F, Armani A, Paik JH, Frasson L, et al. Regulation of autophagy and the ubiquitin–proteasome system by the FoxO transcriptional network during muscle atrophy. Nat Commun. 2015 Apr 10;6(1):6670.

56. Hershko A, Ciechanover A. THE UBIQUITIN SYSTEM. Annu Rev Biochem. 1998 Jun;67(1):425–79.

57. Koepp DM. Cell Cycle Regulation by Protein Degradation. In 2014. p. 61–73.

58. Henry KW, Wyce A, Lo WS, Duggan LJ, Emre NCT, Kao CF, et al. Transcriptional activation via sequential histone H2B ubiquitylation and deubiquitylation, mediated by SAGA-associated Ubp8. Genes Dev. 2003 Nov 1;17(21):2648–63.

59. Goldberg AL. Protein degradation and protection against misfolded or damaged proteins. Nature. 2003 Dec;426(6968):895–9.

60. Duan S, Pagano M. Ubiquitin ligases in cancer: Functions and clinical potentials. Cell Chem Biol. 2021 Jul;28(7):918–33.

61. Rubinsztein DC. The roles of intracellular protein-degradation pathways in neurodegeneration. Nature. 2006 Oct 18;443(7113):780–6.

62. Lecker SH. Ubiquitin-protein ligases in muscle wasting: multiple parallel pathways? Curr Opin Clin Nutr Metab Care. 2003 May;6(3):271–5.

63. Hershko A, Ciechanover A, Heller H, Haas AL, Rose IA. Proposed role of ATP in protein breakdown: conjugation of protein with multiple chains of the polypeptide of ATP-dependent proteolysis. Proceedings of the National Academy of Sciences. 1980 Apr;77(4):1783–6.

64. Hershko A, Heller H, Elias S, Ciechanover A. Components of ubiquitin-protein ligase system. Resolution, affinity purification, and role in protein breakdown. J Biol Chem. 1983 Jul 10;258(13):8206–14.

65. Joazeiro CAP, Weissman AM. RING Finger Proteins. Cell. 2000 Sep;102(5):549–52.

66. Pickart CM, Eddins MJ. Ubiquitin: structures, functions, mechanisms. Biochimica et Biophysica Acta (BBA) - Molecular Cell Research. 2004 Nov;1695(1–3):55–72.

67. Ikeda F, Dikic I. Atypical ubiquitin chains: New molecular signals. “Protein Modifications: Beyond the Usual Suspects” Review Series. Vol. 9, EMBO Reports. 2008. p. 536–42.

68. Komander D, Rape M. The Ubiquitin Code. Annu Rev Biochem. 2012 Jul 7;81(1):203–29.

69. Kulathu Y, Komander D. Atypical ubiquitylation — the unexplored world of polyubiquitin beyond Lys48 and Lys63 linkages. Nat Rev Mol Cell Biol. 2012 Aug 23;13(8):508–23.

70. Heride C, Urbé S, Clague MJ. Ubiquitin code assembly and disassembly. Current Biology. 2014 Mar;24(6):R215–20.

71. McDowell GS, Philpott A. Non-canonical ubiquitylation: Mechanisms and consequences. Int J Biochem Cell Biol. 2013 Aug;45(8):1833–42.

72. Li X, Han M, Zhang H, Liu F, Pan Y, Zhu J, et al. Structures and biological functions of zinc finger proteins and their roles in hepatocellular carcinoma. Biomark Res. 2022 Dec 9;10(1):2.

73. Husnjak K, Dikic I. Ubiquitin-Binding Proteins: Decoders of Ubiquitin-Mediated Cellular Functions. Annu Rev Biochem. 2012 Jul 7;81(1):291–322.

74. Ciechanover A. The ubiquitin-proteasome proteolytic pathway. Cell. 1994 Oct;79(1):13–21.

75. Smith DM, Chang SC, Park S, Finley D, Cheng Y, Goldberg AL. Docking of the Proteasomal ATPases' Carboxyl Termini in the 20S Proteasome's α Ring Opens the Gate for Substrate Entry. Mol Cell. 2007 Sep;27(5):731–44.

76. Finley D. Recognition and Processing of Ubiquitin-Protein Conjugates by the Proteasome. Annu Rev Biochem. 2009 Jun 1;78(1):477–513.

77. Groll M, Ditzel L, Löwe J, Stock D, Bochtler M, Bartunik HD, et al. Structure of 20S proteasome from yeast at 2.4Å resolution. Nature. 1997 Apr;386(6624):463–71.

78. Haas AL, Rose IA. The mechanism of ubiquitin activating enzyme. A kinetic and equilibrium analysis. J Biol Chem. 1982 Sep 10;257(17):10329–37.

79. Schulman BA, Wade Harper J. Ubiquitin-like protein activation by E1 enzymes: the apex for downstream signalling pathways. Nat Rev Mol Cell Biol. 2009 May 8;10(5):319–31.

80. Henneberg LT, Schulman BA. Decoding the messaging of the ubiquitin system using chemical and protein probes. Cell Chem Biol. 2021 Jul;28(7):889–902.

81. Nandi D, Tahiliani P, Kumar A, Chandu D. The ubiquitin-proteasome system. J Biosci. 2006 Mar 1;31(1):137–55.

82. Michelle C, Vourc'h P, Mignon L, Andres CR. What Was the Set of Ubiquitin and Ubiquitin-Like Conjugating Enzymes in the Eukaryote Common Ancestor? J Mol Evol. 2009 Jun 19;68(6):616–28.

83. Deshaies RJ, Joazeiro CAP. RING Domain E3 Ubiquitin Ligases. Annu Rev Biochem. 2009 Jun 1;78(1):399–434.

84. Rotin D, Kumar S. Physiological functions of the HECT family of ubiquitin ligases. Nat Rev Mol Cell Biol. 2009 Jun 13;10(6):398–409.

85. Freemont PS. Ubiquitination: RING for destruction? Current Biology. 2000;10(2):84–7.

86. Lorick KL, Jensen JP, Fang S, Ong AM, Hatakeyama S, Weissman AM. RING fingers mediate ubiquitin-conjugating enzyme (E2)-dependent ubiquitination. Proceedings of the National Academy of Sciences. 1999 Sep 28;96(20):11364–9.

87. Aravind L, Koonin E V. The U box is a modified RING finger — a common domain in ubiquitination. Current Biology. 2000 Feb;10(4):R132–4.

88. Breckel CA, Hochstrasser M. Ubiquitin Ligase Redundancy and Nuclear-Cytoplasmic Localization in Yeast Protein Quality Control. Biomolecules. 2021 Dec 3;11(12):1821.

89. Wenzel DM, Lissounov A, Brzovic PS, Klevit RE. UBCH7 reactivity profile reveals parkin and HHARI to be RING/HECT hybrids. Nature. 2011 Jun 1;474(7349):105–8.

90. Cornelissen T, Vilain S, Vints K, Gounko N, Verstreken P, Vandenberghe W. Deficiency of parkin and PINK1 impairs age-dependent mitophagy in Drosophila. Elife. 2018 May 29;7.

91. Centner T, Yano J, Kimura E, McElhinny AS, Pelin K, Witt CC, et al. Identification of muscle specific ring finger proteins as potential regulators of the titin kinase domain. J Mol Biol. 2001;306(4):717–26.

92. Centner T, Yano J, Kimura E, McElhinny AS, Pelin K, Witt CC, et al. Identification of muscle specific ring finger proteins as potential regulators of the titin kinase domain. J Mol Biol. 2001;306(4):717–26.

93. Bodine SC, Latres E, Baumhueter S, Lai VKM, Nunez L, Clarke BA, et al. Identification of ubiquitin ligases required for skeletal Muscle Atrophy. Science (1979). 2001;294(5547):1704–8.

94. McElhinny AS, Kakinuma K, Sorimachi H, Labeit S, Gregorio CC. Muscle-specific RING finger-1 interacts with titin to regulate sarcomeric M-line and thick filament structure and may have nuclear functions via its interaction with glucocorticoid modulatory element binding protein-1. Journal of Cell Biology. 2002;157(1):125–36.

95. Clarke BA, Drujan D, Willis MS, Murphy LO, Corpina RA, Burova E, et al. The E3 Ligase MuRF1 Degrades Myosin Heavy Chain Protein in Dexamethasone-Treated Skeletal Muscle. Cell Metab. 2007;6(5):376–85.

96. Bodine SC, Latres E, Baumhueter S, Lai VKM, Nunez L, Clarke BA, et al. Identification of ubiquitin ligases required for skeletal Muscle Atrophy. Science (1979). 2001;294(5547):1704–8.

97. Labeit S, Kohl CH, Witt CC, Labeit D, Jung J, Granzier H. Modulation of muscle atrophy, fatigue and MLC phosphorylation by MuRF1 as indicated by hindlimb suspension studies on MuRF1-KO mice. J Biomed Biotechnol. 2010;

98. Baehr LM, Furlow JD, Bodine SC. Muscle sparing in muscle RING finger 1 null mice: Response to synthetic glucocorticoids. Journal of Physiology. 2011;589(19):4759–76.

99. Hwee DT, Baehr LM, Philp A, Baar K, Bodine SC. Maintenance of muscle mass and load-induced growth in Muscle RING Finger 1 null mice with age. Aging Cell. 2014;13(1):92–101.

100. Cohen S, Brault JJ, Gygi SP, Glass DJ, Valenzuela DM, Gartner C, et al. During muscle atrophy, thick, but not thin, filament components are degraded by MuRF1-dependent ubiquitylation. Journal of Cell Biology. 2009;185(6):1083–95.

101. Hirner S, Krohne C, Schuster A, Hoffmann S, Witt S, Erber R, et al. MuRF1-dependent Regulation of Systemic Carbohydrate Metabolism as Revealed from Transgenic Mouse Studies. J Mol Biol. 2008 Jun;379(4):666–77.

102. Willis MS, Schisler JC, Li L, Rodríguez JE, Hilliard EG, Charles PC, et al. Cardiac Muscle Ring Finger-1 Increases Susceptibility to Heart Failure In Vivo. Circ Res. 2009 Jul 2;105(1):80–8.

103. Chen SN, Czernuszewicz G, Tan Y, Lombardi R, Jin J, Willerson JT, et al. Human molecular genetic and functional studies identify TRIM63, encoding muscle RING finger protein 1, as a novel gene for human hypertrophic cardiomyopathy. Circ Res. 2012;111(7):907–19.

104. Jokela M, Baumann P, Huovinen S, Penttilä S, Udd B. Homozygous Nonsense Mutation p.Q274X in TRIM63 (MuRF1) in a Patient with Mild Skeletal Myopathy and Cardiac Hypertrophy. J Neuromuscul Dis. 2019 Jan 30;6(1):143–6.

105. Salazar-Mendiguchía J, Ochoa JP, Palomino-Doza J, Domínguez F, Díez-López C, Akhtar M, et al. Mutations in TRIM63 cause an autosomal-recessive form of hypertrophic cardiomyopathy. Heart. 2020 Sep;106(17):1342–8.

106. Bodine SC, Baehr LM. Skeletal muscle atrophy and the E3 ubiquitin ligases MuRF1 and MAFbx/atrogin-1. Am J Physiol Endocrinol Metab. 2014;307(6):E469–84.

107. Stewart MD, Ritterhoff T, Klevit RE, Brzovic PS. E2 enzymes: More than just middle men. Cell Res. 2016;26(4):423–40.

108. Polge C, Cabantous S, Deval C, Claustre A, Hauvette A, Bouchenot C, et al. A muscle-specific MuRF1-E2 network requires stabilization of MuRF1-E2 complexes by telethonin, a newly identified substrate. J Cachexia Sarcopenia Muscle. 2018;9(1):129–45.

109. Jackman RW, Kandarian SC. The molecular basis of skeletal muscle atrophy. American Journal of Physiology-Cell Physiology. 2004 Oct;287(4):C834–43.

110. Mrosek M, Labeit D, Witt S, Heerklotz H, von Castelmur E, Labeit S, et al. Molecular determinants for the recruitment of the ubiquitin-ligase MuRF-1 onto M-line titin. The FASEB Journal. 2007;21(7):1383–92.

111. Mrosek M, Meier S, Ucurum-Fotiadis Z, Von Castelmur E, Hedbom E, Lustig A, et al. Structural analysis of B-box 2 from MuRF1: Identification of a novel self-association pattern in a RING-like fold. Biochemistry. 2008;47(40):10722–30.

112. Higashikuse Y, Mittal N, Arimura T, Yoon SH, Oda M, Enomoto H, et al. Perturbation of the titin/MURF1 signaling complex is associated with hypertrophic cardiomyopathy in a fish model and in human patients. DMM Disease Models and Mechanisms. 2019;12(11).

113. Bowen TS, Adams V, Werner S, Fischer T, Vinke P, Brogger MN, et al. Small-molecule inhibition of MuRF1 attenuates skeletal muscle atrophy and dysfunction in cardiac cachexia. J Cachexia Sarcopenia Muscle. 2017 Dec;8(6):939–53.

114. Bogomolovas J, Fleming JR, Franke B, Manso B, Simon B, Gasch A, et al. Titin kinase ubiquitination aligns autophagy receptors with mechanical signals in the sarcomere. EMBO Rep. 2021;22(10):1–14.

115. Scalabrin M, Adams V, Labeit S, Bowen TS. Emerging strategies targeting catabolic muscle stress relief. Int J Mol Sci. 2020;21(13):1–18.

Chapter 5 The Mechanisms of MuRF1

- A Review

Title: The Mechanisms of MuRF1 Ubiquitylation

Journal submission: Physical Activity (Asian Society of Kinesiology)

Authorship: Peter W.J. Dawson[1,2] Jimi Ng [1], and Yu-Chiang Lai[1,2,3,a]

Affiliations:

[1]School of Sport, Exercise and Rehabilitation Sciences, University of Birmingham, Birmingham, UK.

[2]MRC Versus Arthritis Centre for Musculoskeletal Ageing Research, University of Birmingham, Birmingham, UK.

[3]Institute of Metabolism and Systems Research, University of Birmingham, Birmingham, UK.

[a] **Corresponding Author:**

Dr. Yu-Chiang Lai[1,2,3]

5.1 Abstract

MuRF1 (TRIM63) has been long known as a critical regulator in skeletal muscle atrophy. Over two decades of research has made evident that MuRF1's expression is critical to the development of muscle atrophy. However, the development of atrophy inhibiting pharmaceuticals targeting MuRF1 has been hindered as MuRF1's ubiquitin E3 ligase activity remains uncharacterised. The mechanism regulating MuRF1 activity, substrate recognition, and downstream effectors are unclear. This review aims to highlight the current research of molecular mechanisms by providing insights regarding MuRF1's cooperating UBE2s, the topology of MuRF1 ubiquitylation, and the fates of MuRF1 substrates.

ABBREVIATIONS

AR, Acidic Region; ATG7, Autophagy Related 7; CHIP, carboxy-terminus of Hsc70 interacting protein; COS, C-terminal Subgroup One Signature; DCAF8, DDB1 And CUL4 Associated Factor 8; FBxl22, F-Box And Leucine Rich Repeat Protein 22; IGF1, Insulin-like growth factor 1; IL-6, interleukin 6; IRS-1, Insulin receptor substrate 1; MAFbx, Muscle Atrophy F-box; MFC, MuRF Family Conserved; MPB, Muscle Protein Breakdown; MPS, Muscle Protein Synthesis; UPS, Ubiquitin-Proteasome System; MuRF1, Muscle-specific RING finger protein 1; MUSA1, muscle ubiquitin ligase of SCF complex in atrophy-1 (Also, F-box protein 30); MYLPF, Mylpf myosin light chain, phosphorylatable, fast skeletal muscle; NBR1, Neighbor of BRCA1 gene 1; PDK-1, Phosphoinositide-dependent kinase-1; PI3K, Phosphoinositide 3-kinase; PKB, Protein

kinase B; PTM, Post-translational Modification; RBCC, RING–B-box–coiled-coil; RING, Really Interesting New Gene; SUMO, Small Ubiquitin-like Modifier; TNF, Tumour Necrosis Factor; TRIM, Tripartite motif; UBE1, Ubiquitin Activating Enzyme; UBE2, Ubiquitin Conjugating Enzyme; UBE3, Ubiquitin Ligase Enzyme.

5.2 Murf1 As A Critical Regulator Of Skeletal Muscle Atrophy

Introduction

Skeletal muscle atrophy occurs as a response to behavioural changes (e.g. inactivity, bed rest, and malnutrition). Atrophy is a symptom of many pathologies, such as cancer, diabetes, and sepsis, which is directly associated with increased mortality of those diseases (1). The long-term atrophy present in ageing (sarcopenia), and the associated strength loss, are correlated with decreased lifespan (2,3). To uncover the underlying mechanism of atrophy, most of the previous research has focussed on the Ubiquitin-Proteasome system (UPS) as the primary contributor of muscle protein breakdown (4–7). Ubiquitin is a small modifying protein involved in post-translational modification (PTM) known as ubiquitylation. This is an enzymatic process where ubiquitin is covalently attached to a substrate protein, determined by an E3 ligase enzyme. For the UPS, ubiquitylated proteins are recognised and degraded by 26S proteasome. Muscle-specific RING finger protein 1 (MuRF1; gene name TRIM63) has captured the interest of researchers as a regulator of muscle atrophy, because it is ubiquitously expressed in most of atrophic conditions and its deletion preserves muscle from atrophy.

Discovery of MuRF1 in Skeletal Muscle Atrophy

MuRF1 was first identified by characterising myofibrillar proteins interacting with the kinase domain of Titin (8). It was found to be exclusively expressed in muscle tissue, implying its unique functioning role in muscle. At a similar time, Bodine et al. used transcriptional profiling to identify atrophy-specific genes in rats and found that MuRF1/TRIM63 gene is highly expressed in models of atrophy, including dexamethasone treatment, interleukin-1 treatment, denervation, immobilisation, and limb unloading (9). Having established MuRF1 expression in multiple atrophic models, Bodine et al. went on to demonstrate MuRF1 as an atrophic mediator. They showed that mice with MuRF1 deletion were spared 36% of the muscle loss induced by denervation (9). Following studies have reinforced MuRF1's role in atrophy, as its genetic deletion perturbs multiple atrophic phenotypes. Dexamethasone is a glucocorticoid, commonly used for the treatment of inflammation, such as rheumatic conditions and for post-surgery recovery. Recently dexamethasone was used as an effective treatment for Covid-19 induced lung damage, increasing the survival rates of hospitalised patients (10). Unfortunately, dexamethasone is known to induce muscle loss through regular high-dose administration, making dexamethasone treatment a useful atrophy model. Mice with MuRF1 gene knock-out (MuRF1-KO) are spared the decreases in muscle mass following dexamethasone treatment (11). This protective effect of MuRF1-KO also prevents immobilisation- and ageing-induced atrophy (12,13). MuRF1's universal role in underpinning muscle atrophy cemented its role as a regulator of muscle atrophy.

Mechanisms of muscle protein turnover

Skeletal muscle mass is determined by muscle protein turnover, a product of muscle protein synthesis (MPS) and muscle protein breakdown (MBP). MPS has been well explored by its sequence of phosphorylation events. With well-characterised protein kinases and known phosphorylated residues, resulting in increased protein synthesis (Figure 5.1) (14). In contrast, the MBP signalling pathway is poorly characterised. There are several known stimuli, such as inflammation, cancer, or ageing, which cause an atrophic phenotype resulting in the expression of MuRF1, MAFbx, and other E3 ligases. The increased expression of E3-ligases is associated with an increase in ubiquitylated proteins (15). Despite best efforts to profile these proteins, a comprehensive list remains incomplete. Furthermore, how these ubiquitylated proteins contribute to MPB remains unclear. Despite the activity of the proteasomal and lysosomal degradation increasing during atrophy (16), evidence has suggested that not all ubiquitylated proteins are destined for breakdown (11). The ubiquitylation of some protein could act as a signal to enhance proteasomal or lysosomal activity in MPB (Without being subject to degradation themselves).

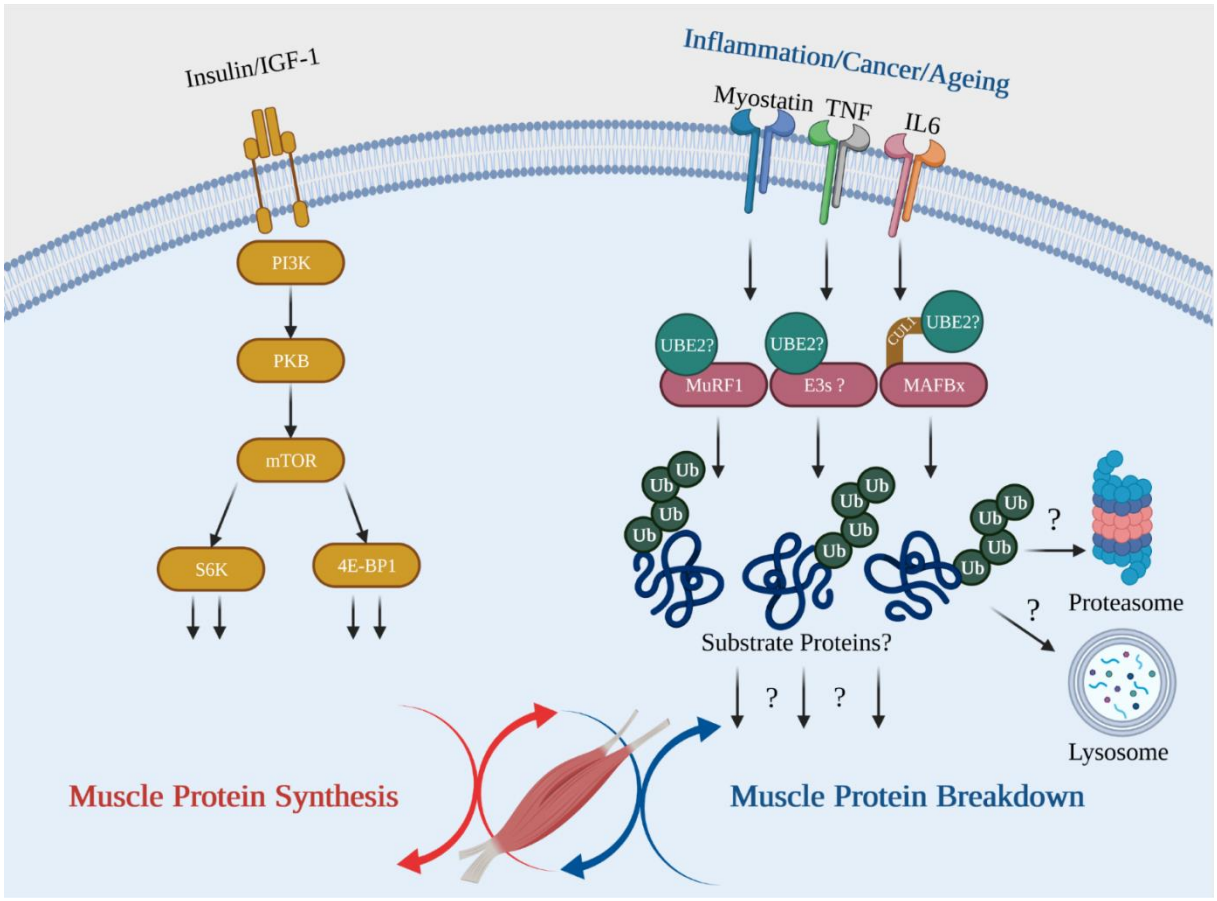

Figure 5. 1 - Schematic diagram showing the pathways regulating muscle protein synthesis and muscle protein breakdown.

UPS accounts for 60% of MPB (16) and as MuRF1 is a ubiquitin E3-ligase, research has focused on its role in UPS-mediated degradation. Studies showed that both MuRF1's expression (17) and function (18) are essential for the degradation of myofibrillar proteins, supporting the hypothesis that MuRF1 is a mediator of MPB. However, some studies have challenged this hypothesis. For example, MuRF1-KO mice showed increases in proteasomal activity in muscles following denervation-induced atrophy (19). Furthermore, recent proteomic screening reveals that the majority of MuRF1 targets are not subject to degradation (11). Therefore, the role of

MuRF1's contribution to atrophy requires further investigation.

Ubiquitylation

As a ubiquitin E3 ligase, MuRF1 functions to modify proteins by the process of ubiquitylation. Ubiquitylation is a sequential process involving three enzymes: Ubiquitin Activating Enzyme (UBE1), which uses ATP to activate free ubiquitin; Ubiquitin Conjugating Enzyme (UBE2) binds to the activated ubiquitin; (RING-type) Ubiquitin Ligase Enzyme (UBE3), coordinated with UBE2 and a target substrate to transfer ubiquitin to an available lysine or n-terminal methionine. Ubiquitylation is a sophisticated post-translational modification (PTM). Ubiquitin can be attached as three topologies, as either mono-ubiquitin (a single ubiquitin bound to a substrate), multi-ubiquitin (many single ubiquitin added to different residues of one substrate), or poly-ubiquitin chains (a polymer of ubiquitin that can be linear or branched). Poly-ubiquitin chains are further distinguished by their ubiquitin-ubiquitin binding at seven lysines (K6, K11, K27, K29, K33, K48, and K63) or on their N-terminal methionine (M1) (20,21). Early experiments have shown that K48 is a dominant chain causing proteasomal degradation (22). Further evidence suggests that K11, K29, and K63 linkages can also initiate proteasomal degradation (23). As research has progressed, ubiquitin is implicated in other degradation systems. For example, mono-ubiquitylation and K63 chains have been identified as regulators of lysosome-mediated autophagy (24). Sometimes, ubiquitylation can provide activation/inhibition of enzymatic activity (For review see (20)). However, this diversity of ubiquitylation function has not been studied in relation to MuRF1. MuRF1 has been shown to

generate both K48 and K63 chains (25,26), suggesting functionality beyond proteasomal degradation. The recently characterised ubiquitylome of MuRF1 identified 56 ubiquitylated proteins, only one of which decreased in abundance and 22 increasing in abundance (11). This suggests the direct ubiquitylation by MuRF1 is not exclusively mediating degradation.

MuRF1 is evidently an important regulator of muscle mass. However, researchers are presented with the challenge: elucidating how MuRF1 contributes to muscle atrophy. To overcome this challenge, researchers must explore the biochemical properties of MuRF1 and its biological functioning as a E3-ligase. The aim of this review is to present an overview of the current literature of MuRF1's biochemical mechanisms, with particular attention to MuRF1's structure, interacting UBE2s, MuRF1-mediated ubiquitin architecture, and the fate of MuRF1 substrates. This is to highlight the areas that require research and some potential targets that can be exploited for new therapeutic strategies.

5.3 Murf1 As A Trim/Rbcc Ubiquitin E3 Ligase

TRIM Proteins

MuRF1 is part of a family of over 70 proteins, called tripartite motif (TRIM) or RING–B-box–coiled-coil (RBCC) (27–29). This protein family shares three conserved structures, a RING (Really interesting new gene) domain, one or two B-box motifs,

and a coiled-coil domain (27), and is classified as RING-type E3-ligase. In fact, the RING-type E3-ligases have no catalytic activity alone but act as a scaffold to recruit both a UBE2 and substrate, thereby allowing UBE2 to transfer ubiquitin to an available lysine or n-terminal methionine.

RING, MFC, and B-Box domains

The N-terminal of MuRF1 begins with the RING domain (residues 14 to 79), a subclass of the zinc finger domain. (Figure 5.2A). The RING domain is responsible for the interaction of UBE2s (30–32). The MuRF family conserved (MFC; residue 80-113) region is exclusive to MuRF proteins, located directly after the N-terminal RING domain. To date, no function of this domain has been identified. The B-Box 2 domain (Residue 117-159) is another zinc finger domain with a different conserved peptide sequence to RING domain. Structural analysis of MuRF1 B-Box 2 predicted its role in the stabilisation of MuRF1 dimerisation (33).

Coiled-coil, COS-Box, and Acidic Region

The coiled-coil (Residues 166-269) domain is a helical structure. Its stability is dependent on its flanking domains—B-Box and COS—securing the correct self-assembly (34). The coil-coil functions to dimerise in an antiparallel arrangement, resulting in a homodimer with the coiled-coils centred between 2 RING-B-Box domains (Figure 5.2C) (35). This also allows for repeat recruitment of further proteins or enzymes into an oligomer (36), therefore further post-translational modification can be introduced. Oligomerisation has been reported as crucial to auto-ubiquitylation for

TRIM-type E3 ligases (37,38). The C-terminal of MuRF1 contains a COS-Box and unstructured acidic region (AR). The COS-Box (Residues 269-328) forms part of the helical structure with the coiled-coil domain. The use of immunostaining and microscopy shows that the COS-Box domain causes MuRF1 localisation to the Z-line/M-line area in muscle (34). With C-terminal structures being unique to each TRIM protein, the COS-Box and AR place a critical role in the recognition of MuRF1 specific substrate.

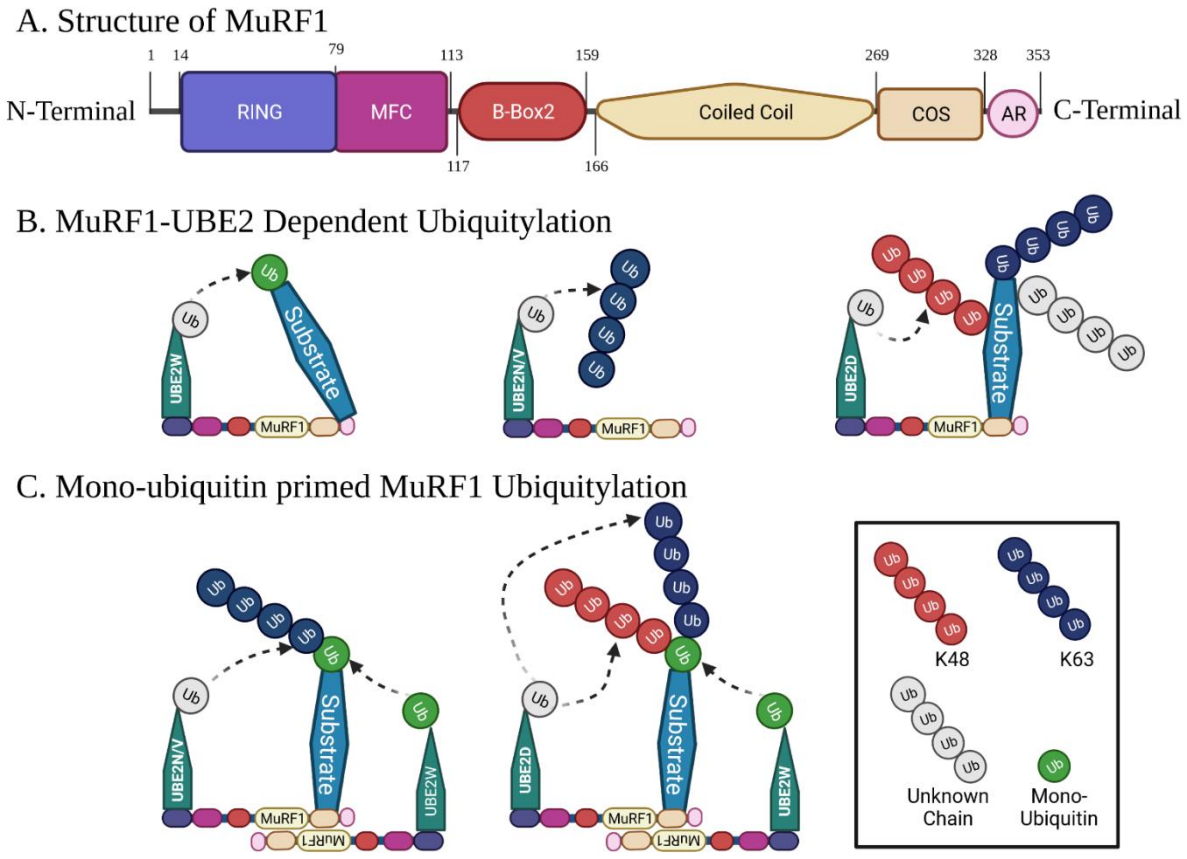

Figure 5. 2 - The structural domains of MuRF1 and its known ubiquitylation mechanisms with UBE2.

A) The structure of MuRF1 contains six discrete conserved domains: The Really

Interesting New Gene (RING) domain, MuRF Family Conserved (MFC) domain, B-Box Zinc Finger 2 (B-Box2) domain, coiled-coil domain, C-terminal Subgroup One Signature (COS-Box), and Acidic Region.

B) MuRF1 generated ubiquitin linkage types are dependent on different interacting UBE2s. When cooperating with MuRF1, UBE2W generates mono-ubiquitylation. UBE2N/V and MuRF1 generates unanchored K63 poly-ubiquitin chains. UBE2D and MuRF1 generate K48 and K63 poly-ubiquitin chains.

C) Paired MuRF1 and UBE2W generate mono-ubiquitylation, acting as a priming site for further poly-ubiquitin chain formation. Utilising the antiparallel dimerisation of multiple MuRF1, multiple UBE2s can be utilised at the same time. This allows MuRF1 to partner with UBE2N/V to anchor K63 poly-ubiquitin onto the UBE2W-generated mono-ubiquitin priming site. Similarly, a dimerised MuRF1 can anchor further UBE2D generated poly-ubiquitin chains (including K48 and K63) onto the mono-ubiquitin priming site.

5.4 The Biochemical Mechanism Of Murf1 Ubiquitylation

MuRF1-UBE2 Function

MuRF1's catalytic activity requires interaction with a UBE2. In such case, UBE2 not only transfers ubiquitin to the substrate, but also plays a key role in determining the form of ubiquitylation. This includes the ubiquitin topology (mono- or poly-ubiquitylation) and the structural arrangement of poly-ubiquitin chains (e.g. K48, K63

etc). As the ubiquitin chain types determine the fate of substrate protein (e.g. degradation, relocalisation, and enzymatic activation/inhibition), it is critical to identify which UBE2(s) partners with MuRF1 providing ligase activity toward the substrate.

MuRF1-E2 Characterisation - Interaction

A few studies have aimed to identify MuRF1 interacting UBE2s using binding assays. Polge et al. assessed a panel of 14 UBE2s affinity with MuRF1 using surface plasmon resonance (SPR) and yeast two-hybrid assays. They identified UBE2E1, G1, J1, and L3 as MuRF1 interacting UBE2s. Furthermore, SPR analysis revealed that Telethonin is required to stabilise the interaction between MuRF1 and partnering UBE2E1 and J1. To confirm this in a cellular model, they showed that overexpression of UBE2E1, G1, J1, or L3 with MuRF1 decreases Telethonin (A muscle-specific protein that regulates sarcomeric assembly) abundance in HEK293T cells (39). Later work in C2C12 myotubes demonstrated that UBE2L3 knockdown perturbs dexamethasone-induced muscle atrophy (40). Although the explanation of these results is not straight-forward, these earlier works have identified four UBE2s interacting/binding with MuRF1 or playing a role in the MuRF1-dependent networks. However, none of these studies provide evidence that these UBE2s can generate ubiquitin E3-ligase activity with MuRF1.

MuRF1-E2 Characterisation - Ubiquitylation Activity Assays

Our lab has recently deployed a screening approach of all human ubiquitin-specific UBE2s with MuRF1 (41). We used *in-vitro* ubiquitylation assays to directly

demonstrate ubiquitin E3-ligase activity produced by the cooperation between MuRF1 and UBE2s. We found MuRF1 can partner with 10 UBE2s—UBE2D family (D1, D2, D3 and D4), UBE2E family (E1, E2 and E3), UBE2N/V family (N/V1 and N/V2), and UBE2W—to generate ubiquitylation activity (41). ELISA-based assays have shown that MuRF1 interacts with UBE2D2 or UBE2D3 to generate ubiquitylation activity (42). As the UBE2D family interact universally with all RING-type E3-ligases (43), they have been used in previous MuRF1 *in-vitro* research (44–47). This promiscuity makes UBE2D a useful tool to characterise substrate ubiquitylation. However, its biological function in atrophy is difficult to define as all members of the UBE2D family offer redundancy. Literature regarding the UBE2E family with MuRF1 is scarce and inconsistent. Nevertheless, it is reported that MuRF1 can interact with UBE2E1 (39) and all other UBE2E family to generate ubiquitylation activity (41). However, another study showed that UBE2E1 knockdown does not preserve dexamethasone-induced atrophy in C2C12 myotubes. (48).

MuRF1-E2 Generated Ubiquitin Chain types

MuRF1 has been previously shown to interact with UBE2D1 to form multiple poly-ubiquitin chains with all seven ubiquitin lysines (26). Looking at MuRF1-UBE2 cooperation *in-vitro*, we were able to ascertain that chain types were formed in a UBE2-dependent manner; MuRF1 is able to form poly-ubiquitin chains through partnering with UBE2D and UBE2E families (Figure 5.2B); UBE2N/V1 and N/V2 were only able to form unanchored poly-ubiquitin chains (not anchored to MuRF1 or its substrates); For the first time, UBE2W was found to be able to generate mono-

ubiquitylation with MuRF1 (41)(Figure 5.2B). UBE2W is well characterised for its unique ability to target the α-amino groups on the N-termini of a substrate (49–51). To explore this further, our group used MuRF1 and UBE2W in combination with other UBE2s and identified a two-step mechanism: 1) MuRF1 can generate a mono-ubiquitin site on a substrate by cooperation with UBE2W, and 2) this acts as an anchor point for further poly-chain elongation (Figure 5.2C). The addition of UBE2W causes UBE2N/V1 or N/V2 ubiquitin chains to become anchored onto the substrate (41). MuRF1 primed mono-ubiquitylation, cooperating with a network of other E3-ligases, expands the number of potential fates of MuRF1 substrates (e.g. with DCAF8, MuRF2, MuRF3, CHIP, MAFbx, TRIM32, FBxL22 and MUSA1), This implies that MuRF1 can have a diverse role in mediating biological effects through ubiquitylation.

Fate of MuRF1 Substrates

Our work also established that MuRF1 can form K48 and K63 poly-ubiquitin chains with UBE2D (1, 2 ,3, and 4) and UBE2E (1, 2, and 3). This highlights that MuRF1 has a large pool of UBE2s to generate proteasomal-preferential K48 chains. However, no direct evidence has been presented to show MuRF1-mediated K48 ubiquitylation leading to degradation of substrate. The UBE2D, UBE2E, and UBE2N/V (NV1 and N/V2) were all able to generate K63 chains in cooperation with MuRF1 (Figure 5.2B). The biological role of K63 poly-ubiquitin chains in autophagy is well documented in the literature (See review Dósa et al (24)). Indeed, an earlier study has demonstrated that autophagy increases during fasting-induced atrophy and its perturbation, through deletion of autophagy regulator ATG7, preserves muscle mass and function (52).

Using Titin as a substrate, MuRF1 has been found to cause ubiquitylation-induced autophagy in cardiomyocytes (53). The MuRF1 interacting region of titin has been well characterised by structural biologists using truncated titin region A168-170 (54). Further cell studies revealed that the titin 170-M1 region interacts with MuRF1 causing the recruitment of autophagic receptors p62 and Nbr1 (55). Our recent study highlighted that the MuRF1 can anchor UBE2N/V-generated K63 ubiquitin chains to titin A168-A170 using a mono-ubiquitin anchor (41). Due to its extremely large size, titin has only been recently shown to be ubiquitylated with K63 poly-ubiquitin chains in cardiomyocytes, using high-resolution agar-strengthened SDS-PAGE. In that study, they also demonstrated that titin was degraded through the lysosome system in a MuRF1 dependent manner (53). Taken together this evidence presents the possibility that MuRF1 directly ubiquitylates titin with K63 chains, which were then used as a signal to recruit Nbr1 and p62. As a result, titin can be engulfed with auto-phagosome and therefore degrading by lysosome-mediated autophagy. This extends MuRF1's role in muscle atrophy to also regulating autophagy.

The fate of MuRF1 ubiquitylated proteins is still yet to be fully understood. Baehr et al. (2021) demonstrated that most MuRF1 substrate abundance didn't change. Some substrates were even increased with MuRF1 overexpression. In fact, only one MuRF1-dependent substrate, MYLPF, was shown to be decreased; Desmin was reported to increase in abundance (11). While previous work demonstrated Desmin to be ubiquitylated and degraded during atrophy, this has not been attributed to MuRF1 (56). However, Desmin has been reported as requiring phosphorylation in

order to be ubiquitylated (56). This highlights that other PTMs may be a necessary component in the ubiquitin-mediated degradation process. Nonetheless, both MYLPF and Desmin are direct substrates of MuRF1 via the same UBE2-dependent mechanism (41). All these studies imply that MuRF1 ubiquitylated proteins are not all directly degraded via UPS. Further research should aim to understand how MuRF1-mediated ubiquitylation on each substrate contribute to MPB.

5.5 Conclusion And Remarks

Skeletal muscle atrophy is a driving cause of poor life- and health-span. However, the mechanism of action remains obscure. Identifying atrophy-induced genes led to the discovery of MuRF1 as a crucial regulator of muscle atrophy. Yet, with over twenty years of research, the progress of understanding MuRF1's mechanistic regulation has been at a slow pace. This is partly due to the field of ubiquitylation being in its adolescence. Nevertheless, the rate of progression in MuRF1 research lacks behind the characterisation of other ubiquitin E3 ligases.

The conserved domains of MuRF1 have been long known, but each of their functional contributions to ubiquitylation activity remains unclear. Through a systematic MuRF1-UBE2 screening, UBE2W-dependant ubiquitylation was discovered to facilitate MuRF1 mono-ubiquitylation of substrates. This mono-ubiquitin can act as an initiator for further MuRF1 dependant poly-ubiquitylation. However, the possibility of secondary ubiquitylation by interacting with other UBE2s or E3 ligases offers a

greater amount of potential ubiquitylation outcomes. This finding expands the downstream functions of MuRF1 beyond direct protein degradation. With the knowledge of MuRF1 interaction with UBE2s, future research will be able to characterise the structural properties necessary for MuRF1-UBE2 cooperation. This will be a crucial step in developing specific inhibitors to perturb MuRF1-UBE2 interaction and MuRF1 dependent signalling in the progression of muscle atrophy. Furthermore, regulators of MuRF1 E3-ligase activity are another area that can be exploited for pharmaceutical intervention. For example, MuRF1 can auto-ubiquitylate (41) and is reported to be SUMOylated (57). It will be interesting to explore how these PTMs impact on MuRF1 E3-ligase activity or alter its interacting partners and localisation.

Skeletal muscle mass is a result of balance between muscle protein synthesis (MPS) and muscle protein breakdown (MBP). MPS signalling is well-characterised cascade of phosphorylation events. For example, the insulin or insulin-like growth factor 1 (IGF1) causes the surface receptor to recruit and tyrosine-phosphorylate insulin receptor substrate 1 (IRS-1). IRS1 then coordinates with phosphoinositide 3-kinases (PI3K) to convert phosphatidylinositol (4,5)-bisphosphate to phosphatidylinositol (3,4,5)-trisphosphate. Phosphatidylinositol (3,4,5)-trisphosphate recruits Protein *kinase* B (*PKB; also called AKT*) and PDK-1, resulting in PDK-1 phosphorylating PKB. PKB activates mTOR by interrupting the mTOR inhibitor Rheb. mTOR then enhances transcriptional regulation of MPS by phosphorylation of S6K and disinhibition of 4E-BP1, promoting translational initiation. The MPB signalling pathway is initiated by a plurality of stimuli, such as inflammation cytokines (e.g. TNF, IL6, and myostatin etc). These cytokines increase expression of several E3 ligases, such as MuRF1 and MAFbx, that are known to be involved in atrophy. Atrophy causes an increase in the abundance of ubiquitylated proteins which are thought to be driven by the increase of E3 ligases. However, the contribution that ubiquitylated proteins make to MPB is still unclear. Although proteasomal activity and lysosomal autophagy are increased during atrophy, the question remains whether ubiquitylated proteins are direct substrates for degradation or function as a signalling protein to activate degradation.

AUTHOR CONTRIBUTIONS

P.W.J.D. and Y-C.L. draft, edited and revised the manuscript.

ACKNOWLEDGEMENT

Y-C.L. and P.W.J.D. was supported by MRC Versus Arthritis Centre for Musculoskeletal Ageing Research (MR/P021220/1).

CONFLICT OF INTEREST

The authors have no conflicts of interest to declare

5.6 References

1. von Haehling S, Anker MS, Anker SD. Prevalence and clinical impact of cachexia in chronic illness in Europe, USA, and Japan: facts and numbers update 2016. J Cachexia Sarcopenia Muscle. 2016;7(5):507–9.

2. Arango-Lopera VE, Arroyo P, Gutiérrez-Robledo LM, Perez-Zepeda MU, Cesari M. Mortality as an adverse outcome of sarcopenia. J Nutr Heal Aging. 2013;17(3):259–62.

3. Metter EJ, Talbot LA, Schrager M, Conwit R. Skeletal muscle strength as a predictor of all-cause mortality in healthy men. Journals Gerontol - Ser A Biol Sci Med Sci. 2002;57(10):B359–65.

4. Amm I, Sommer T, Wolf DH. Protein quality control and elimination of protein waste: The role of the ubiquitin-proteasome system. Biochim Biophys Acta - Mol Cell Res. 2014;1843(1):182–96.

5. Vilchez D, Saez I, Dillin A. The role of protein clearance mechanisms in organismal ageing and age-related diseases. Nat Commun. 2014;5:5659.

6. Pohl C, Dikic I. Cellular quality control by the ubiquitin-proteasome system and autophagy. Science. 2019;366(6467):818–22.

7. Nishimura Y, Musa I, Holm L, Lai YC. Recent advances in measuring and understanding the regulation of exercise-mediated protein degradation in skeletal muscle. Am J Physiol - Cell Physiol. 2021;321(2):C276–87.

8. Centner T, Yano J, Kimura E, McElhinny AS, Pelin K, Witt CC, et al. Identification of muscle specific ring finger proteins as potential regulators of the titin kinase domain. J Mol Biol. 2001;306(4):717–26.

9. Bodine SC, Latres E, Baumhueter S, Lai VKM, Nunez L, Clarke BA, et al. Identification of ubiquitin ligases required for skeletal Muscle Atrophy. Science. 2001;294(5547):1704–8.

10. RECOVERY Collaborative Group. Dexamethasone in Hospitalized Patients with Covid-19. N Engl J Med. 2021;384(8):693–704.

11. Baehr LM, Hughes DC, Lynch SA, Van Haver D, Maia TM, Marshall AG, et al. Identification of the MuRF1 Skeletal Muscle Ubiquitylome Through Quantitative Proteomics. Function. 2021;2(4):1–18.

12. Labeit S, Kohl CH, Witt CC, Labeit D, Jung J, Granzier H. Modulation of muscle atrophy, fatigue and MLC phosphorylation by MuRF1 as indicated by hindlimb suspension studies on MuRF1-KO mice. J Biomed Biotechnol. 2010;

13. Hwee DT, Bodine SC. Age-related deficit in load-induced skeletal muscle growth. Journals Gerontol - Ser A Biol Sci Med Sci. 2009;64(6):618–28.

14. Sartorelli V, Fulco M. Molecular and cellular determinants of skeletal muscle atrophy and hypertrophy. Sci STKE. 2004;244(244):1–10.

15. Wing SS, Haas AL, Goldberg AL. Increase in ubiquitin-protein conjugates concomitant with the increase in proteolysis in rat skeletal muscle during starvation and atrophy denervation. Biochem J. 1995;307(3):639–45.

16. Zhao J, Zhai B, Gygi SP, Goldberg AL. MTOR inhibition activates overall protein degradation by the ubiquitin proteasome system as well as by autophagy. Proc Natl Acad Sci U S A. 2015;112(52):15790–7.

17. Clarke BA, Drujan D, Willis MS, Murphy LO, Corpina RA, Burova E, et al. The E3 Ligase MuRF1 Degrades Myosin Heavy Chain Protein in Dexamethasone-Treated Skeletal Muscle. Cell Metab. 2007;6(5):376–85.

18. Cohen S, Brault JJ, Gygi SP, Glass DJ, Valenzuela DM, Gartner C, et al. During muscle atrophy, thick, but not thin, filament components are degraded by MuRF1-dependent ubiquitylation. J Cell Biol. 2009;185(6):1083–95.

19. Gomes A V., Waddell DS, Siu R, Stein M, Dewey S, Furlow JD, et al. Upregulation of proteasome activity in muscle RING finger 1-null mice following denervation. FASEB J. 2012;26(7):2986–99.

20. Komander D, Rape M. The ubiquitin code. Annu Rev Biochem. 2012;81:203–29.

21. Swatek KN, Komander D. Ubiquitin modifications. Cell Res. 2016;26(4):399–422.

22. Chau V, Tobias JW, Bachmair A, Marriott D, Ecker DJ, Gonda DK, et al. A Multiubiquitin Chain Is Confined to Specific Lysine in a Targeted Short-Lived Protein. Science. 1989;243(4898):1576–83.

23. van Kruijsbergen I, Mulder MPC, Uckelmann M, van Welsem T, de Widt J, Spanjaard A, et al. Strategy for Development of Site-Specific Ubiquitin Antibodies. Front Chem. 2020;8:1–13.

24. Dósa A, Csizmadia T. The role of K63 - linked polyubiquitin in several types of autophagy. Biol Futur. 2022;DOI: 10.1007/s42977-022-00117-4.

25. Li HH, Du J, Fan YN, Zhang ML, Liu DP, Li L, et al. The ubiquitin ligase MuRF1 protects against cardiac ischemia/reperfusion injury by its proteasome-dependent degradation of phospho-c-Jun. Am J Pathol. 2011;178(3):1043–58.

26. Hyoung TK, Kwang PK, Lledias F, Kisselev AF, Scaglione KM, Skowyra D, et al. Certain pairs of ubiquitin-conjugating enzymes (E2s) and ubiquitin-protein ligases (E3s) synthesize nondegradable forked ubiquitin chains containing all possible isopeptide linkages. J Biol Chem. 2007;282(24):17375–86.

27. Meroni G, Diez-Roux G. TRIM/RBCC, a novel class of “single protein RING finger” E3 ubiquitin ligases. BioEssays. 2005;27(11):1147–57.

28. Ozato K, Shin D-M, Chang T-H, Morse HC. TRIM family proteins and their emerging roles in innate immunity. Nat Rev Immunol. 2008;8(11):849–60.

29. Yang W, Gu Z, Zhang H, Hu H. To TRIM the Immunity: From Innate to Adaptive Immunity. Front Immunol. 2020;11:1–18.

30. Napolitano LM, Jaffray EG, Hay RT, Meroni G. Functional interactions between ubiquitin E2 enzymes and TRIM proteins. Biochem J. 2011;434(2):309–19.

31. Budhidarmo R, Nakatani Y, Day CL. RINGs hold the key to ubiquitin transfer. Trends Biochem Sci. 2012;37(2):58–65.

32. Gundogdu M, Walden H. Structural basis of generic versus specific E2–RING E3 interactions in protein ubiquitination. Protein Sci. 2019;28(10):1758–70.

33. Mrosek M, Meier S, Ucurum-Fotiadis Z, Von Castelmur E, Hedbom E, Lustig A, et al. Structural analysis of B-box 2 from MuRF1: Identification of a novel self-association pattern in a RING-like fold. Biochemistry. 2008;47(40):10722–30.

34. Franke B, Gasch A, Rodriguez D, Chami M, Khan MM, Rudolf R, et al. Molecular basis for the fold organization and sarcomeric targeting of the muscle atrogin MuRF1. Open Biol. 2014;4:130172.

35. Stevens M, Franke B, Skorupka KA, Cafiso DS, Pornillos O, Mayans O, et al. Exploration of the TRIM Fold of MuRF1 Using EPR Reveals a Canonical Antiparallel Structure and Extended COS-Box. J Mol Biol. 2019;431(15):2900–9.

36. Fiorentini F, Esposito D, Rittinger K. Does it take two to tango? RING domain self-association and activity in TRIM E3 ubiquitin ligases. Biochem Soc Trans. 2020;48(6):2615–24.

37. Balaji V, Hoppe T. Regulation of E3 ubiquitin ligases by homotypic and heterotypic assembly. F1000Research. 2020;9(6):88.

38. Yin Q, Lin S-C, Lamothe B, Lu M, Lo Y-C, Hura G, et al. E2 interaction and dimerization in the crystal structure of TRAF6. Nat Struct Mol Biol. 2009;16(6):658–66.

39. Polge C, Koulmann N, Claustre A, Jarzaguet M, Serrurier B, Combaret L, et al. UBE2D2 is not involved in MuRF1-dependent muscle wasting during hindlimb suspension. Int J Biochem Cell Biol. 2016;79:488–93.

40. Peris-Moreno D, Malige M, Claustre A, Armani A, Coudy-Gandilhon C, Deval C, et al. Ube2l3, a partner of murf1/trim63, is involved in the degradation of myofibrillar actin and myosin. Cells. 2021;10(8):1–18.

41. Dawson PWJ, Baehr LM, Hughes DC, Knowles TJ, Sridhar P, Bodine SC, et al. The Role of UBE2-Conjugating Enzymes in the Mechanism of MuRF1 Ubiquitylation. Bioarchive. 2022;44(0):1–29.

42. Marblestone JG, Butt S, McKelvey DM, Sterner DE, Mattern MR, Nicholson B, et al. Comprehensive Ubiquitin E2 Profiling of Ten Ubiquitin E3 Ligases. Cell Biochem Biophys. 2013;67(1):161–7.

43. Brzovic PS, Klevit RE. Ubiquitin transfer from the E2 perspective: Why is UbcH5 so promiscuous? Cell Cycle. 2006;5(24):2867–73.

44. Kedar V, McDonough H, Arya R, Li HH, Rockman HA, Patterson C. Muscle-specific RING finger 1 is a bona fide ubiquitin ligase that degrades cardiac troponin I. Proc Natl Acad Sci U S A. 2004;101(52):18135–40.

45. Koyama S, Hata S, Witt CC, Ono Y, Lerche S, Ojima K, et al. Muscle RING-Finger Protein-1 (MuRF1) as a Connector of Muscle Energy Metabolism and Protein Synthesis. J Mol Biol. 2008;376(5):1224–36.

46. Chen SN, Czernuszewicz G, Tan Y, Lombardi R, Jin J, Willerson JT, et al. Human molecular genetic and functional studies identify TRIM63, encoding muscle RING finger protein 1, as a novel gene for human hypertrophic cardiomyopathy. Circ Res. 2012;111(7):907–19.

47. Polge C, Heng A, Jarzaguet M, Ventadour S, Claustre A, Combaret L, et al. Muscle actin is polyubiquitinylated in vitro and in vivo and targeted for breakdown by the E3 ligase MuRF1 . FASEB J. 2011;25(11):3790–802.

48. Cécile P, Julien A, Andrea A, Agnès C, Cécile CG, Clara T, et al. UBE2E1 is preferentially expressed in the cytoplasm of slow-twitch fibers and protects skeletal muscles from exacerbated atrophy upon dexamethasone treatment. Cells. 2018;7(11).

49. Tatham MH, Plechanovová A, Jaffray EG, Salmen H, Hay RT. Ube2W conjugates ubiquitin to α-amino groups of protein N-termini. Biochem J. 2013;453(1):137–45.

50. Scaglione KM, Basrur V, Ashraf NS, Konen JR, Elenitoba-Johnson KSJ, Todi S V., et al. The ubiquitin-conjugating enzyme (E2) ube2w ubiquitinates the N terminus of substrates. J Biol Chem. 2013;288(26):18784–8.

51. Vittal V, Shi L, Wenzel DM, Scaglione KM, Duncan ED, Basrur V, et al. Intrinsic disorder drives N-terminal ubiquitination by Ube2w. Nat Chem Biol. 2015;11(1):83–9.

52. Masiero E, Agatea L, Mammucari C, Blaauw B, Loro E, Komatsu M, et al. Autophagy Is Required to Maintain Muscle Mass. Cell Metab. 2009;10(6):507–15.

53. Müller E, Salcan S, Bongardt S, Barbosa DM, Krüger M, Kötter S. E3-ligase knock down revealed differential titin degradation by autopagy and the ubiquitin proteasome system. Sci Rep. 2021;11(1):1–13.

54. Mrosek M, Labeit D, Witt S, Heerklotz H, von Castelmur E, Labeit S, et al. Molecular determinants for the recruitment of the ubiquitin-ligase MuRF-1 onto M-line titin. FASEB J. 2007;21(7):1383–92.

55. Bogomolovas J, Fleming JR, Franke B, Manso B, Simon B, Gasch A, et al. Titin kinase ubiquitination aligns autophagy receptors with mechanical signals in the sarcomere. EMBO Rep. 2021;22(10):1–14.

56. Cohen S, Zhai B, Gygi SP, Goldberg AL. Ubiquitylation by Trim32 causes coupled loss of desmin, Z-bands, and thin filaments in muscle atrophy. J Cell Biol. 2012;198(4):575–89.

57. Heras G, Namuduri AV, Traini L, Shevchenko G, Falk A, Bergström Lind S, et al. Muscle RING-finger protein-1 (MuRF1) functions and cellular localization are regulated by SUMO1 post-translational modification. J Mol Cell Biol. 2019;11(5):356–70

Chapter 6

Conclusion and Discussion

6.1 Discussion

The aim of this thesis was to examine MuRF1's ubiquitylation activity to better understand the molecular mechanisms governing skeletal muscle atrophy. Muscle atrophy results in deleterious health consequences associated with aging and disease such as increased mortality risk, loss of function and independence. MuRF1 has robustly correlated with atrophy and been implicated in its regulation, though precisely how remained unclear. Elucidating MuRF1's molecular activity is essential for developing diagnostic and therapeutic interventions.

Past research largely relied on MuRF1 mRNA expression as an atrophy marker, providing only inferential links to its function. MuRF1 upregulation accompanies diverse catabolic states, and gene deletion partially rescues wasting, yet direct evidence of its regulatory activity was lacking. Transgenic MuRF1 overexpression reduced cardiac but not skeletal muscle mass, indicating tissue-specific roles warranting deeper investigation.

In this thesis, the first study aimed to identify the ubiquitin-conjugating enzymes (UBE2s) that interact with the E3 ligase MuRF1 to mediate ubiquitylation. An *in-vitro* ubiquitylation assay was developed using purified recombinant proteins including ubiquitin, E1 ubiquitin-activating enzyme, all known relevant human E2s, and MuRF1 tagged with maltose-binding protein (MBP). Interactions between MuRF1 and each UBE2 were screened by incubating them together in the ubiquitylation reaction mixture containing all the enzymes and substrates required for ubiquitylation.

Products were then analysed by western blotting to detect polyubiquitin chains or single ubiquitin molecules attached to MuRF1, indicating its interaction with UBE2s.

This assay revealed that MuRF1 interacts with the UBE2D, UBE2E, UBE2N/V families and UBE2W to produce different ubiquitin chain linkages. Further experiments showed MuRF1 undergoes autoubiquitylation in a two-step manner using UBE2W to first attach a single ubiquitin, acting as an anchor for UBE2N/V to generate K63-linked polyubiquitin chains. To investigate substrate ubiquitylation, known MuRF1 substrates including Titin A168-A170, Desmin, and MYLPF were added to the reaction and detected by western blotting. To explore the correlation of MuRF1 upregulation with UBE2, qPCR of UBE2 genes was performed during a time course of atrophy in a rodent model. Gene expression of UBE2W, UBE2N and UBE2V2 was found to increase 14 days after denervation in mouse muscle, correlating with MuRF1 upregulation and atrophy.

Further experiments were performed to investigate the nature of MuRF1-Substrate interaction, using Titin A168-A170 as a substrate. Site-directed mutagenesis was used to mutate the predicted MuRF1 binding site on Titin A168-A170. Co-precipitation assays showed mutation did not abolish interaction between MuRF1 and titin. However, *in-vitro* ubiquitylation revealed mutation impaired but did not eliminate titin ubiquitylation by MuRF1.

Furthermore, mass spectrometry identified candidate ubiquitylation sites on Titin A168-A170 ubiquitylated by MuRF1 *in-vitro*. Targeted mutagenesis of the predicted

lysine residue did not fully disrupt ubiquitylation, suggesting MuRF1 promiscuously modified accessible amino acids. Finally, the ability of a reported MuRF1 inhibitor to block ubiquitylation was investigated *in-vitro* but no effect was observed.

It is important to consider the nuances of an *in-vitro* methods, and how this should be interpreted in context of a whole organism. While the purpose of this research has been to isolate the essential biochemical characteristics of MuRF1, using an *in-vitro* method doesn't account for the variables that influence its activity; *in-vitro* ubiquitylation assays provide a simplified system to study protein interactions and modification but cannot fully recapitulate the complexity of cellular environments. *In-vitro* assays fail to account for additional regulatory mechanisms present in cells/tissues that could influence protein modification. Furthermore, using recombinant overexpression systems to produce purified proteins runs the risk of proteins misfolding or adopting non-native structures that impact their interactions and functions. Screening a library of UBE2 enzymes *in-vitro* only identifies those capable of directly transferring ubiquitin in isolation; indirect or cell/tissue-specific interactions may be missed. Predicting interaction interfaces based on homology modelling is an approximation and mutation of putative residues may not fully disrupt the interaction, as was discovered. Additionally, co-precipitation assays can only detect protein-protein interactions but provide no information about specific functional outcomes like ubiquitylation activity.

However, the combination of *in-vitro* biochemical techniques, protein interaction assays, targeted mutagenesis, and mass spectrometry allowed rigorous examination of MuRF1 activity at a molecular level, providing novel insights into interacting

enzymes, ubiquitylation mechanisms, and substrates. These reductionist methods established a strong basis for further investigation and hypothesis generation to understand MuRF1's role in muscle wasting and may point to potential strategies for creating diagnostic tools or modulating its function for the purpose of future therapies.

Initially, it is imperative to demonstrate the validity of MuRF1's *in-vitro* characteristics within a physiologically relevant model. To facilitate this understanding 3 tools would need to be developed:

1. An atrophy model in-cell – A cell model in which trophy can be induced to observe the increase in MuRF1 and its correlating change on substrate abundance (Such as Desmin, Titin, and MYLPF)

2. An overexpression of MuRF1 model in-cell. This can be used to show a dose dependant response on substrate abundance following MuRF1 expression.

3. A knockout model of MuRF1 in-cell – Using a MuRF1 knockout model, to observe if substrates are preserved if MuRF1 is not expressed during atrophy.

Using these three tools as wild type, positive, and negative controls, it would be possible to explore the impact of UBE2s during atrophy. Such as using siRNA or shRNA knockdown of the UBE2s identified as MuRF1 interactors in this thesis.

Downstream of MuRF1-E2 interaction and the addition of ubiquitin chains, the fate of MuRF1 substrates could be explored. Firstly, using an in-cell atrophy model, the proteasome could be inhibited (Such as using Bortazomib or MG132) to preserve

MuRF1 substrates. These substrates could be purified using immunoprecipitation and blotted to identify the type of ubiquitin chains covalently attached to them

Further to exploring the role of MuRF1 being involved in a greater process of atrophy, MuRF1 and substrates could be transfected alone in a non-muscle cell-line and the ubiquitylation and potential degradation of the substrate occurs. This would highlight if MuRF1 requires cooperation with other proteins to facilitate protein degradation.

With an established model in-cell or *in-vivo*, it will then be possible to explore the fate of MuRF1 ubiquitylated substrates, the importance of each E2 to MuRF1 function, the role of additional PTMs and the potential role of MuRF1-E3 interaction. Current research in the field of ubiquitylation is examining the therapeutic use of deubiquitylates (DUBs), a family of enzymes that cleave ubiquitin from substrates. Screening panels of DUBs in an atrophy model would open the door for exploring potential therapies that could perturb MuRF1 induced atrophy in addition to identifying the molecular mechanisms of MuRF1.

This research provides an important foundational stone in understanding the molecular mechanisms of muscle wasting. This can be built upon to develop more sophisticated hypotheses and ultimately benefit those suffering from muscle-wasting conditions.